

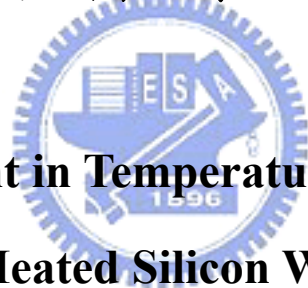
國立交通大學

機械工程學系

碩士論文

利用晶圓旋轉和/或位移改善燈源

加熱晶圓之等溫性研究



**Improvement in Temperature Uniformity
of a Lamp-Heated Silicon Wafer through
Wafer Rotation and/or Translation**

研究生：賴信介

指導教授：林清發博士

中華民國九十三年六月

誌 謝

時光飛逝，回首在新竹這幾年來的點點滴滴，與當年隻身到交大求學的我相比，在交大這充滿學術氣息的环境下似乎讓我在知識上成長茁壯許多。個人經歷在交大大學部、研究所的歲月裡，師長的敦敦教誨，同學間的相互砥礪，學弟妹的鼓勵等等，使我在這幾年來不僅獲得是知識上的成長，在生活上也得到許多寶貴的經驗，這些我將永遠不能忘懷並時時銘記在心。本論文之所以可以順利完成，首先要感謝的是指導老師 林清發教授嚴謹及殷切的指導，使學生能培養出獨立思考、釐清並自行解決問題的能力；更在學生撰寫論文時，不辭辛勞逐字斧正文稿，在此獻上最高謝意。在研究所期間，要特別感謝博士班謝瑞青學長在實驗設備設計及架設上的協助指導，亦要感謝博士班杜志龍、謝雅意、郭威伸、賴佑民、陳尚緯、謝汎鈞等博士班學長在生活及課業上指導與建議，使我受益匪淺，謝謝您們。

榮源、峰慶、佳鴻這群不只是求學中的同學，更是生活上的好朋友。研究所之所以能在緊湊忙碌又充滿歡樂中的氣氛中度過，即是靠這些同學兼好友的夥伴們相互協助幫忙，令我永生難忘。另外也要感謝 文賢、召漢、立傑、家銘等一群努力的學弟幫忙及合作，希望你們能繼續保持實驗室優良傳統，並帶著實驗室進步。

最後更要感謝父母對於我的支持及教誨，有他們無怨無悔付出及支持，使我可以無後顧之憂的專注於研究，並且可無憂無慮過求學生活。最後，僅以本份成果願與關心我的人及我關心的人分享。

今日我以交大為榮 願他日交大以我為榮

信 介

2004. 6. 于交大風城


利用晶圓旋轉和/或位移改善燈源 加熱晶圓之等溫性研究

研究生：賴信介

指導教授：林清發 博士

國立交通大學機械工程學系

中文摘要



本篇論文是藉由量測八吋矽晶圓表面溫度，去探討在快速加熱製程(RTP)中利用燈源加熱晶圓的溫度均勻性研究。本論文的重點是在於，使用燈源加熱使晶圓升溫的過程中，藉由將晶圓加以旋轉或位移以及旋轉加位移，來改善加熱過程中晶圓表面之不均勻性。另外也探討燈源距離晶圓垂直距離對於晶圓溫度均勻性之影響；在本實驗中其參數範圍分別為，燈源到晶圓距離由 30 mm 到 90 mm，晶圓旋轉速率為 0 rpm 至 200 rpm 並且晶圓位移速率為 0 mm/s 到 20 mm/s。

由實驗數據結果可知，在有限範圍內增加晶圓旋轉和位移速率，可改善晶圓的不均溫性，但超過此範圍將獲得反效果。除此以外還發現增加燈源到晶圓的距離對溫度的均勻性也有所改善。最後，在本實驗系統中選擇一適當之晶圓旋轉速率和位移速率可得到一個較佳溫度均勻性；在一顆燈加熱，晶圓平均溫度為 140 °C 時，可有一個最佳溫度不均勻性 $\approx 0.5^{\circ}\text{C}$ 。

Improvement in Temperature Uniformity of a Lamp-Heated Silicon Wafer through Wafer Rotation and/or Translation

Student: Hsin-Chieh Lai

Advisor: Dr. Tsing-Fa Lin

**Department (Institute) of Mechanical Engineering
National Chaio Tung University**

The logo of National Chaio Tung University is a circular emblem with a gear-like outer border. Inside the circle, there is a stylized building and the year '1896' at the bottom. The word 'ABSTRACT' is superimposed in bold, black, uppercase letters across the center of the logo.

ABSTRACT

Temperature measurement on the surface of an eight-inch a silicon wafer is conducted in the present study to explore the temperature uniformity of a lamp heated wafer during a model rapid thermal processing. The possible improvement of the wafer temperature uniformity during the ramp-up period by the wafer rotation and/or translation are explored. The effects of the lamp-to-wafer separation distance on the wafer temperature uniformity are also examined. In the experiment the lamp-to-wafer separation distance is varied from 30 mm to 90 mm, the rotation rate of the wafer is varied from 0 to 200 rpm , the wafer translation speed is varied from 0 to 20 mm/s.

The measured data clearly show that increasing the wafer rotation rate and translation speed to certain levels can significantly improve the temperature uniformity of the wafer. Beyond these levels opposite effects are noted. Besides, we also observe that for a longer lamp-to-wafer distance the wafer temperature is more uniform. Finally, the temperature nonuniformity on the wafer can be rather small for a

suitable choice of the wafer rotation rate and translation speed.



TABLE OF CONTENTS

ABSTRACT	I
TABLE OF CONTENTS	III
LIST OF TABLES	V
LIST OF FIGURES	VI
NOMENCLATURE	X V
CHAPTER 1 INTRODUCTION	1
1.1 Motivation of the Present Study	1
1.2 Literature Review	2
1.3 Objectives and Scope of Present Study	6
CHAPTER 2 EXPERIMENTAL APPARATUS AND PROCEDURES	7
2.1 Experimental Apparatus	7
2.1.1 Processing Chamber	7
2.1.2 Heating Lamp Unit	8
2.1.3 Temperature Measurement and Data Acquisition Unit	8
2.1.4 Control Unit	8
2.1.5 Rotation and displacement Unit	9
2.1.6 Susceptor Unit	9

2.2 Experimental Procedures	10
CHAPTER 3 UNCERTAINTY ANALYSIS	18
CHAPTER 4 RESULTS AND DISCUSSION	21
4.1 Effects of Lamp Power Level on Wafer Temperature	22
Nonuniformity	
4.2 Effects of Wafer Rotational Speed on Wafer	23
Temperature Uniformity	
4.3 Effects of Wafer Translation on Wafer Temperature	24
Uniformity	
4.4 Effects of Lamp-to-Wafer Separation Distance on	25
Wafer Temperature Uniformity	
4.5 Effects of Lamp Arrangement on Wafer Temperature	26
Uniformity	
4.6 Optimum design for Wafer Temperature Uniformity	27
CHAPTER 5 CONCLUDING REMARKS	95
REFERENCES	96

LIST OF TABLES

Table 3.1 Summary of uncertainty analysis



LIST OF FIGURES

- Fig. 2.1 Schematic diagram of the experiment apparatus.
- Fig. 2.2 Schematic of the heating lamp arrangement (a)one lamp, and (b)three lamps-first arrangement, and (c)three lamps-second arrangement.
- Fig. 2.3 Schematic of the measured wafer temperature at selected locations for the wafer temperature measurement.
- Fig. 2.4 Schematic of the feedback control point above the wafer with(a)one lamp, (b)three lamps lamps-first arrangement, and (c)three lamps-second arrangement..
- Fig. 2.5 Schematic diagram of the rotation unit.
- Fig. 2.6 Schematic diagram of translation system.
- Fig. 2.7 Schematic diagram of the susceptor.
- Fig. 4.1 Time variation of the wafer temperature measured at the geometric center of the wafer during the ramp-up period for the wafer heated by a single lamp for $H=90$ mm, $\omega=150$ rpm, and $V_d=15$ mm/s.
- Fig. 4.2 Time variation of the wafer temperature measured at the geometric center of the wafer during the ramp-up period for the wafer heated by three lamp for $H=60$ mm, $\omega=150$ rpm, and $V_d=15$ mm/s.
- Fig. 4.3 The measured wafer temperature at selected locations for $H=30$ mm, $V_d=0$ mm/s and $\omega=0$ rpm for the wafer heated by one lamp during the ramp-up period.
- Fig. 4.4 The measured wafer temperature at selected locations for $H=30$ mm, $V_d=0$ mm/s and $\omega=0$ rpm for the wafer heated by three lamps during the ramp-up period.
- Fig. 4.5 The measured wafer temperature at selected locations for (a) $\omega=0$ rpm, (b) $\omega=50$ rpm, (c) $\omega=100$ rpm, (d) $\omega=150$ rpm and (e) $\omega=200$ rpm at

$H=30$ mm and $V_d=0$ mm/s for the wafer heated by one lamp.

Fig. 4.6 The measured wafer temperature at selected locations for (a) $\omega=0$ rpm, (b) $\omega=50$ rpm, (c) $\omega=100$ rpm, (d) $\omega=150$ rpm and (e) $\omega=200$ rpm at $H=60$ mm and $V_d=0$ mm/s for the wafer heated by one lamp.

Fig. 4.7 The measured wafer temperature at selected locations for (a) $\omega=0$ rpm, (b) $\omega=50$ rpm, (c) $\omega=100$ rpm, (d) $\omega=150$ rpm and (e) $\omega=200$ rpm at $H=30$ mm and $V_d=5$ mm/s for the wafer heated by one lamp.

Fig. 4.8 The measured wafer temperature at selected locations for (a) $\omega=0$ rpm, (b) $\omega=50$ rpm, (c) $\omega=100$ rpm, (d) $\omega=150$ rpm and (e) $\omega=200$ rpm at $H=60$ mm and $V_d=5$ mm/s for the wafer heated by one lamp.

Fig. 4.9 The measured wafer temperature at selected locations for (a) $\omega=0$ rpm, (b) $\omega=50$ rpm, (c) $\omega=100$ rpm, (d) $\omega=150$ rpm and (e) $\omega=200$ rpm at $H=30$ mm and $V_d=10$ mm/s for the wafer heated by one lamp

Fig. 4.10 The measured wafer temperature at selected locations for (a) $\omega=0$ rpm, (b) $\omega=50$ rpm, (c) $\omega=100$ rpm, (d) $\omega=150$ rpm and (e) $\omega=200$ rpm at $H=60$ mm and $V_d=10$ mm/s for the wafer heated by one lamp.

Fig. 4.11 The measured wafer temperature at selected locations for (a) $\omega=0$ rpm, (b) $\omega=50$ rpm, (c) $\omega=100$ rpm, (d) $\omega=150$ rpm and (e) $\omega=200$ rpm at $H=30$ mm and $V_d=15$ mm/s for the wafer heated by one lamp.

Fig. 4.12 The measured wafer temperature at selected locations for (a) $\omega=0$ rpm, (b) $\omega=50$ rpm, (c) $\omega=100$ rpm, (d) $\omega=150$ rpm and (e) $\omega=200$ rpm at $H=60$ mm and $V_d=15$ mm/s for the wafer heated by one lamp.

Fig. 4.13 The measured wafer temperature at selected locations for (a) $\omega=0$ rpm, (b) $\omega=50$ rpm, (c) $\omega=100$ rpm, (d) $\omega=150$ rpm and (e) $\omega=200$ rpm at $H=30$ mm and $V_d=0$ mm/s for the wafer heated by three lamps.

Fig. 4.14 The measured wafer temperature at selected locations for (a) $\omega=0$ rpm, (b) $\omega=50$ rpm, (c) $\omega=100$ rpm, (d) $\omega=150$ rpm and (e) $\omega=200$ rpm at $H=60$ mm and $V_d=0$ mm/s for the wafer heated by three lamps.

- Fig. 4.15 The measured wafer temperature at selected locations for (a) $\omega=0$ rpm, (b) $\omega=50$ rpm, (c) $\omega=100$ rpm, (d) $\omega=150$ rpm and (e) $\omega=200$ rpm at $H=30$ mm and $V_d=5$ mm/s for the wafer heated by three lamps.
- Fig. 4.16 The measured wafer temperature at selected locations for (a) $\omega=0$ rpm, (b) $\omega=50$ rpm, (c) $\omega=100$ rpm, (d) $\omega=150$ rpm and (e) $\omega=200$ rpm at $H=60$ mm and $V_d=5$ mm/s for the wafer heated by three lamps.
- Fig. 4.17 The measured wafer temperature at selected locations for (a) $\omega=0$ rpm, (b) $\omega=50$ rpm, (c) $\omega=100$ rpm, (d) $\omega=150$ rpm and (e) $\omega=200$ rpm at $H=30$ mm and $V_d=10$ mm/s for the wafer heated by three lamps.
- Fig. 4.18 The measured wafer temperature at selected locations for (a) $\omega=0$ rpm, (b) $\omega=50$ rpm, (c) $\omega=100$ rpm, (d) $\omega=150$ rpm and (e) $\omega=200$ rpm at $H=60$ mm and $V_d=10$ mm/s for the wafer heated by three lamps.
- Fig. 4.19 The measured wafer temperature at selected locations for (a) $\omega=0$ rpm, (b) $\omega=50$ rpm, (c) $\omega=100$ rpm, (d) $\omega=150$ rpm and (e) $\omega=200$ rpm at $H=30$ mm and $V_d=15$ mm/s for the wafer heated by three lamps.
- Fig. 4.20 The measured wafer temperature at selected locations for (a) $\omega=0$ rpm, (b) $\omega=50$ rpm, (c) $\omega=100$ rpm, (d) $\omega=150$ rpm and (e) $\omega=200$ rpm at $H=60$ mm and $V_d=15$ mm/s for the wafer heated by three lamps.
- Fig. 4.21 The measured wafer temperature at selected locations during the ramp-up period for (a) $V_d=0$ mm/s, (b) $V_d=5$ mm/s, (c) $V_d=10$ mm/s and (d) $V_d=15$ mm/s with the wafer heated by a single lamp at $\omega=0$ rpm and $H=60$ mm for the final wafer temperature set at 140°C .
- Fig. 4.22 The measured wafer temperature at selected locations during the ramp-up period for (a) $V_d=0$ mm/s, (b) $V_d=5$ mm/s, (c) $V_d=10$ mm/s and (d) $V_d=15$ mm/s with the wafer heated by a single lamp at $\omega=100$ rpm and $H=60$ mm for the final wafer temperature set at 140°C .
- Fig. 4.23 The measured wafer temperature at selected locations during the ramp-up period for (a) $V_d=0$ mm/s, (b) $V_d=5$ mm/s, (c) $V_d=10$ mm/s and (d) $V_d=15$ mm/s with the wafer heated by a single lamp at $\omega=200$ rpm and $H=60$ mm for the final wafer temperature set at 140°C .

Fig. 4.24 The measured wafer temperature at selected locations during the ramp-up period for (a) $V_d=0$ mm/s, (b) $V_d=5$ mm/s, (c) $V_d=10$ mm/s and (d) $V_d=15$ mm/s with the wafer heated by a single lamp at $\omega=0$ rpm and $H=30$ mm for the final wafer temperature set at 140°C .

Fig. 4.25 The measured wafer temperature at selected locations during the ramp-up period for (a) $V_d=0$ mm/s, (b) $V_d=5$ mm/s, (c) $V_d=10$ mm/s and (d) $V_d=15$ mm/s with the wafer heated by a single lamp at $\omega=100$ rpm and $H=30$ mm for the final wafer temperature set at 140°C .

Fig. 4.26 The measured wafer temperature at selected locations during the ramp-up period for (a) $V_d=0$ mm/s, (b) $V_d=5$ mm/s, (c) $V_d=10$ mm/s and (d) $V_d=15$ mm/s with the wafer heated by a single lamp at $\omega=200$ rpm and $H=30$ mm for the final wafer temperature set at 140°C .

Fig. 4.27 The measured wafer temperature at selected locations during the ramp-up period for (a) $V_d=0$ mm/s, (b) $V_d=5$ mm/s, (c) $V_d=10$ mm/s and (d) $V_d=15$ mm/s with the wafer heated by a single lamp at $\omega=0$ rpm and $H=90$ mm for the final wafer temperature set at 140°C .

Fig. 4.28 The measured wafer temperature at selected locations during the ramp-up period for (a) $V_d=0$ mm/s, (b) $V_d=5$ mm/s, (c) $V_d=10$ mm/s and (d) $V_d=15$ mm/s with the wafer heated by a single lamp at $\omega=100$ rpm and $H=90$ mm for the final wafer temperature set at 140°C .

Fig. 4.29 The measured wafer temperature at selected locations during the ramp-up period for (a) $V_d=0$ mm/s, (b) $V_d=5$ mm/s, (c) $V_d=10$ mm/s and (d) $V_d=15$ mm/s with the wafer heated by a single lamp at $\omega=200$ rpm and $H=90$ mm for the final wafer temperature set at 140°C .

Fig. 4.30 The measured wafer temperature at selected locations during the ramp-up period for (a) $V_d=0$ mm/s, (b) $V_d=5$ mm/s, (c) $V_d=10$ mm/s and (d) $V_d=15$ mm/s with three heating lamps at $\omega=0$ rpm and $H=60$ mm for the final wafer temperature set at 200°C .

Fig. 4.31 The measured wafer temperature at selected locations during the ramp-up period for (a) $V_d=0$ mm/s, (b) $V_d=5$ mm/s, (c) $V_d=10$ mm/s and

(d) $V_d=15$ mm/s with three heating lamps at $\omega=100$ rpm and $H= 60$ mm for the final wafer temperature set at 200°C .

Fig. 4.32 The measured wafer temperature at selected locations during the ramp-up period for (a) $V_d=0$ mm/s, (b) $V_d=5$ mm/s, (c) $V_d=10$ mm/s and (d) $V_d=15$ mm/s with three heating lamps at $\omega=200$ rpm and $H= 60$ mm for the final wafer temperature set at 200°C .

Fig. 4.33 The measured wafer temperature at selected locations during the ramp-up period for (a) $V_d=0$ mm/s, (b) $V_d=5$ mm/s, (c) $V_d=10$ mm/s and (d) $V_d=15$ mm/s with three heating lamps at $\omega=0$ rpm and $H= 30$ mm for the final wafer temperature set at 200°C .

Fig. 4.34 The measured wafer temperature at selected locations during the ramp-up period for (a) $V_d=0$ mm/s, (b) $V_d=5$ mm/s, (c) $V_d=10$ mm/s and (d) $V_d=15$ mm/s with three heating lamps at $\omega=100$ rpm and $H= 30$ mm for the final wafer temperature set at 200°C .

Fig. 4.35 The measured wafer temperature at selected locations during the ramp-up period for (a) $V_d=0$ mm/s, (b) $V_d=5$ mm/s, (c) $V_d=10$ mm/s and (d) $V_d=15$ mm/s with three heating lamps heating at $\omega=200$ rpm, and $H= 30$ mm for the final wafer temperature set at 200°C .

Fig. 4.36 The measured wafer temperature at selected locations during the ramp-up period for (a) $V_d=0$ mm/s, (b) $V_d=5$ mm/s, (c) $V_d=10$ mm/s and (d) $V_d=15$ mm/s with three heating lamps heating at $\omega=0$ rpm, and $H= 90$ mm for the final wafer temperature set at 200°C .

Fig. 4.37 The measured wafer temperature at selected locations during the ramp-up period for (a) $V_d=0$ mm/s, (b) $V_d=5$ mm/s, (c) $V_d=10$ mm/s and (d) $V_d=15$ mm/s with three heating lamps heating at $\omega=100$ rpm, and $H= 90$ mm for the final wafer temperature set at 200°C .

Fig. 4.38 The measured wafer temperature at selected locations during the ramp-up period for (a) $V_d=0$ mm/s, (b) $V_d=5$ mm/s, (c) $V_d=10$ mm/s and (d) $V_d=15$ mm/s with three heating lamps heating at $\omega=200$ rpm, and $H= 90$ mm for the final wafer temperature set at 200°C .

- Fig. 4.39 The measured wafer temperature at selected locations during the ramp-up period for (a) H=30 mm, (b) H=60 mm, and (c) H=90 mm with a heating lamps heating at $\omega=0$ rpm, and $V_d=0$ mm/s for the final wafer temperature set at 140°C .
- Fig. 4.40 The measured wafer temperature at selected locations during the ramp-up period for (a) H=30 mm, (b) H=60 mm, and (c) H=90 mm with a heating lamps heating at $\omega=100$ rpm, and $V_d=0$ mm/s for the final wafer temperature set at 140°C .
- Fig. 4.41 The measured wafer temperature at selected locations during the ramp-up period for (a) H=30 mm, (b) H=60 mm, and (c) H=90 mm with a heating lamps heating at $\omega=200$ rpm, and $V_d=0$ mm/s for the final wafer temperature set at 140°C .
- Fig. 4.42 The measured wafer temperature at selected locations during the ramp-up period for (a) H=30 mm, (b) H=60 mm, and (c) H=90 mm with a heating lamps heating at $\omega=0$ rpm, and $V_d=5$ mm/s for the final wafer temperature set at 140°C .
- Fig. 4.43 The measured wafer temperature at selected locations during the ramp-up period for (a) H=30 mm, (b) H=60 mm, and (c) H=90 mm with a heating lamps heating at $\omega=100$ rpm, and $V_d=5$ mm/s for the final wafer temperature set at 140°C .
- Fig. 4.44 The measured wafer temperature at selected locations during the ramp-up period for (a) H=30 mm, (b) H=60 mm, and (c) H=90 mm with a heating lamps heating at $\omega=200$ rpm, and $V_d=5$ mm/s for the final wafer temperature set at 140°C .
- Fig. 4.45 The measured wafer temperature at selected locations during the ramp-up period for (a) H=30 mm, (b) H=60 mm, and (c) H=90 mm with a heating lamps heating at $\omega=0$ rpm, and $V_d=10$ mm/s for the final wafer temperature set at 140°C .
- Fig. 4.46 The measured wafer temperature at selected locations during the ramp-up period for (a) H=30 mm, (b) H=60 mm, and (c) H=90 mm with a heating lamps heating at $\omega=100$ rpm, and $V_d=10$ mm/s for the final

wafer temperature set at 140°C.

Fig. 4.47 The measured wafer temperature at selected locations during the ramp-up period for (a) H=30 mm, (b) H=60 mm, and (c) H=90 mm with a heating lamps heating at $\omega=200\text{rpm}$, and $V_d=10\text{ mm/s}$ for the final wafer temperature set at 140°C.

Fig. 4.48 The measured wafer temperature at selected locations during the ramp-up period for (a) H=30 mm, (b) H=60 mm, and (c) H=90 mm with a heating lamps heating at $\omega=0\text{rpm}$, and $V_d=15\text{ mm/s}$ for the final wafer temperature set at 140°C.

Fig. 4.49 The measured wafer temperature at selected locations during the ramp-up period for (a) H=30 mm, (b) H=60 mm, and (c) H=90 mm with a heating lamps heating at $\omega=100\text{rpm}$, and $V_d=15\text{ mm/s}$ for the final wafer temperature set at 140°C.

Fig. 4.50 The measured wafer temperature at selected locations during the ramp-up period for (a) H=30 mm, (b) H=60 mm, and (c) H=90 mm with a heating lamps heating at $\omega=200\text{rpm}$, and $V_d=15\text{ mm/s}$ for the final wafer temperature set at 140°C.

Fig. 4.51 The measured wafer temperature at selected locations during the ramp-up period for (a) H=30 mm, (b) H=60 mm, and (c) H=90 mm with a heating lamps heating at $\omega=0\text{rpm}$, and $V_d=0\text{ mm/s}$ for the final wafer temperature set at 200°C.

Fig. 4.52 The measured wafer temperature at selected locations during the ramp-up period for (a) H=30 mm, (b) H=60 mm, and (c) H=90 mm with three heating lamps heating at $\omega=100\text{rpm}$, and $V_d=0\text{ mm/s}$ for the final wafer temperature set at 200°C.

Fig. 4.53 The measured wafer temperature at selected locations during the ramp-up period for (a) H=30 mm, (b) H=60 mm, and (c) H=90 mm with three heating lamps heating at $\omega=200\text{rpm}$, and $V_d=0\text{ mm/s}$ for the final wafer temperature set at 200°C.

Fig. 4.54 The measured wafer temperature at selected locations during the ramp-up period for (a) H=30 mm, (b) H=60 mm, and (c) H=90 mm with

three heating lamps heating at $\omega=0$ rpm, and $V_d=5$ mm/s for the final wafer temperature set at 200°C .

Fig. 4.55 The measured wafer temperature at selected locations during the ramp-up period for (a) $H=30$ mm, (b) $H=60$ mm, and (c) $H=90$ mm with three heating lamps heating at $\omega=100$ rpm, and $V_d=5$ mm/s for the final wafer temperature set at 200°C .

Fig. 4.56 The measured wafer temperature at selected locations during the ramp-up period for (a) $H=30$ mm, (b) $H=60$ mm, and (c) $H=90$ mm with three heating lamps heating at $\omega=200$ rpm, and $V_d=5$ mm/s for the final wafer temperature set at 200°C .

Fig. 4.57 The measured wafer temperature at selected locations during the ramp-up period for (a) $H=30$ mm, (b) $H=60$ mm, and (c) $H=90$ mm with three heating lamps heating at $\omega=0$ rpm, and $V_d=10$ mm/s for the final wafer temperature set at 200°C .

Fig. 4.58 The measured wafer temperature at selected locations during the ramp-up period for (a) $H=30$ mm, (b) $H=60$ mm, and (c) $H=90$ mm with three heating lamps heating at $\omega=100$ rpm, and $V_d=10$ mm/s for the final wafer temperature set at 200°C .

Fig. 4.59 The measured wafer temperature at selected locations during the ramp-up period for (a) $H=30$ mm, (b) $H=60$ mm, and (c) $H=90$ mm with three heating lamps heating at $\omega=200$ rpm, and $V_d=10$ mm/s for the final wafer temperature set at 200°C .

Fig. 4.60 The measured wafer temperature at selected locations during the ramp-up period for (a) $H=30$ mm, (b) $H=60$ mm, and (c) $H=90$ mm with three heating lamps heating at $\omega=0$ rpm, and $V_d=15$ mm/s for the final wafer temperature set at 200°C .

Fig. 4.61 The measured wafer temperature at selected locations during the ramp-up period for (a) $H=30$ mm, (b) $H=60$ mm, and (c) $H=90$ mm with three heating lamps heating at $\omega=100$ rpm, and $V_d=15$ mm/s for the final wafer temperature set at 200°C .

Fig. 4.62 The measured wafer temperature at selected locations during the ramp-up period for (a) $H=30$ mm, (b) $H=60$ mm, and (c) $H=90$ mm with three heating lamps heating at $\omega=200$ rpm, and $V_d=15$ mm/s for the final wafer temperature set at 200°C .

Fig. 4.63 The measured wafer temperature at selected locations for the wafer Heated by three lamps arranged as Fig. 2.2(c) at $\omega=0$ rpm, $V_d=0$ mm/s and $H=60$ mm for the final wafer temperature set at 200°C

Fig. 4.64 The measured wafer temperature at selected locations for the wafer Heated by three lamps arranged as Fig. 2.2(b) at $\omega=0$ rpm, $V_d=0$ mm/s and $H=60$ mm for the final wafer temperature set at 200°C .

Fig. 4.65 The measured wafer temperature at selected locations during the ramp-up period for (a) $\omega=0$ rpm, (b) $\omega=50$ rpm, (c) $\omega=100$ rpm, (d) $\omega=150$ rpm and (e) $\omega=200$ rpm with a heating lamps heating at $H=60$ mm and $V_d=0$ mm/s for the final wafer temperature set at 200°C .

Fig. 4.66 The measured wafer temperature at selected locations during the ramp-up period for (a) $\omega=0$ rpm, (b) $\omega=50$ rpm, (c) $\omega=100$ rpm, (d) $\omega=150$ rpm and (e) $\omega=200$ rpm with a heating lamps heating at $H=60$ mm and $V_d=15$ mm/s for the final wafer temperature set at 200°C .

Fig. 4.67 The measured wafer temperature at selected locations during the ramp-up period for (a) $V_d=15$ mm/s, (b) $V_d=16$ mm/s, (c) $V_d=17$ mm/s and (d) $V_d=18$ mm/s with a heating lamp at $\omega=170$ rpm and $H=90$ mm for the final wafer temperature set at 140°C .

NONMENCLTURE

D_{cu}	diameter of copper disk, (mm)
D_w	diameter of wafer, (mm)
H	distance between wafer and lamp, (mm)
N	number of lamp
T_a	ambient temperature, ($^{\circ}C$)
T_{mean}	mean temperature, ($^{\circ}C$)
T_{set}	set temperature of produce , ($^{\circ}C$)
V_d	translating speed of wafer, (mm/s)
ΔT_{max}	maximum temperature difference, ($^{\circ}C$)
ω	speed of rotating susceptor (rpm)
Φ	wafer temperature nonuniformity (%)



CHAPTER 1

INTRODUCTION

1.1 Motivation of the Present Study

Following the quick technological progress in the growth of semiconductor thin crystal films, the line widths in IC (Integrated Circuits) chips have been reduced considerably and we can fabricate sophisticated circuits for multimedia, communication and computing applications. Thus, Ultra Large-Scale Integrated (ULSI) circuits are widely used in information technology and computer system. Among various growth technologies single-wafer rapid thermal processing (RTP), which uses thermal energy from lamps to directly heat the wafer, has emerged as a key manufacturing technique for semiconductor device fabrication. In addition, the low thermal mass of a single wafer (as compared to a batch processing) allows the RTP system to rapidly increase wafer temperature [1]. This can be ascribed to the fact that the rapid thermal processing not only allows for minimization of processing and cycle times but also enables a significant reduction in the thermal budget. In many practical applications, RTP has been proven to be a key technology in single wafer processing due to the smaller thermal budget and higher throughput [2&3]. In order to obtain good thin film properties, temperature uniformity of the wafer during the processing is important in steady operation as well as in the transient ramp-up and ramp-down stages. The improvement of the wafer temperature uniformity during ramp-up and ramp-down stages by adding a high thermal conductivity copper plate right below the wafer was illustrated by Yin et al.[4]. Over the past, several methods have been attempted to improve the wafer temperature uniformity, such as the better arrangement of lamps, optimal power control of lamps, wafer rotation, etc. In the

present study an experiment is conducted to investigate the possible improvement of the wafer temperature uniformity by the wafer rotation and/or translation.

1.2 Literature Review

It has been identified by Dilhac et al.[5] that in a RTP processor temperature nonuniformity on wafer surface is caused by nonuniform light illumination from heating lamps, radiation from the wafer, thermal radiation absorption, larger heat loss from the wafer edge than from center of wafer, and gas cooling. For heat loss at the wafer edge, Öztürk et al.[6] show that some techniques have been employed to compensate for the large heat losses at the wafer edge. These include: (a) alter the center of the furnace windows so that the light entering here is scattered to some extent and less light reaches the center of the wafer than does the edge; (b) supply higher power to the outer lamps to increase the radiation at the edge of the wafer; (c) use a susceptor of some kind which effectively makes the wafer appear larger than it actually is; (d) employ a mirror system to focus or reflect more light on the wafer edges.

The improvement in the wafer temperature uniformity has been attempted by means of adopting new arrangement of heating lamps, better chamber geometry, independent control of lamp power, and feedback control. The important aspects associated with the new arrangement of heating lamps for RTP include thermal environment, power efficiency, spectral and spatial distribution of power, transient response, and reliability[7]. Timans[8] and Yoo[9] used linear arrays of lamps to heat the wafer. Here the linear lamp arrays mean that the different groups of lamps are gathered together as a zone. Sorrell et al.[10] moved further to install flat reflectors for the lamps. They then found that curved reflectors could focus the radiation on a small area and therefore improved the uniformity of wafer temperature. A symmetric

arrangement tungsten halogen lamps were proposed by Lord [11] and Gyurcsik et al. [12]. Wong et al.[13] add quartz isolation tube between lamps and wafer to increase thermal uniformity of wafer. Furthermore, Hirasawa et al. [14] and Balakrishnan and Edgar [15] used rod-type lamps with tungsten filament coils in quartz tubes. The tungsten-halogen lamp tubes were also used by Liu et al. [16]. They examined the wafer temperature uniformity influenced by the distance between the lamps and the wafer. The results showed that at a longer distance the wafer temperature was more uniform. But the edge of the wafer was found to have more heat loss than the center, which would cause some temperature nonuniformity on the surface of the wafer. In addition, Cho et al.[17] arranged linear halogen lamps into a hexagonal shape and the hexagonal-shaped lamp groups were stacked vertically. They showed that a temperature difference within 1.5°C could be achieved over a 6- in wafer at steady state. The advantage of the hexagonal-shaped lamp banks is that it allows us to achieve excellent temperature uniformity without any angular dependence over wafer. Stuber et al. [18] installed a lower zone heating lamps to compensate the heat loss at the periphery of the wafer. Besides, Poscher and Theiler [19] suggested to use two halogen lamp heating units mounted respectively above and below the wafer surface. The wafer temperature uniformity was improved substantially.

Haung et al. [20], Zöllner et al.[21], Chen et al.[22], Fukada et al.[23] and Urban et al.[24] studied a cold-wall RTP system heated with three concentric lamp rings. The concentric arrangement of lamps was noted to produce more uniform illumination on the surface of the wafer and hence improved the wafer temperature uniformity. Similar lamp arrangement was adopted by Apte and Saraswat [25] and Norman [26] and Choi et al. [27]. The lamp heating unit employed by Yin et al.[4] contains two lamp rings with focusing reflectors. The wafer heated with the focusing reflectors was at a more uniform temperature. The wafer heated by the concentric

rings of lamps still faces with the larger heat loss from the edge of the wafer (Cho et al.[28], Liu et al. [29], Park et al. [30], Norman [31], and Gyugyi and Roy[32]). To compensate the larger heat loss from the wafer edge, Jan and Lin[33] and Theodoropoulou et al.[34] installed one concentric circular lamp zone around the wafer edge. Rotating the wafer was also found to enhance the wafer temperature uniformity by Poscher and Theiler [19]. The tungsten halogen lamp is often used in RTP systems. Öztürk et al.[6] proposed to use arc lamps for RTP systems. The advantages of using the arc lamps are that they are much more powerful than the tungsten halogen lamps and the emission spectrum of an arc lamp extends from $\sim 0.2 \mu\text{m}$ to $\sim 0.4 \mu\text{m}$. This emission spectrum range is close to the absorption spectrum range of the silicon wafer. A disadvantage of the arc lamp is its relatively high price compared to the tungsten halogen lamp. In addition, Lee et al.[35] used concentric Si rings on a planar quartz or Si susceptor to improve the wafer temperature distribution. It was noted that although the use of a guard ring can improve the wafer temperature uniformity, significant temperature gradient can still exist in the ring causing it to become warped.

The control of lamp power is also considered to be rather important in improving the temperature uniformity of the wafer surface. Schaper et al.[36] proposed three necessary conditions to achieve uniform and repeatable manufacturing for lamp power control for RTP systems, namely , the lamp heating unit (a) should be capable of manipulating the spatial distribution of radiative energy flux to the wafer in real-time, (b) must have repeatable noninvasive temperature sensing that is insensitive to the change in the wafer surface conditions and lamp power fluctuations, and (c) needs to possess a flexible multivariable control system that can push the RTP lamp and sensing equipment to its limit of performance in terms of temperature uniformity and repeatability. Gyurcsik et al.[1] suggested three elements in a real-time control of

RTP systems: (1) real-time absolute temperature control, (2) real-time temperature uniformity control, and (3) real-time temperature correction. Two basic control methods are normally employed. The one without using the feedback signals from the real time wafer temperature measurement is named as the open-loop control and the other obviously is called the close-loop control. At first, only one control point with single input single output (SISO) was employed and it is named as the scalar control. But this often results in a large experiment error. Later, the multiple-input multiple-output (MIMO) control algorithm was used to enhance the accuracy of the control which is the so called a multivariable control [31]. Besides, the wafer temperature nonuniformity caused by the larger heat loss from the edge of the wafer was improved by raising the power level of the outer lamp zones[37]. Independent control of each lamp zone was shown to be effective for the wafer temperature uniformity by Zöllner et al. [21] and Huang et al. [20], Choi et al.[27] , Yin et al.[4] , Park et al.[30], and Urban et al.[24]. Furthermore, Apte and Saraswat [25] and Chen et al.[22] used a multivariable dynamical control of the lamp power by dynamically controlling the multiple inputs to the lamps. Four control strategies were examined by Yu et al.[38], namely, the open-loop control , pyrometer control , pyrometer control with corrected emissivity , programmed open loop control (POLC). The results showed that the use of POLC led to a best wafer temperature uniformity. Sorrell et al.[39] tested a feedback control algorithm combining with proportional (P), proportional and differential (PD), and complete proportional, differential, and integral (PDI) controls. The conventional PID (Proportional-Integral-Derivative) control was used by Gyurcsik [12] and Hirasawa et al.[40]. In addition, Hirasawa et al. showed that when heating power was properly controlled the average temperature distribution in the wafers during heating could be maintained within $\pm 1^{\circ}\text{C}$ at 1000°C . Finally, Kersch and Schafbauer [41] investigated conventional PID control, scheduled

PID control, and optimal power control for the lamp power distribution. The total lamp power was controlled in the conventional PID control and scheduled PID control. But the individual lamp power was adjusted in the optimal power control. They showed that the optimal power control gave the best results. Lin and Jan [42] combined a least square feedforward controller with an output feedback proportional plus integral (PI) controller. A high-order nonlinear model describing the temperature dynamics of a RTP system was used in a feedforward controller design by Emami-Naeini et al. [43]. The result showed that the wafer temperature nonuniformity could be within 1-2 °C. A linear model based on a desired uniform steady-state temperature was used for the design of the multiinput-multioutput PI controller. Cho and Kailath[44] indicated that a lamplight interference elimination could increase the wafer temperature uniformity.

1.3 Objective and Scope of present study

The purpose of the present study is to investigate how the rotation and/or linear translation of the wafer affect the temperature uniformity of a lamp heated silicon wafer during the ramp-up period. The effects of the susceptor rotation and translation speeds and the lamp-to-wafer separation distance on the wafer temperature uniformity will be experimentally examined for different lamp power levels.

In this study the wafer rotation intends to improve the axisymmetric and circumferential temperature uniformity of the wafer. The problem of higher thermal radiation from the lamps at the geometric center of the wafer is expected to be reduced to a certain degree by the linear translation of the wafer.

CHAPTER 2

EXPERIMENTAL APPARATUS AND PROCEDURES

In order to investigate the effects of the wafer rotation and/or translation on the wafer temperature uniformity, we build a simplified RTP system with a single silicon wafer heated by lamps to simulate that encountered in a real rapid thermal processing.

2.1 Experimental Apparatus

The experimental apparatus established in the present study is schematically shown in Fig. 2.1. The system is an experimental, simplified lamp heated, single wafer rapid thermal processor designed mainly to study how the rotating and translating motions of the wafer affect the wafer temperature uniformity during the ramp-up stage. The system consists of six major parts: (1) processing chamber, (2) heating lamp unit, (3) temperature measurement and data acquisition unit, (4) control unit, (5) rotation and translation unit, and (6) susceptor unit. They are described briefly in the following.

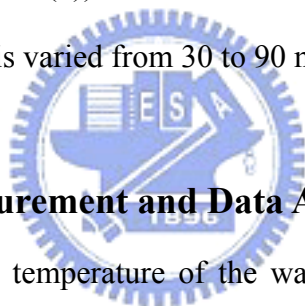
2.1.1 Processing Chamber

The processing chamber of the present experimental processor is chosen to be rectangular in shape and is 570 mm long, 300 mm wide and 560 mm high. Its sidewall is made of 2 mm thick stainless steel plate acting as the reflecting surface for the light from the lamps and the shield to the light. An 8-in actual silicon wafer is used in the experiment, which is fixed on a susceptor of 240 mm in diameter and 5 mm in thickness. The susceptor is connected to a circular rod which is rotated by a motor. Five T-type thermocouples are stuck on the back surface of the wafer at selected

locations to measure the temperature variations over the wafer.

2.1.2 Heating Lamp Unit

The lamp-heating unit consists of one or three lamps, a DC power supply and a reflection plate. The number of lamp is varied in this experiment intending to change the power level delivered to the wafer. The lamps provide the thermal radiative energy to the wafer. More specifically, we use 1000W & 120V OSRAM halogen photo optic lamps with a flat reflector. The power input to each lamp can be automatically or non-automatically adjusted in real time using variable resistance circuits for optimal wafer temperature uniformity. The diagram of the heating lamp arrangement is shown in Fig. 2.2. Note that two different arrangements are tested for the heating unit including three lamps (FIG. 2.2(b)). The vertical distance from the lamps to the geometric center of the wafer is varied from 30 to 90 mm.



2.1.3 Temperature Measurement and Data Acquisition Unit

As mentioned above, the temperature of the wafer is measured by five T-type thermocouples at selected locations on the backside of the wafer. The detection locations are schematically indicated in Fig. 2.3. Note that the five thermocouples are positioned at two concentric circles at a radial interval around 5 cm. A 20-channel data logger (YOKOGAWA DA-100) along with a personal computer are employed to acquire and process the data from various transducers. The voltage signals from the thermocouples are converted to temperature by the internal calibration equation in the computer and are displayed on the screen simultaneously.

2.1.4 Control Unit

To control the input power to the lamps, a PID control algorithm is used. Every lamp is controlled by a microprocessor temperature controller. The apparatus not only

can control the lamp power directly but also can accept the measured temperature signal at the feedback point on the wafer surface. The signal is employed in a PID control algorithm to control the lamp power for a given preset average temperature of the wafer surface. Then the feedback control points and the number of the lamps to be used are decided. The locations of the feedback control points are schematically shown in Fig. 2.4.

2.1.5 Rotation and Translation Unit

The wafer rotation is driven by a stepper motor (Fig. 2.5). A slipping is used to allow the thermocouples to measure the temperature of the rotating wafer. The wafer also moves along a straight line. This translating motion of the wafer is also driven by a motor. The translating speed and distance are controlled by a trimming switch(Fig. 2.6).



2.1.6 Susceptor Unit

The susceptor of the present experimental processor is chosen to be in the form of a concentric disk of 160-mm inside diameter, 240-mm outside diameter and 5-mm in thickness. The susceptor is made of stainless steel and the susceptor is then fixed on a copper plate and both are leveled horizontally. The copper plate is connected to a circular rod which is rotated by a motor. To support the wafer, three conic pins are fixed on the susceptor (Fig. 2.7). The pins are made of quartz to reduce heat loss from the wafer to the susceptor through the pins. To avoid the wafer to fly away during the high speed rotation, four slender cylindrical pins (5-mm in diameter and 15-mm in height) are also installed on the susceptor, as shown in Fig. 2.7.

2.2 Experimental Procedures

Before the experiment, the wafer surface is at the room temperature. The test starts with the lamps turned on at the chosen power level (normally 80% of full power). Besides, the rotation and translation speeds of the wafer, lamp-to-wafer separation distance, and the translation distance of the wafer are kept at the selected values. Then the data acquisition unit begins to record the data from various transducers until the wafer reaches a preset average temperature.



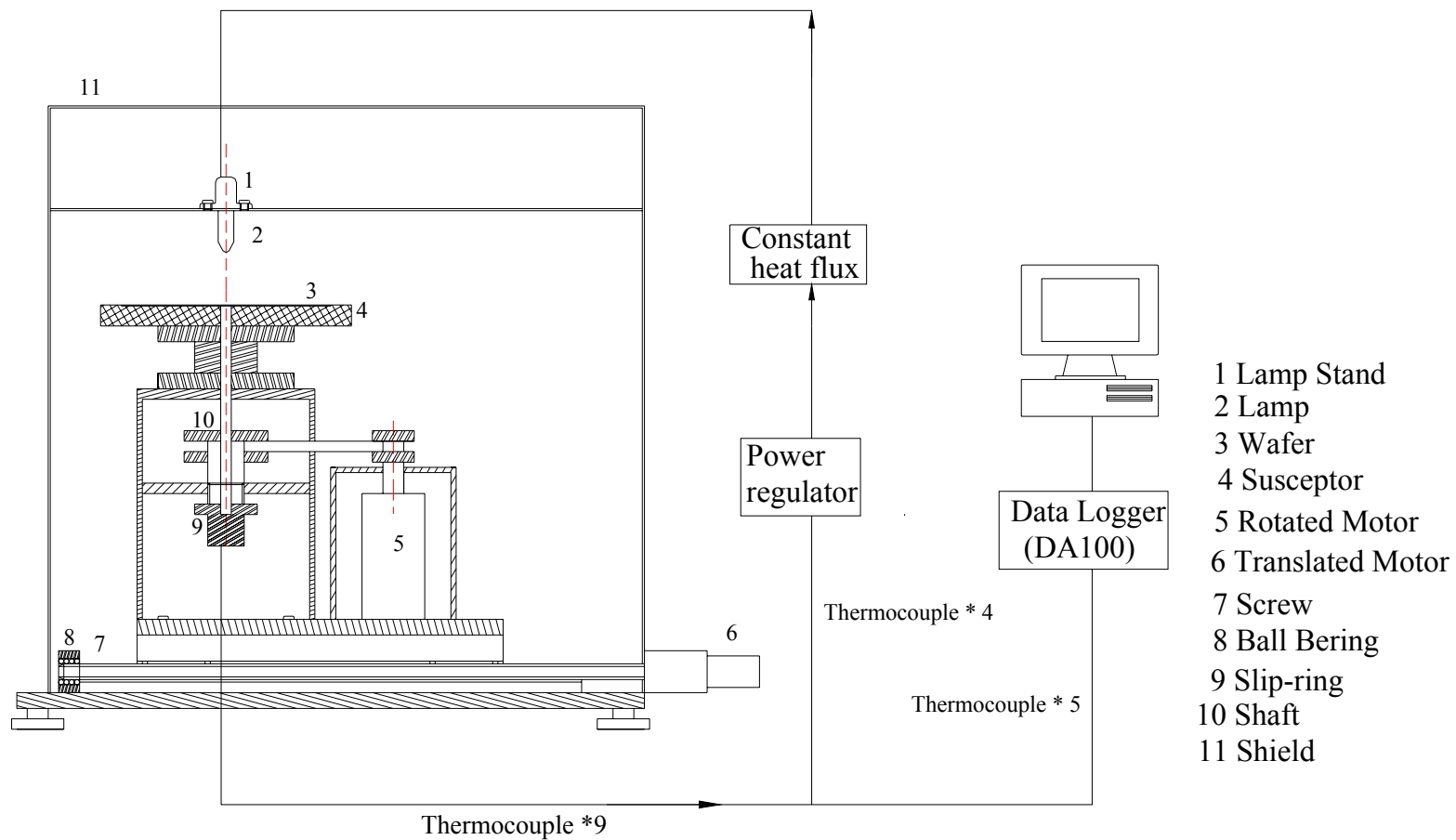


Fig. 2.1 Schematic diagram of the experiment apparatus

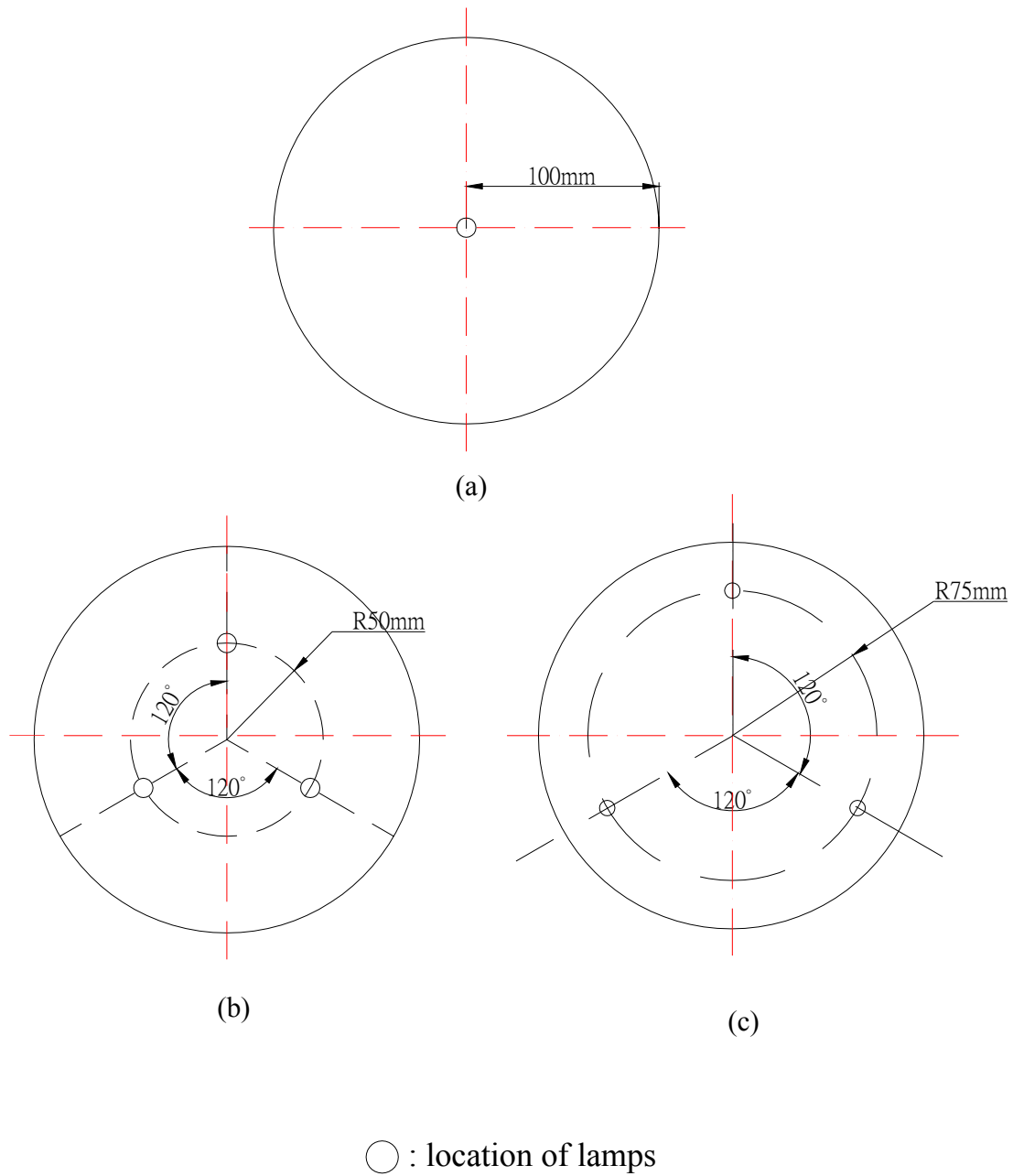


Fig. 2.2 Schematic of the heating lamp arrangement : (a)one lamp, (b)three lamps-first arrangement, and (c)three lamps-second arrangement.

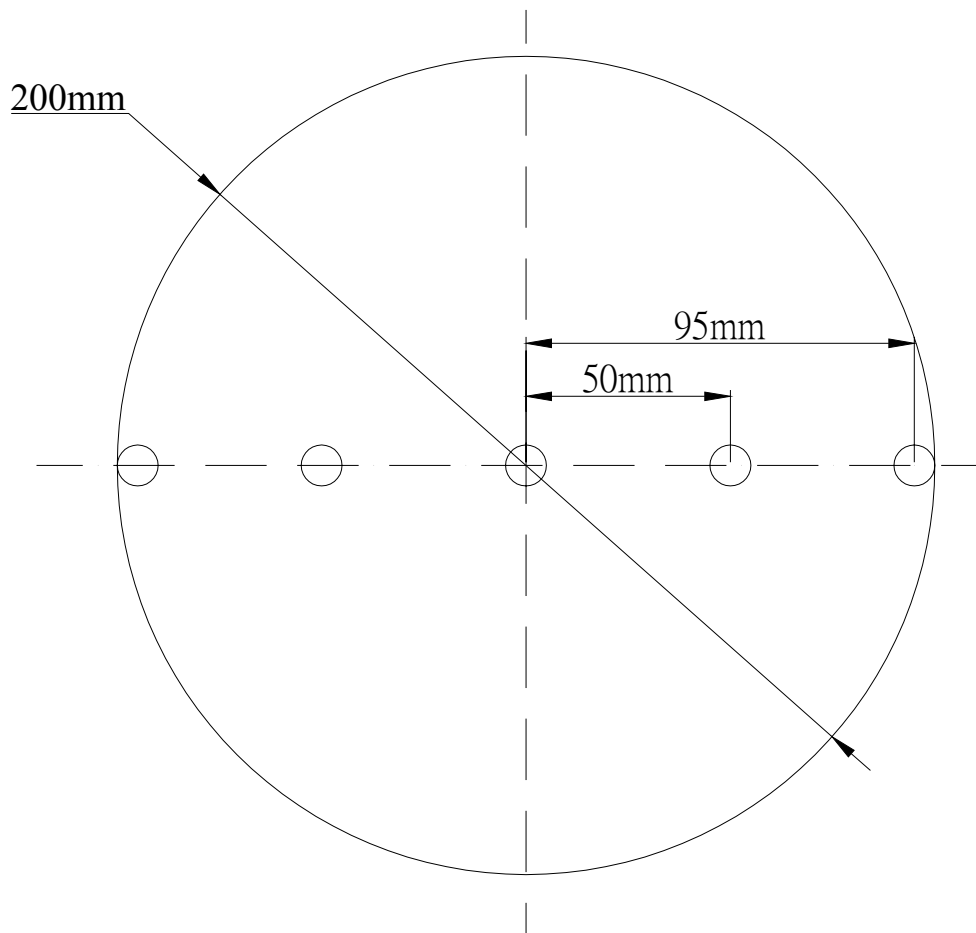


Fig. 2.3 Schematic of the selected detection locations for the wafer temperature measurement.

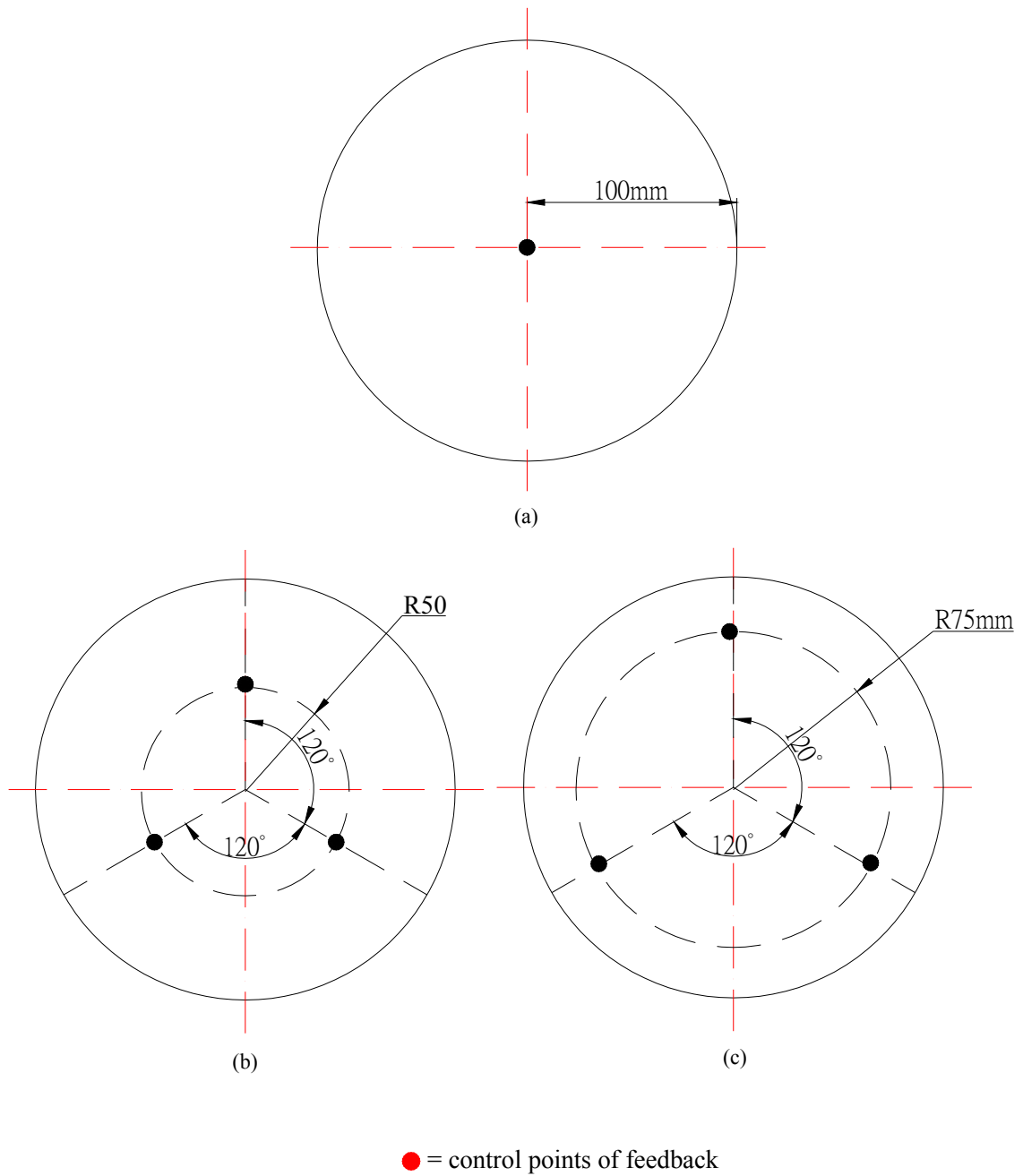


Fig. 2.4 Schematic of the feedback control points on the wafer with (a) one lamp, (b) three lamps-first arrangement, and (c) three lamps-second arrangement.

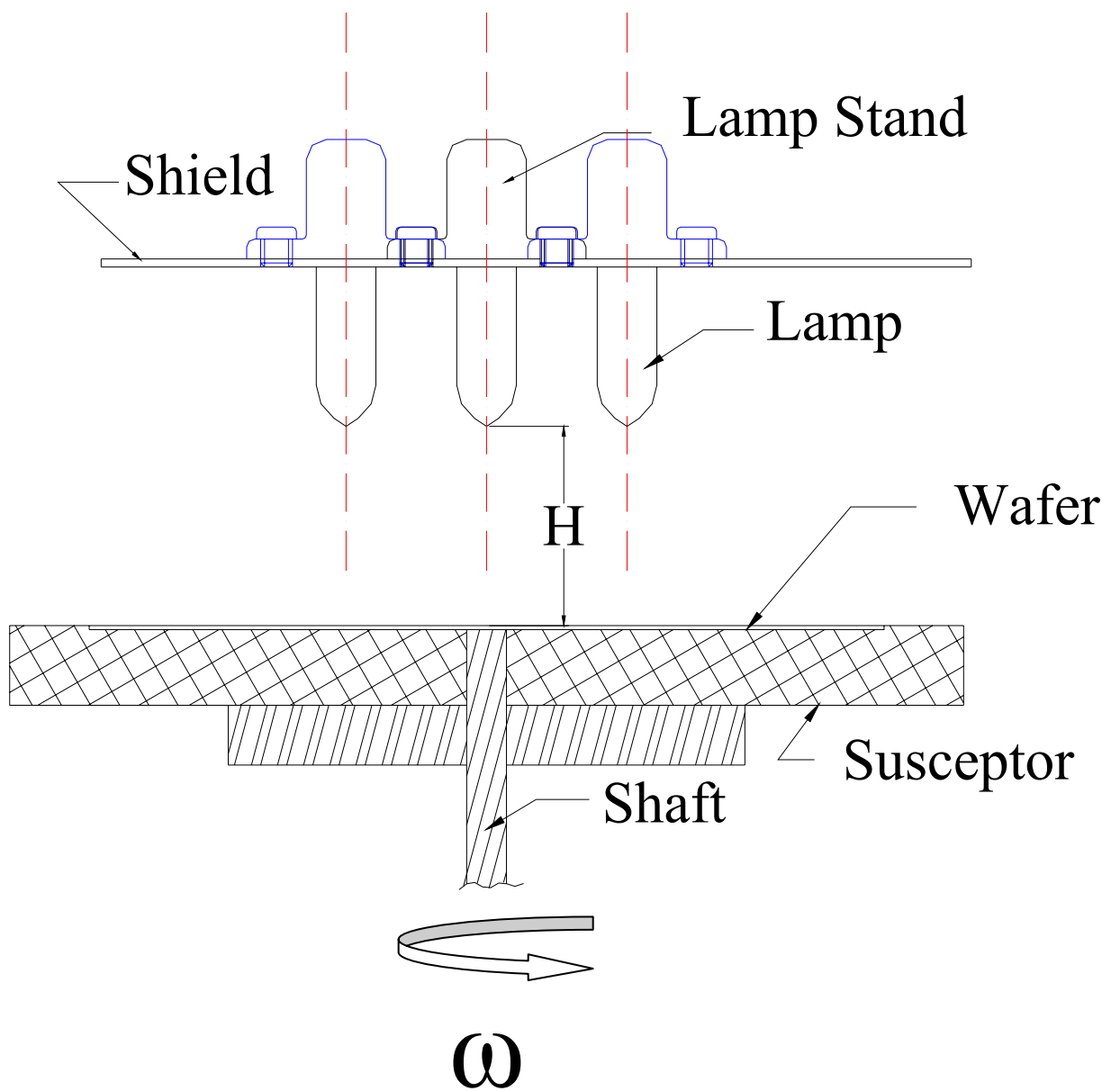


Fig. 2.5 Schematic diagram of the rotation unit

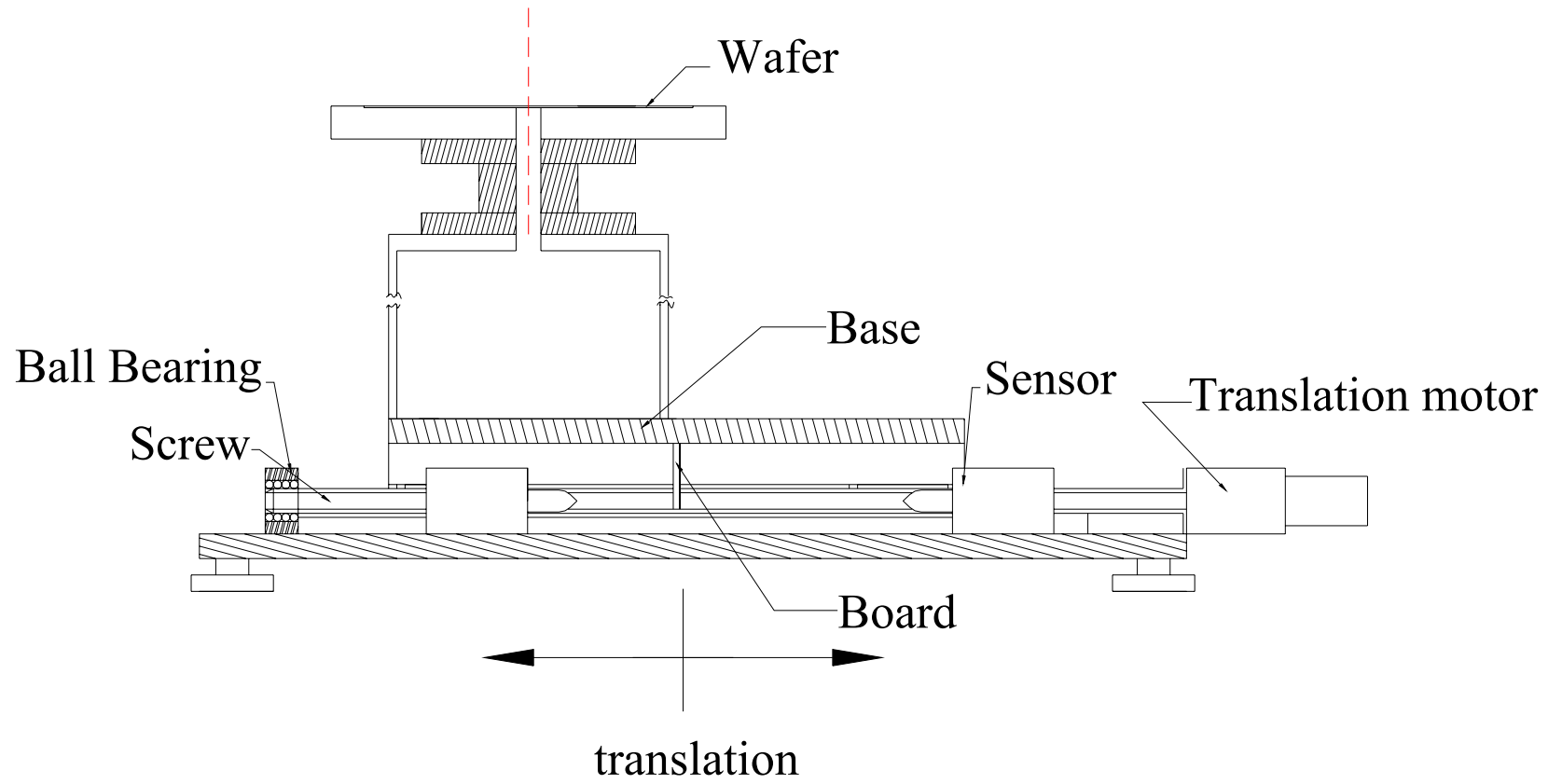
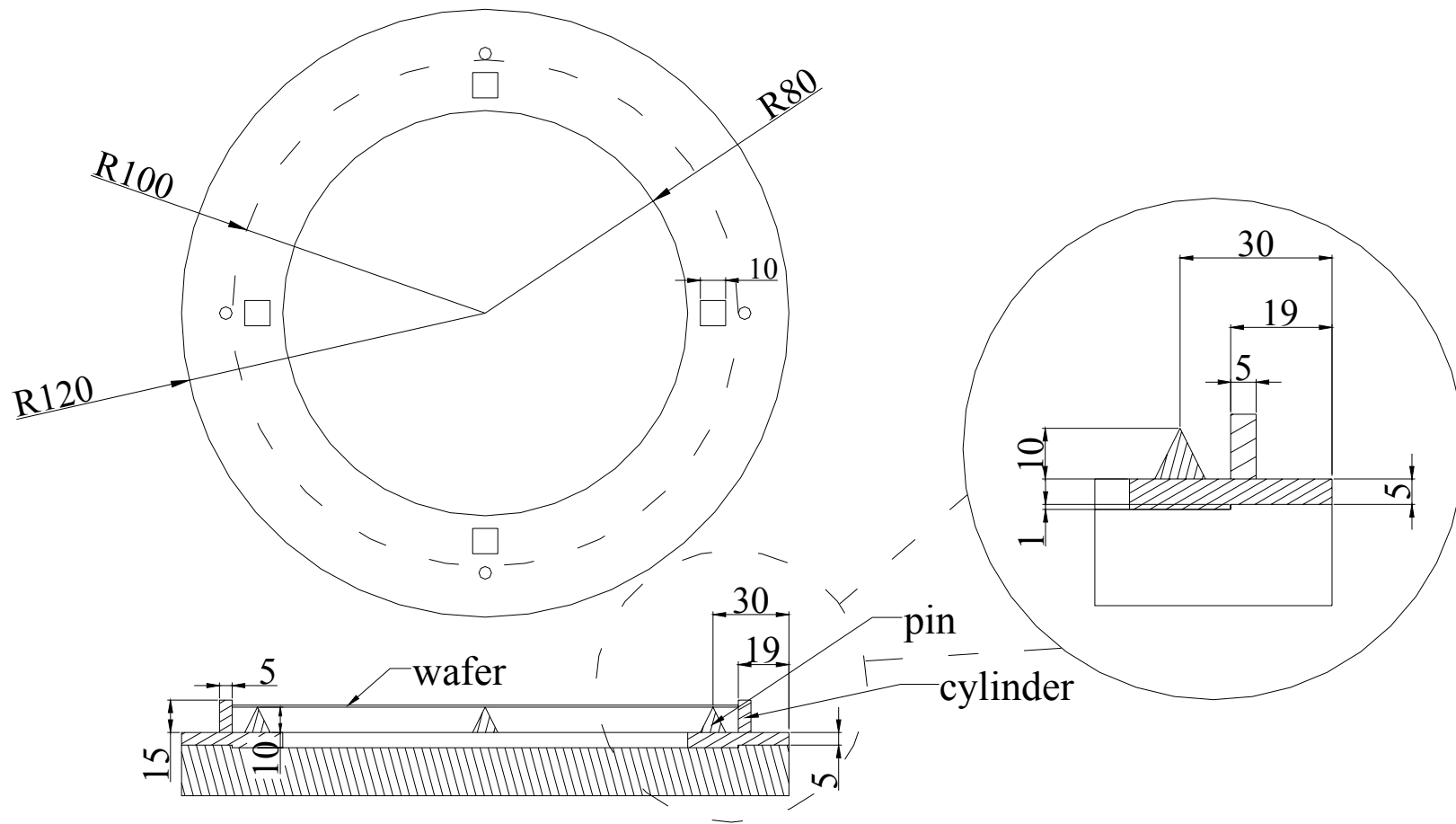


Fig. 2.6 Schematic diagram of the translation unit



Unit:mm

Fig. 2.7 Schematic diagram of the susceptor



CHAPTER 3

UNCERTAINTY ANALYSIS

An uncertainty analysis is carried out here to estimate the uncertainty levels in the experiment. Kline and McClintock [45] proposed a formula for evaluating the uncertainty in the result F as a function of independent variables, X_1, X_2, \dots, X_n ,

$$F = F(X_1, X_2, X_3, \dots, X_n) \quad (3.1)$$

The absolute uncertainty of F is expressed as

$$\delta F = \left\{ \left[\left(\frac{\partial F}{\partial X_1} \right) \delta X_1 \right]^2 + \left[\left(\frac{\partial F}{\partial X_2} \right) \delta X_2 \right]^2 + \left[\left(\frac{\partial F}{\partial X_3} \right) \delta X_3 \right]^2 + \dots + \left[\left(\frac{\partial F}{\partial X_n} \right) \delta X_n \right]^2 \right\}^{1/2} \quad (3.2)$$

and the relative uncertainty of F is

$$\frac{\delta F}{F} = \left\{ \left[\left(\frac{\partial \ln F}{\partial \ln X_1} \right) \left(\frac{\delta X_1}{X_1} \right) \right]^2 + \left[\left(\frac{\partial \ln F}{\partial \ln X_2} \right) \left(\frac{\delta X_2}{X_2} \right) \right]^2 + \dots + \left[\left(\frac{\partial \ln F}{\partial \ln X_n} \right) \left(\frac{\delta X_n}{X_n} \right) \right]^2 \right\}^{1/2} \quad (3.3)$$

If $F = X_1^a X_2^b X_3^c \dots$, then the relative uncertainty is

$$\frac{\delta F}{F} = \left[\left(a \frac{\delta X_1}{X_1} \right)^2 + \left(b \frac{\delta X_2}{X_2} \right)^2 + \left(c \frac{\delta X_3}{X_3} \right)^2 + \dots \right]^{1/2} \quad (3.4)$$

Where $(\partial F / \partial X_i)$ and δX_i are, respectively, the sensitivity coefficient and uncertainty level associated with the variable X_i . The values of the uncertainty intervals δX_i are

obtained by a root-mean-square combination of the precision uncertainty of the instruments and the unsteadiness uncertainty, as recommended by Moffat [46]. The choice of the variable X_i to be included in the calculation of the total uncertainty level of the result F depends on the purpose of the analysis. The uncertainties for the chosen parameters are calculated as follows:

(1) Uncertainty of the measured temperature difference, $\Delta T = T_w - T_a$

$$\delta(T_w - T_a) = [(\delta T_w)^2 + (\delta T_a)^2]^{1/2} \quad (3.5)$$

(2) The dependence of the air properties k , μ , and ν on the temperature (T in K) is

[47]

$$k = 1.195 \times 10^{-6} T^{1.6} / (T + 118)$$

$$\mu = 1.448 \times 10^{-6} T^{1.5} / (T + 118) \quad (3.6)$$

$$\nu = \mu / \rho$$

The uncertainties of the properties are

$$\begin{aligned} \frac{\delta k}{k} &= \frac{T}{k} \frac{\partial k}{\partial T} \frac{\delta T}{T} \\ \frac{\delta \rho}{\rho} &= \frac{T}{\rho} \frac{\partial \rho}{\partial T} \frac{\delta T}{T} \\ \frac{\delta \mu}{\mu} &= \frac{T}{\mu} \frac{\partial \mu}{\partial T} \frac{\delta T}{T} \end{aligned} \quad (3.7)$$

(3) Uncertainty of Rayleigh number, Ra ,

$$Ra = \frac{g\beta(T_w - T_a)H^3}{\alpha\nu} = \frac{g\beta\Delta T H^3}{\alpha\nu} \quad (3.8)$$

$$\frac{\delta Ra}{Ra} = \left[\left(\frac{\delta g\beta}{g\beta} \right)^2 + \left(3 \frac{\delta H}{H} \right)^2 + \left(\frac{\delta \Delta T}{\Delta T} \right)^2 + \left(\frac{\delta \alpha}{\alpha} \right)^2 + \left(\frac{\delta \nu}{\nu} \right)^2 \right]^{1/2} \quad (3.9)$$

The results from this uncertainty analysis are summarized in Table .3.1.

Table 3.1 Summary of uncertainty analysis.

Parameters	Uncertainty
H	± 0.001 m
D	± 0.01 m
ω	± 5 rpm
D_w (m)	± 0.00005 m
$T_w, \Delta T_{\max}$ ($^{\circ}\text{C}$)	$\pm 0.3^{\circ}\text{C}$
$\Delta T(\%)$	0.1%



CHAPTER 4

RESULTS AND DISCUSSION

Selected data obtained in the present study are presented in the following to show how the wafer rotation, wafer translation and lamp-to-wafer separation distance level affect the silicon wafer temperature uniformity during the ramp-up period for the different power levels. In the experiment the rotation speed of wafer ω is varied from 0 to 200 rpm (revolutions per minute), and the lamp-to-wafer separation distance H is fixed at 30 mm, 60 mm or 90 mm with the translating speed of the wafer V_d varied from 0 to 15 mm/s. The wafer is heated by one or three lamps. To signify the improvement in the wafer temperature uniformity by the wafer rotation and translation, we introduce a wafer temperature nonuniformity function Φ based on the reduction in the maximum detected temperature difference on the wafer. The function is defined as

$$\Phi = \left(1 - \frac{\Delta T_{\max}}{\Delta T_{\max,0}} \right) * 100\% \quad (4.1)$$

where ΔT_{\max} is the detected maximum temperature difference over the wafer during the ramp-up period for a given case and the subscript “o” denotes the condition of $\omega = 0$ rpm and $V_d = 0$ mm/s. Specifically, the maximum temperature difference ΔT_{\max} is chosen as the difference between the measured maximum wafer temperature and the average measured wafer temperature at all detection points on the wafer. Note that the instant of time when the lamps are turned on is designated as time $t = 0$. The wafer is heated until it reaches a preset average temperature. To simplify the test procedures, we choose to employ the average measured wafer temperature as the target

temperature level for the lamp heating period. For the wafer heated by one lamp the target is 140 °C. While for the wafer heated by three lamps the target temperature is raised to 200 °C. Typical measured time variations of the temperature at the geometric center of the wafer are shown in Fig. 4.1 and Fig. 4.2, respectively, for the wafer heated by one lamp and three lamps. The ramp-up period ranges from 100 to 500, seconds depending on the input power and H.

4.1 Effects of Lamp Power Level on Wafer Temperature Nonuniformity

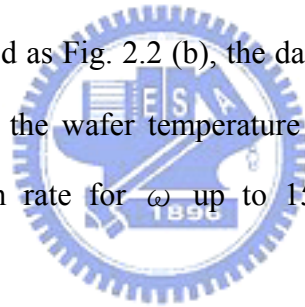
As already mentioned above, the number of lamps used in this experiment reflects the level of the power input to the wafer. The power level is expected to be an important factor for the wafer temperature uniformity. Thus before examining the effects of the wafer rotation and translation, the influences of the power level on the wafer temperature uniformity are discussed. At first, selected data from the wafer temperature measurements for the case with a single heating lamp and no wafer rotation and translation ($\omega=0$, $V_d=0$) are shown in Fig. 4.3. The results indicate that in the initial stage of the ramp-up period the maximum temperature difference among the temperature detection locations is low. For example, at $t=20$ sec the maximum temperature difference ΔT_{\max} is 3.6 °C (Fig. 4.3(a)) and at this instant of time the average wafer temperature T_{mean} is also low at 55.6 °C, indicating that we have relatively small temperature nonuniformity at this early stage of wafer heating. But slightly later at $t=40$ sec the maximum temperature difference increases substantially to 7.1 °C with $T_{\text{mean}}=85.1$ °C (Fig. 4.3(b)). A further increase in ΔT_{\max} is noted for the continuing heating up of the wafer with time. At $t=81$ sec we have a relatively large temperature nonuniformity with $\Delta T_{\max}=8.6$ °C (Fig. 4.3(d)). We also note that the temperature is higher in the region near the geometric center of the wafer and

lower in the region near the wafer edge, implying the larger heat loss from the wafer edge. Besides, near the geometric center the wafer receives more thermal radiation from the lamp. Similar trend is noted for other cases shown in Fig. 4.4 for the wafer heated by three lamps at the same H , ω and V_d . Moreover, the wafer temperature nonuniformity is also highest in the final stage of the wafer ramp-up process. This obviously results from the fact that the wafer temperature near the geometric center rises at a faster rate than the wafer edge. For the wafer heated by three lamps arranged as Fig. 2.2(b) (Fig. 4.4), the maximum temperature difference across the wafer is significantly higher, reflecting the higher power input to the wafer. However, at this higher power input the wafer is ramped up quicker.

4.2 Effects of Wafer Rotation Speed on Wafer Temperature Uniformity

The temperature uniformity of the wafer affected by the rotation rate of the wafer is shown in Fig. 4.5 by presenting the measured wafer temperature at selected locations when the target temperature of the wafer heated by one lamp reaches $140\text{ }^\circ\text{C}$ for various ω for $H=30\text{ mm}$ and $V_d=0\text{ mm/s}$. At $\omega=0\text{ rpm}$, the measured maximum temperature difference across the wafer is $8.6\text{ }^\circ\text{C}$ and Φ defined in Eq.(4.1) is equal to 0% (Fig. 4.5(a)) and at this instant of time the mean wafer temperature $T_{\text{mean}} = 133.3\text{ }^\circ\text{C}$. For the rotational speed raised slightly to 50 rpm the maximum temperature difference across the wafer reduces to $7.7\text{ }^\circ\text{C}$ and hence the temperature nonuniformity is reduced by 10.5% when compared with that for $\omega=0\text{ rpm}$ (Fig.4.5 (b)). A further reduction in ΔT_{max} is noted for a continuing increase in the rotational speed of the wafer. At $\omega=150\text{ rpm}$ we have a still smaller temperature nonuniformity with $\Delta T_{\text{max}} = 6.5\text{ }^\circ\text{C}$ and the wafer temperature nonuniformity is reduced by 24.4% (Fig. 4.5(d)). For a further increase of the rotational speed of the

wafer to 200 rpm ($\omega=200$ rpm), we have $\Delta T_{\max} = 7.7$ °C and the wafer temperature uniformity becomes worse with $\Phi = 10.5\%$ (Fig. 4.5(e)). In other words the wafer temperature nonuniformity increases as ω is raised from 150 to 200 rpm. From the results in Fig. 4.5 the temperature uniformity of the wafer improves with increasing rotation speed of the susceptor before ω reaches 150 rpm. Moreover, the results also manifest that the symmetry of the wafer temperature distribution can be somewhat improved by increasing the rotational speed of the wafer. The measured data for other H and V_d shown in Figs. 4.6 - 4.12 also exhibit a similar trend for the variation of the wafer temperature uniformity with the wafer rotation rate. Note that for case with H = 60.0 mm, $\omega = 150$ rpm and $V_d = 15$ mm/s the wafer temperature uniformity can be improved up to 66.2% , as evident from the results in Fig. 4.12(d). When the wafer is heated by three lamps arranged as Fig. 2.2 (b), the data given in Fig. 4.13 – 4.20 also indicate that improvement in the wafer temperature uniformity can be obtained by increasing the wafer rotation rate for ω up to 150 rpm. For $\omega > 150$ rpm an opposite effect is noted.



4.3 Effects of Wafer Translation on Wafer Temperature Uniformity

Selected data are presented in Figs. 4.21 – 4.29 to illustrate the wafer temperature uniformity affected by the translation of the wafer heated by a single lamp. Figure 4.21 shows that at $\omega = 0$ rpm and H = 60 mm a better wafer temperature uniformity is obtained at a higher wafer translation speed. Specifically, at $V_d = 15$ mm/s the wafer temperature nonuniformity can be reduced by 24.6% when compared with that at $\omega=0$ and $V_d=0$. Note that the wafer translation exhibits a pronounced effect on the wafer temperature uniformity at the higher wafer rotation rate of 100 rpm (Fig. 4.22). A reduction of 58.5% in the wafer temperature nonuniformity results for $V_d = 15$ mm/s (Fig. 4.22(d)). At an even higher ω of 200

rpm the wafer temperature uniformity is also better at a higher V_d . But the degree of improvement is not so high when compared with that for $\omega = 100$ rpm. (Fig. 4.23) The results for $H = 30$ mm & 90 mm given in Figs. 4.24 – 4.29 also show a similar trend.

When the wafer is heated by three lamps, the wafer translation can also improve the wafer temperature uniformity noticeably, as evident from the data given in Figs. 4.30 – 4.38. But the degree of the wafer temperature uniformity is slightly less when compared with the cases of a single lamp heating. This obviously results from the higher power level for the wafer heated by three lamps.

4.4 Effects of Lamp-to-Wafer Separation Distance on Wafer Temperature Uniformity

The results presented in the previous sections clearly indicate that the lamp-to-wafer separation distance is an important factor in influencing the wafer temperature uniformity and hence needs to be examined. This is illustrated in Figs. 4.39 – 4.62 by presenting the data for various H at fixed ω and V_d for the wafer heated by a single lamp and by three lamps. The results distinctly show that increasing lamp-to-wafer separation distance can improve the wafer temperature uniformity to a significant degree. For instance, at $\omega = 0$ rpm and $V_d = 0$ mm/s the wafer temperature nonuniformity is reduced by 59.3% when H is increased from 30 to 90 mm for the wafer subjected to one lamp heating (Fig. 4.39). At a high ω of 100 rpm Fig. 4.40 shows that the reduction in the wafer temperature nonuniformity is raised to 73.3%. Note that at $\omega = 100$ rpm and $V_d = 15$ mm/s the improvement in the wafer temperature uniformity can be up to 87.2% (Fig. 4.49). Now the data give in Figs. 4.51 – 4.62 for the wafer heated by three lamps also manifest that increasing the lamp-to-wafer separation distance significantly improves the wafer temperature

uniformity. Even at $\omega = 0$ rpm the reduction in Φ due to H raised from 30 mm to 90 mm is relatively substantial with Φ all larger than 70% (Figs. 4.51, 4.54, 4.57 and 4.60). The significant reduction in the wafer temperature nonuniformity with an increase in the lamp-to-wafer separation distance can be attributed to the fact that at a higher H the thermal radiation emitted from the lamps distributes more uniformly on the wafer surface. Meanwhile the thermal radiation flux on the wafer is less at a higher H and thus the ramp-up period of the wafer is longer.

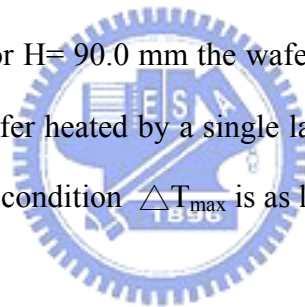
4.5 Effects of Lamp Arrangement on Wafer Temperature Uniformity

In the above discussion, we realize that the wafer temperature uniformity for the wafer heated by a single lamp is somewhat better than that by three lamps. It is legitimate to suspect that this is caused by the relatively nonuniform thermal radiation emitted from the three lamps arranged as that schematically shown in Fig. 2.2(b). Therefore tests are conducted for the wafer heated by a different arrangement of the three lamps as that schematically shown in Fig. 2.2(c), with the lamps located at a longer distance away from the axis of the processor. The data for the measured wafer temperature during the ramp-up period for these two lamp arrangements for $\omega = 0$ rpm and $V_d = 0$ mm/s are given in Figs. 4.63 and 4.64. The results indicate that when the lamps are slightly more separated from each other the wafer temperature is more uniform. This is considered to result from the fact that for the lamp arrangement shown in Fig. 2.2(c) the thermal radiation incident on the wafer is less nonuniform as compared with that for Fig. 2.2 (b). We further illustrate the effects of the lamp arrangement on the wafer temperature uniformity for the wafer rotated at different rates by comparing the data in Figs. 4.14 and 4.65 for $V_d = 0$ mm/s. The results also indicate that separating the lamps slightly away from each other can improve the wafer temperature uniformity even when the wafer is under rotation. Similar

conclusion is noted when the wafer is under rotation and translation, as evident from the results in Figs. 4.20 and 4.66.

4.6 Optimal Condition for Wafer Temperature Uniformity

The results presented above distinctly suggest that the wafer temperature uniformity can be improved by increasing the lamp-to-wafer separation distance and wafer translating speed for the wafer rotated at certain rate. Besides, the wafer heated by a single lamp is at a more uniform temperature. An attempt is made here to search for the optimal condition for the wafer temperature uniformity subjected to the constraints of the present experimental system. In this search ω is tested at an interval of 10 rpm and V_d at an interval of 1 mm/s. The results indicate that at $\omega = 170$ rpm and $V_d = 17$ mm/s for $H = 90.0$ mm the wafer temperature uniformity can be reduced by 85.7 % for the wafer heated by a single lamp. The data are shown in Fig. 4.67. Note that at this optimal condition ΔT_{\max} is as low as 0.5°C .



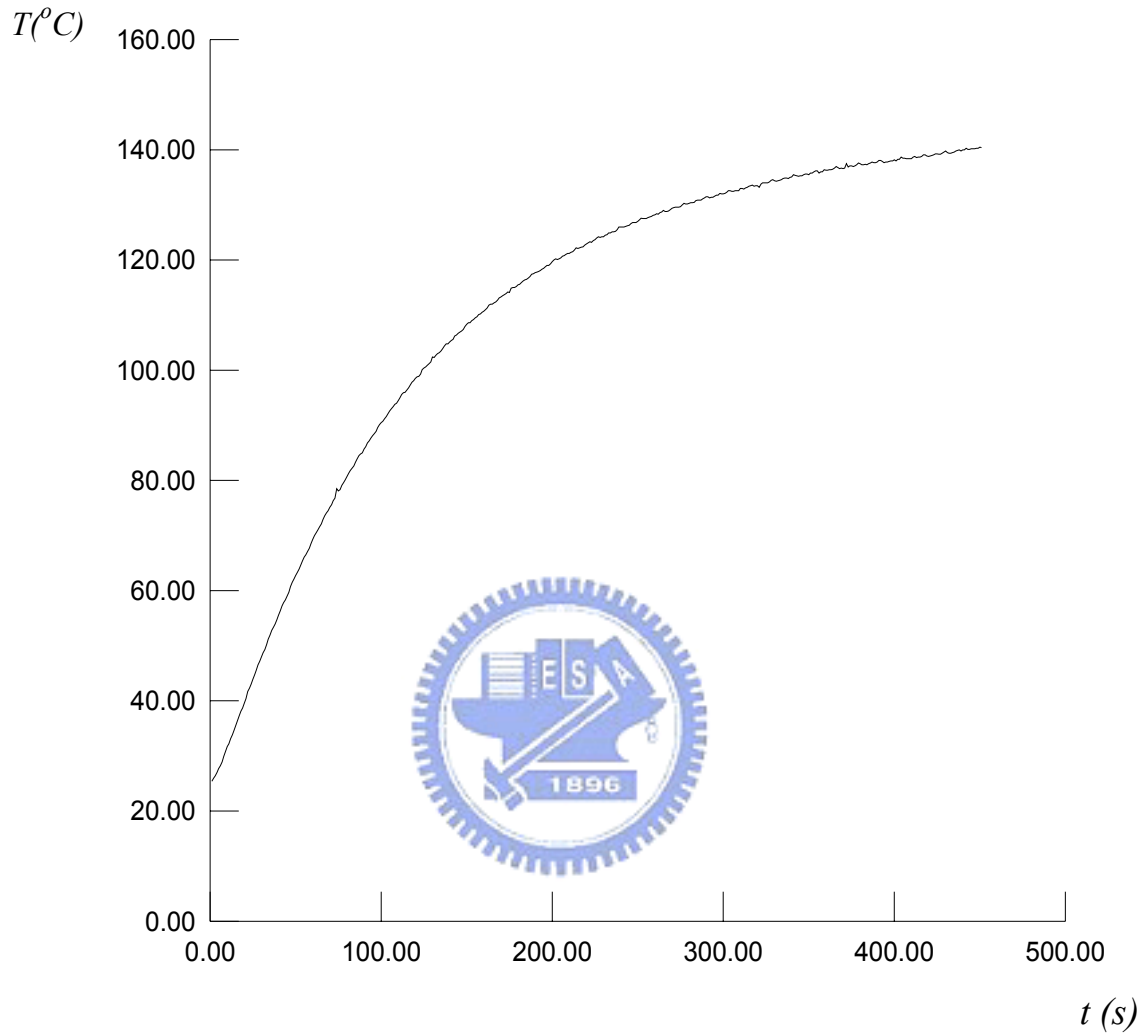


Fig. 4.1 Time variation of the wafer temperature measured at the geometric center of the wafer during the ramp-up period for the wafer heated by a single lamp for $H= 90$ mm, $\omega= 150$ rpm, and $V_d = 15$ mm/s.

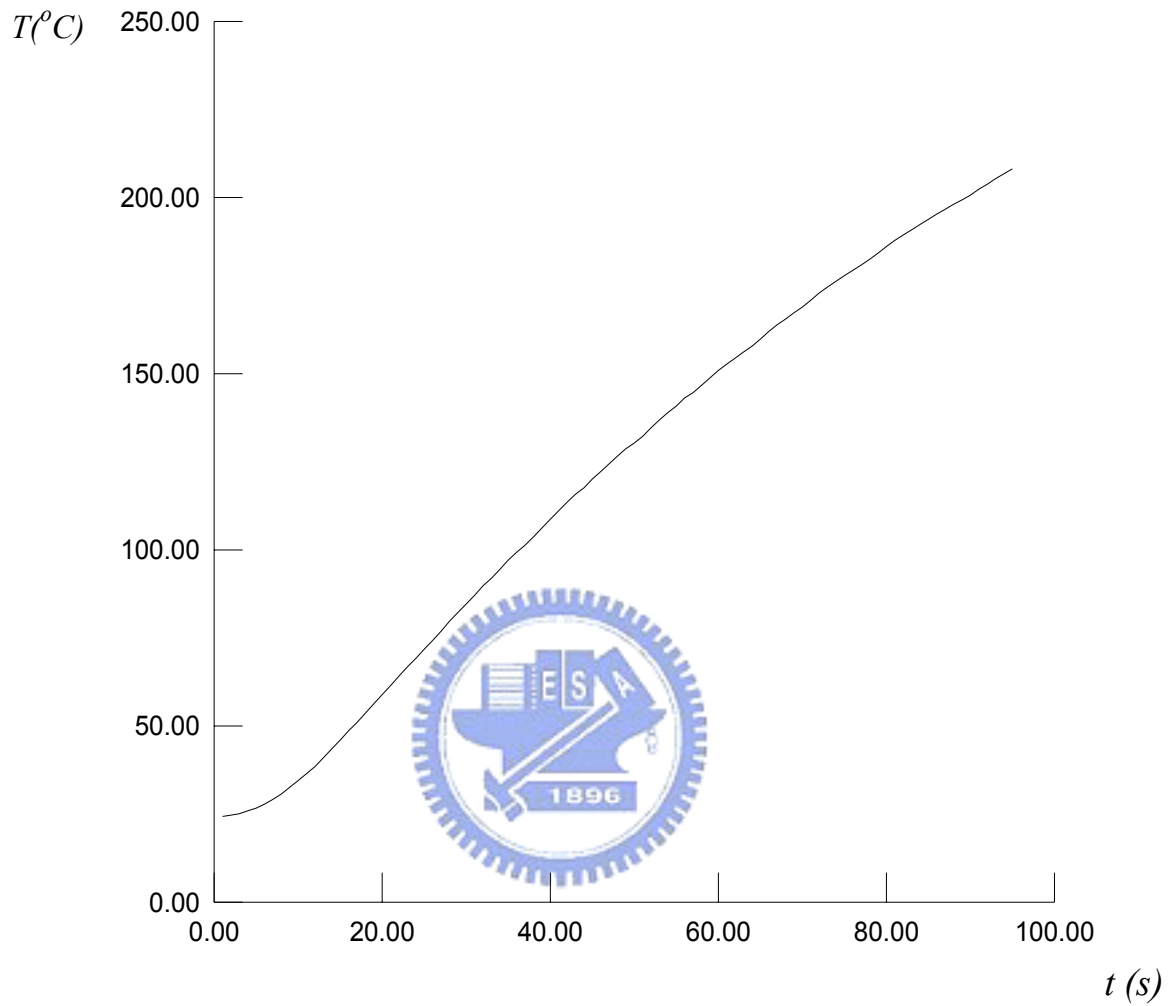
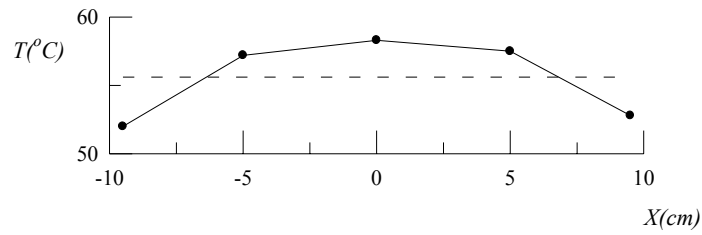
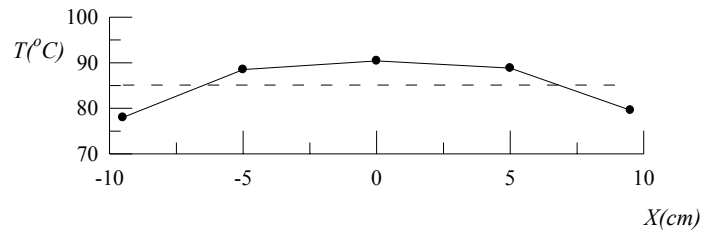


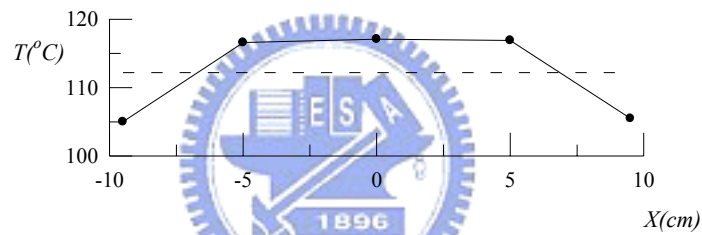
Fig. 4.2 Time variation of the wafer temperature measured at the geometric center of the wafer during the ramp-up period for the wafer heated by three lamps arranged as Fig. 2.2(b) for $H= 60$ mm, $\omega= 150$ rpm, and $V_d = 15$ mm/s.



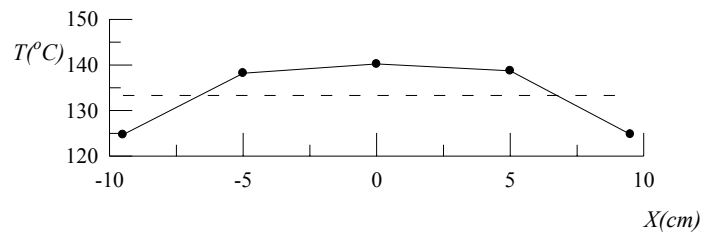
(a) $t=20\text{s}$, $T_{\text{mean}}=55.6^{\circ}\text{C}$ & $\Delta T_{\text{max}}=3.6^{\circ}\text{C}$



(b) $t=40\text{s}$, $T_{\text{mean}}=85.1^{\circ}\text{C}$ & $\Delta T_{\text{max}}=7.1^{\circ}\text{C}$

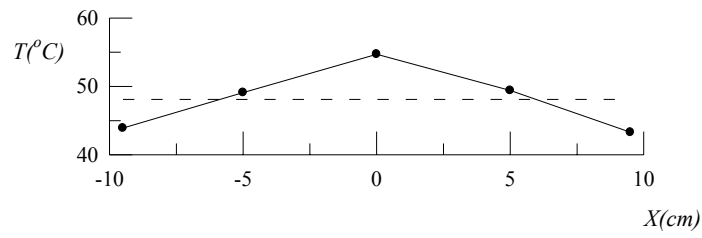


(c) $t=60\text{s}$, $T_{\text{mean}}=122.2^{\circ}\text{C}$ & $\Delta T_{\text{max}}=7.2^{\circ}\text{C}$

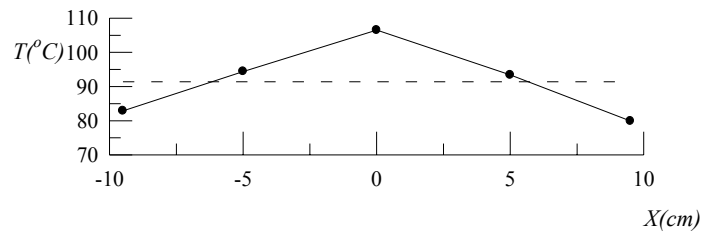


(d) $t=81\text{s}$, $T_{\text{mean}}=133.3^{\circ}\text{C}$ & $\Delta T_{\text{max}}=8.6^{\circ}\text{C}$

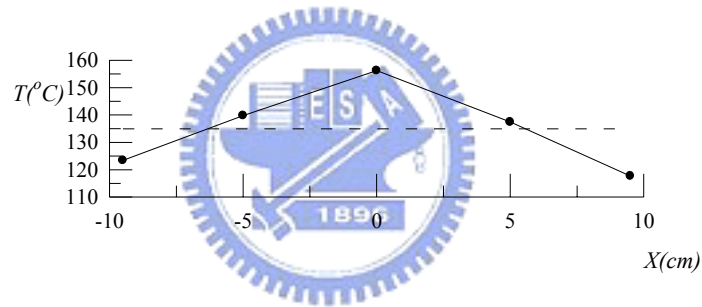
Fig. 4.3 The measured wafer temperature at selected locations for $H=30\text{ mm}$, $V_d=0\text{ mm/s}$ and $\omega=0\text{ rpm}$ for the wafer heated by one lamp during the ramp-up period.



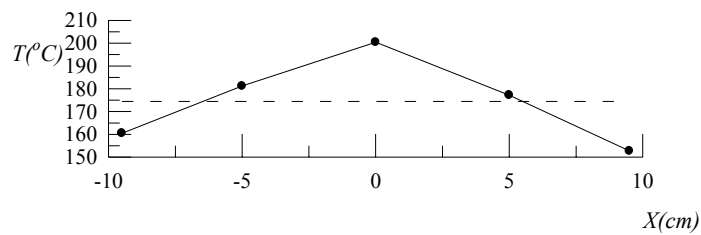
(a) $t = 10\text{s}$, $T_{\text{mean}} = 48.1^{\circ}\text{C}$ & $\Delta T_{\text{max}} = 6.6^{\circ}\text{C}$



(b) $t = 20\text{s}$, $T_{\text{mean}} = 91.4^{\circ}\text{C}$ & $\Delta T_{\text{max}} = 15.1^{\circ}\text{C}$



(c) $t = 30\text{s}$, $T_{\text{mean}} = 134.9^{\circ}\text{C}$ & $\Delta T_{\text{max}} = 21.3^{\circ}\text{C}$



(d) $t = 40\text{s}$, $T_{\text{mean}} = 174.4^{\circ}\text{C}$ & $\Delta T_{\text{max}} = 26^{\circ}\text{C}$

Fig. 4.4 The measured wafer temperature at selected locations for $H=30\text{ mm}$, $V_d=0\text{ mm/s}$ and $\omega=0\text{ rpm}$ for the wafer heated by three lamps during the ramp-up period.

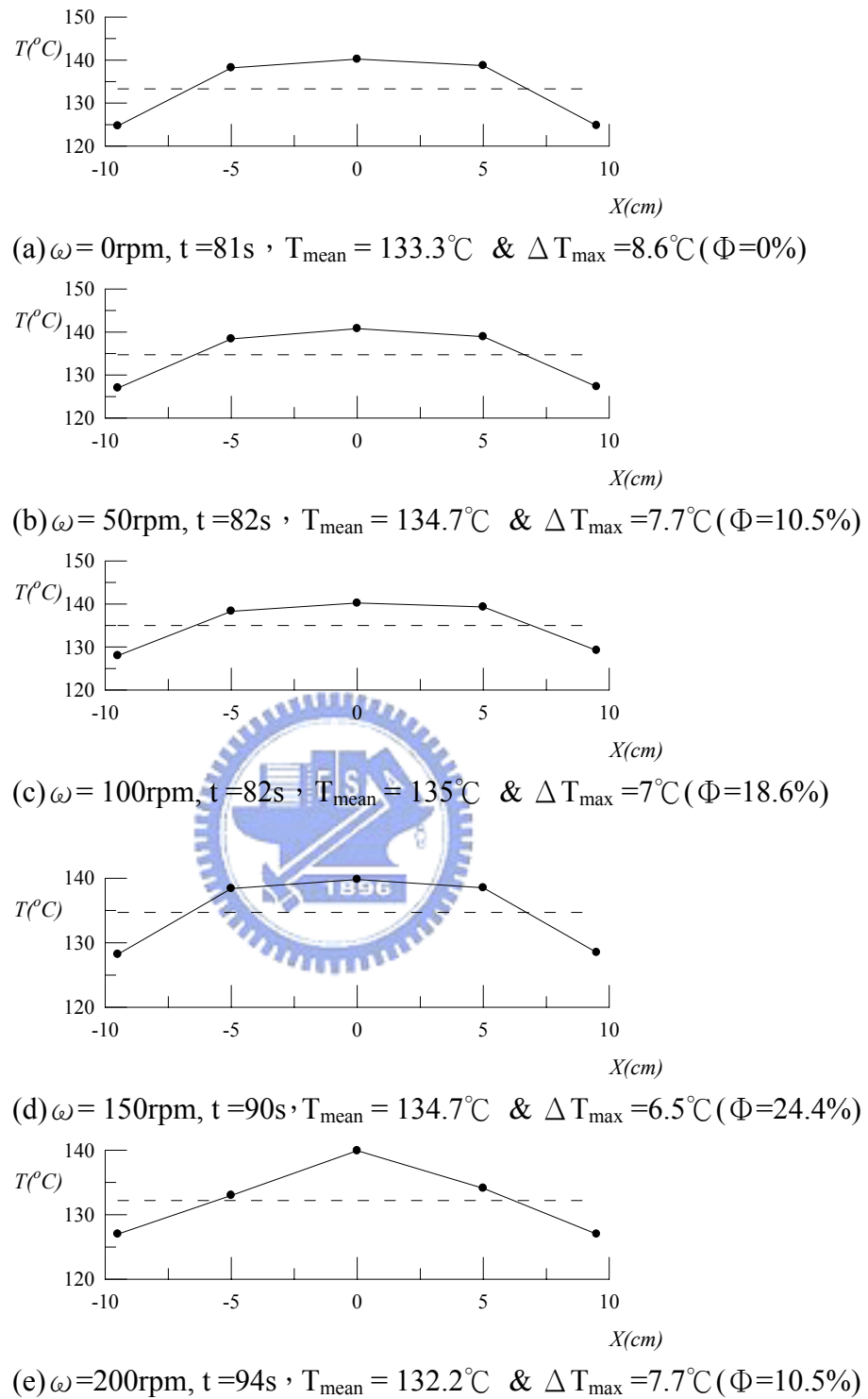


Fig. 4.5 The measured wafer temperature at selected locations for (a) $\omega = 0$ rpm, (b) $\omega = 50$ rpm, (c) $\omega = 100$ rpm, (d) $\omega = 150$ rpm and (e) $\omega = 200$ rpm at $H = 30$ mm and $V_d = 0$ mm/s for the wafer heated by one lamp.

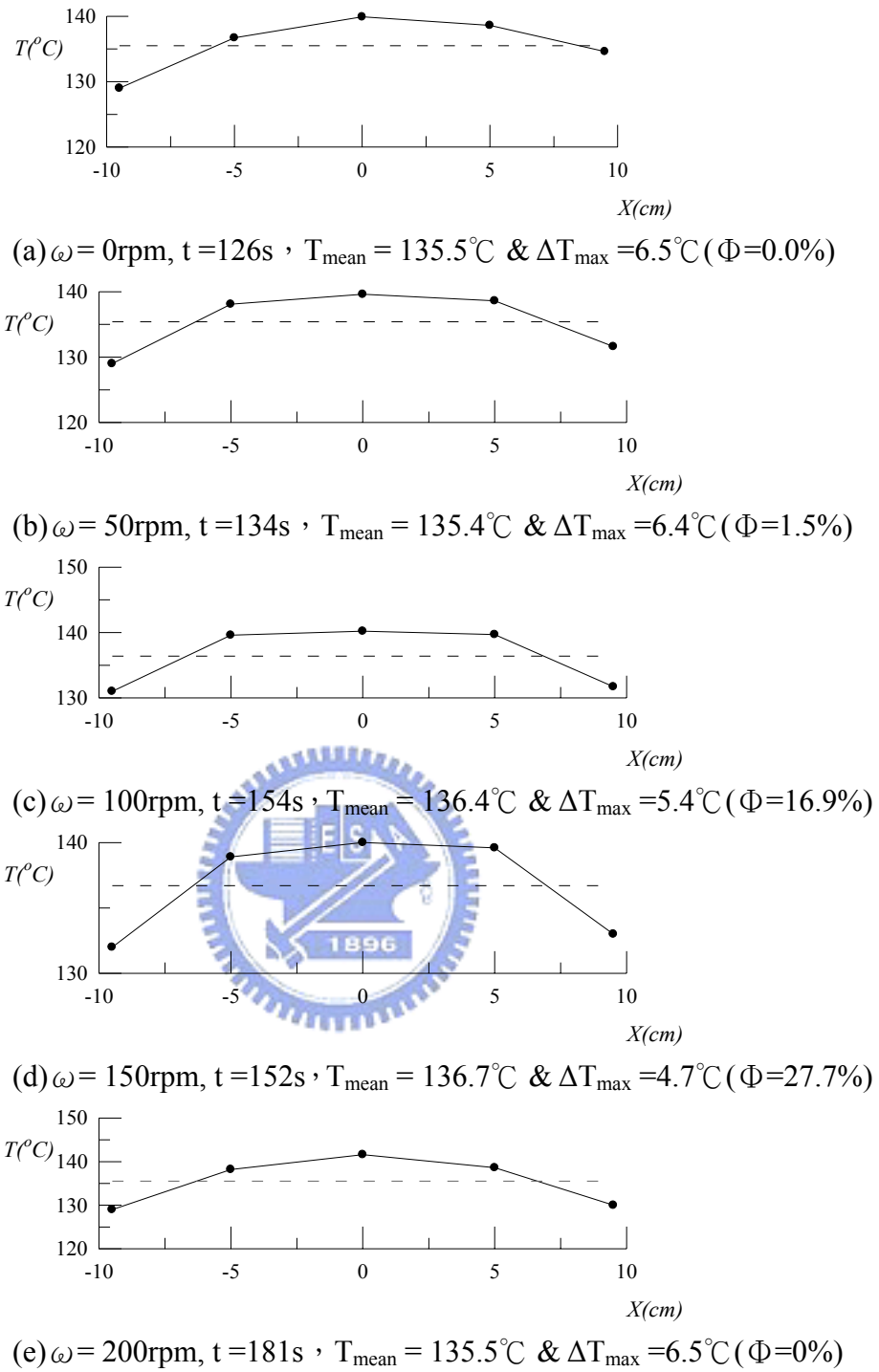


Fig. 4.6 The measured wafer temperature at selected locations for (a) $\omega = 0$ rpm, (b) $\omega = 50$ rpm, (c) $\omega = 100$ rpm, (d) $\omega = 150$ rpm and (e) $\omega = 200$ rpm at $H = 60$ mm and $V_d = 0$ mm/s for the wafer heated by one lamp.

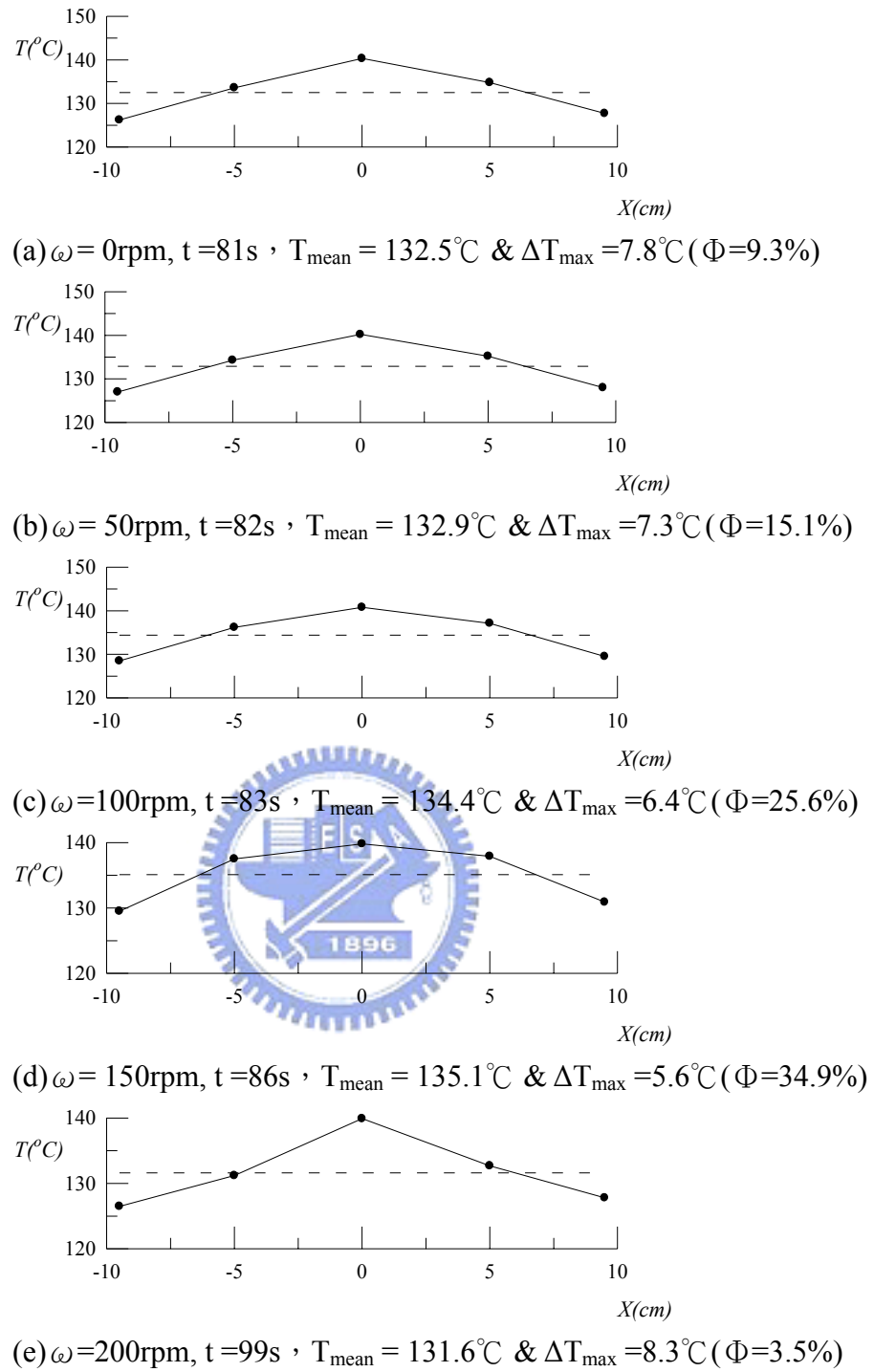


Fig. 4.7 The measured wafer temperature at selected locations for (a) $\omega = 0$ rpm, (b) $\omega = 50$ rpm, (c) $\omega = 100$ rpm, (d) $\omega = 150$ rpm and (e) $\omega = 200$ rpm at $H = 30$ mm and $V_d = 5$ mm/s for the wafer heated by one lamp.

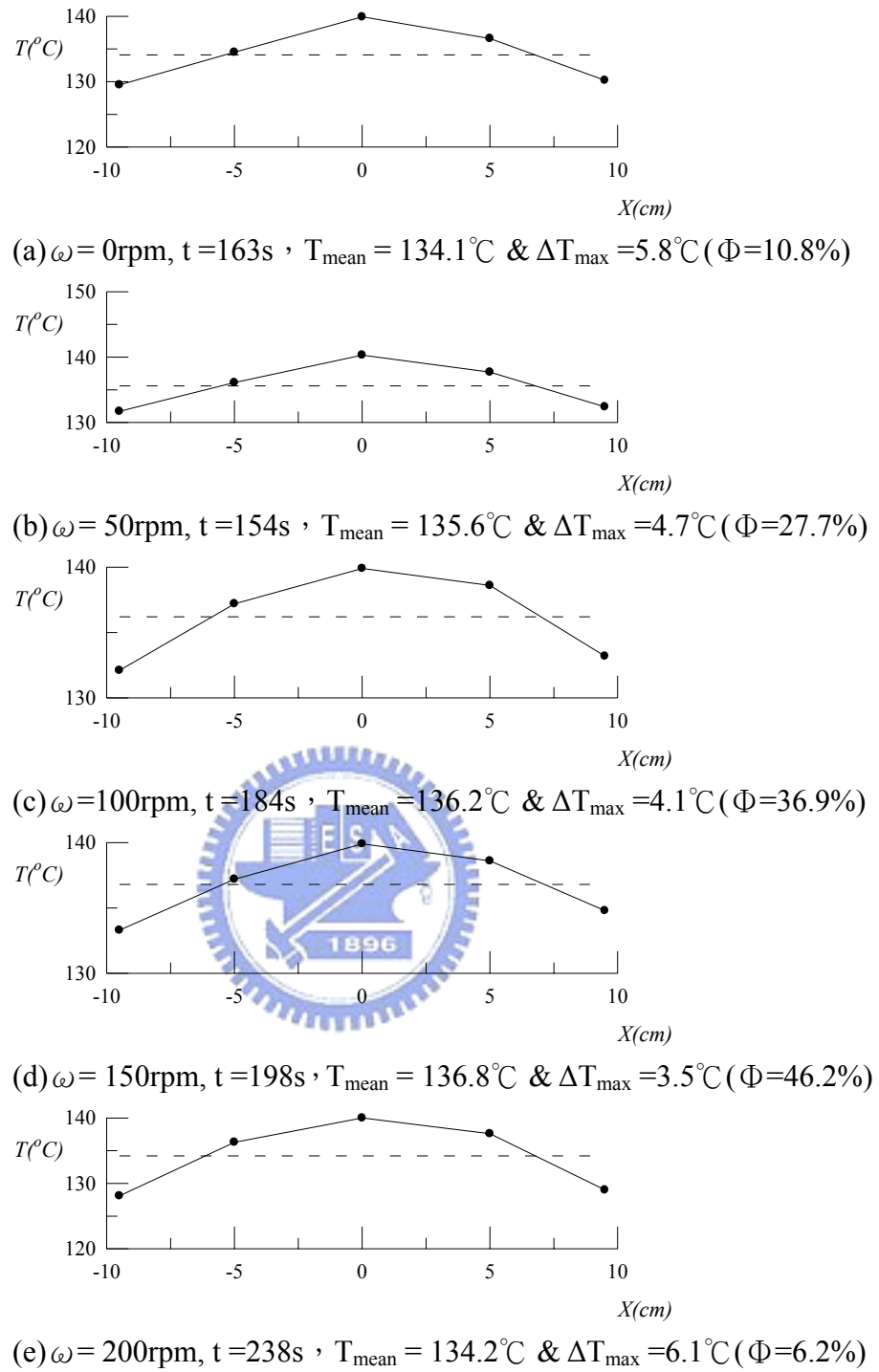
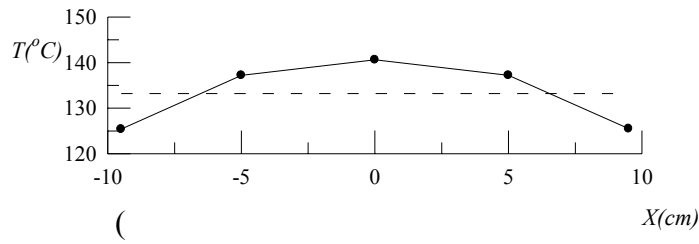
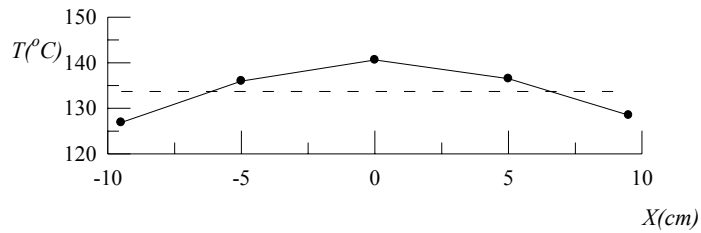


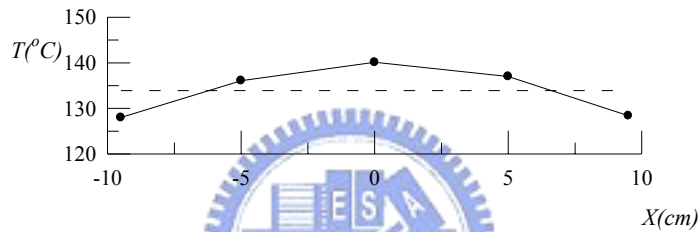
Fig. 4.8 The measured wafer temperature at selected locations for (a) $\omega = 0$ rpm, (b) $\omega = 50$ rpm, (c) $\omega = 100$ rpm, (d) $\omega = 150$ rpm and (e) $\omega = 200$ rpm at $H = 60$ mm and $V_d = 5$ mm/s for the wafer heated by one lamp.



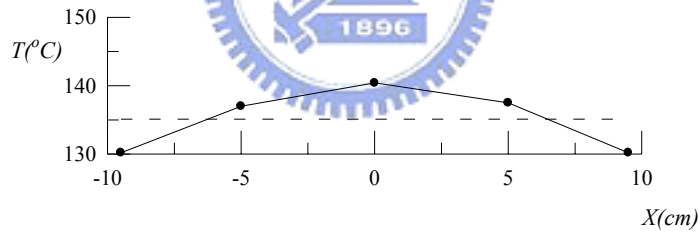
(a) $\omega = 0\text{rpm}$, $t = 91\text{s}$, $T_{\text{mean}} = 133.2^\circ\text{C}$ & $\Delta T_{\text{max}} = 7.4^\circ\text{C}$ ($\Phi = 14.0\%$)



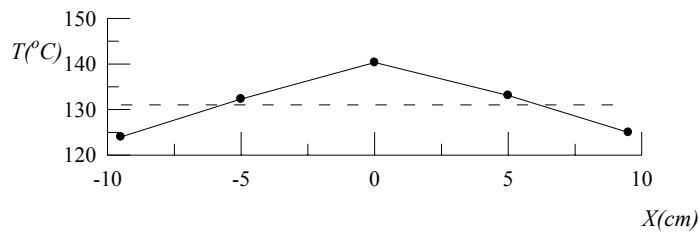
(b) $\omega = 50\text{rpm}$, $t = 88\text{s}$, $T_{\text{mean}} = 133.7^\circ\text{C}$ & $\Delta T_{\text{max}} = 6.9^\circ\text{C}$ ($\Phi = 19.8\%$)



(c) $\omega = 100\text{rpm}$, $t = 91\text{s}$, $T_{\text{mean}} = 133.9^\circ\text{C}$ & $\Delta T_{\text{max}} = 6.2^\circ\text{C}$ ($\Phi = 27.9\%$)

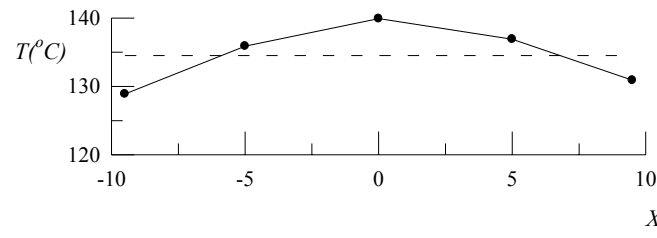


(d) $\omega = 150\text{rpm}$, $t = 92\text{s}$, $T_{\text{mean}} = 135.1^\circ\text{C}$ & $\Delta T_{\text{max}} = 5.3^\circ\text{C}$ ($\Phi = 38.9\%$)

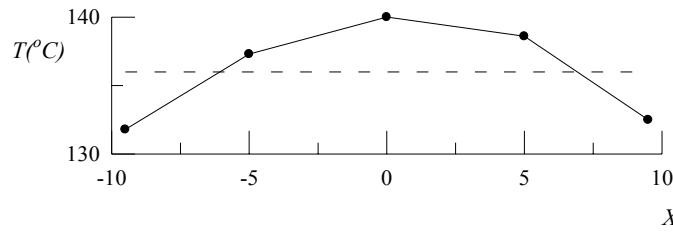


(e) $\omega = 200\text{rpm}$, $t = 104\text{s}$, $T_{\text{mean}} = 131^\circ\text{C}$ & $\Delta T_{\text{max}} = 9.4^\circ\text{C}$ ($\Phi = -9.3\%$)

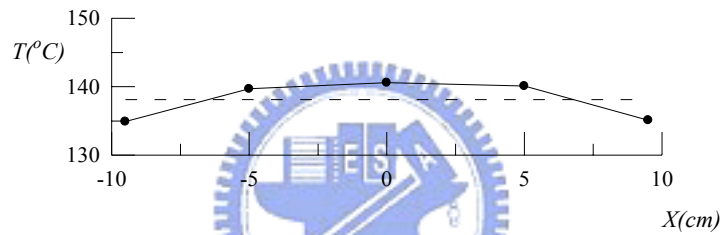
Fig. 4.9 The measured wafer temperature at selected locations for (a) $\omega = 0\text{ rpm}$, (b) $\omega = 50\text{ rpm}$, (c) $\omega = 100\text{ rpm}$, (d) $\omega = 150\text{ rpm}$ and (e) $\omega = 200\text{ rpm}$ at $H = 30\text{ mm}$ and $V_d = 10\text{ mm/s}$ for the wafer heated by one lamp.



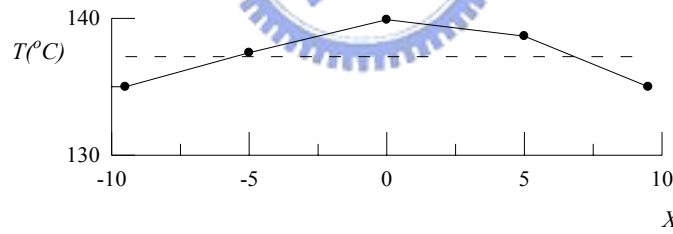
(a) $\omega = 0\text{rpm}$, $t = 157\text{s}$, $T_{\text{mean}} = 134.5^\circ\text{C}$ & $\Delta T_{\text{max}} = 5.6^\circ\text{C}$ ($\Phi = 17.8\%$)



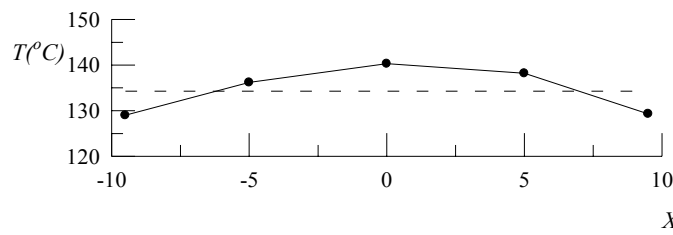
(b) $\omega = 50\text{rpm}$, $t = 174\text{s}$, $T_{\text{mean}} = 136^\circ\text{C}$ & $\Delta T_{\text{max}} = 4.2^\circ\text{C}$ ($\Phi = 35.4\%$)



(c) $\omega = 100\text{rpm}$, $t = 184\text{s}$, $T_{\text{mean}} = 138.1^\circ\text{C}$ & $\Delta T_{\text{max}} = 3.2^\circ\text{C}$ ($\Phi = 50.8\%$)



(d) $\omega = 150\text{rpm}$, $t = 237\text{s}$, $T_{\text{mean}} = 137.2^\circ\text{C}$ & $\Delta T_{\text{max}} = 2.7^\circ\text{C}$ ($\Phi = 58.5\%$)



(e) $\omega = 200\text{rpm}$, $t = 234\text{s}$, $T_{\text{mean}} = 134.6^\circ\text{C}$ & $\Delta T_{\text{max}} = 5.7^\circ\text{C}$ ($\Phi = 12.3\%$)

Fig. 4.10 The measured wafer temperature at selected locations for (a) $\omega = 0\text{rpm}$, (b) $\omega = 50\text{rpm}$, (c) $\omega = 100\text{rpm}$, (d) $\omega = 150\text{rpm}$ and (e) $\omega = 200\text{rpm}$ at $H = 60\text{mm}$ and $V_d = 10\text{mm/s}$ for the wafer heated by one lamp.

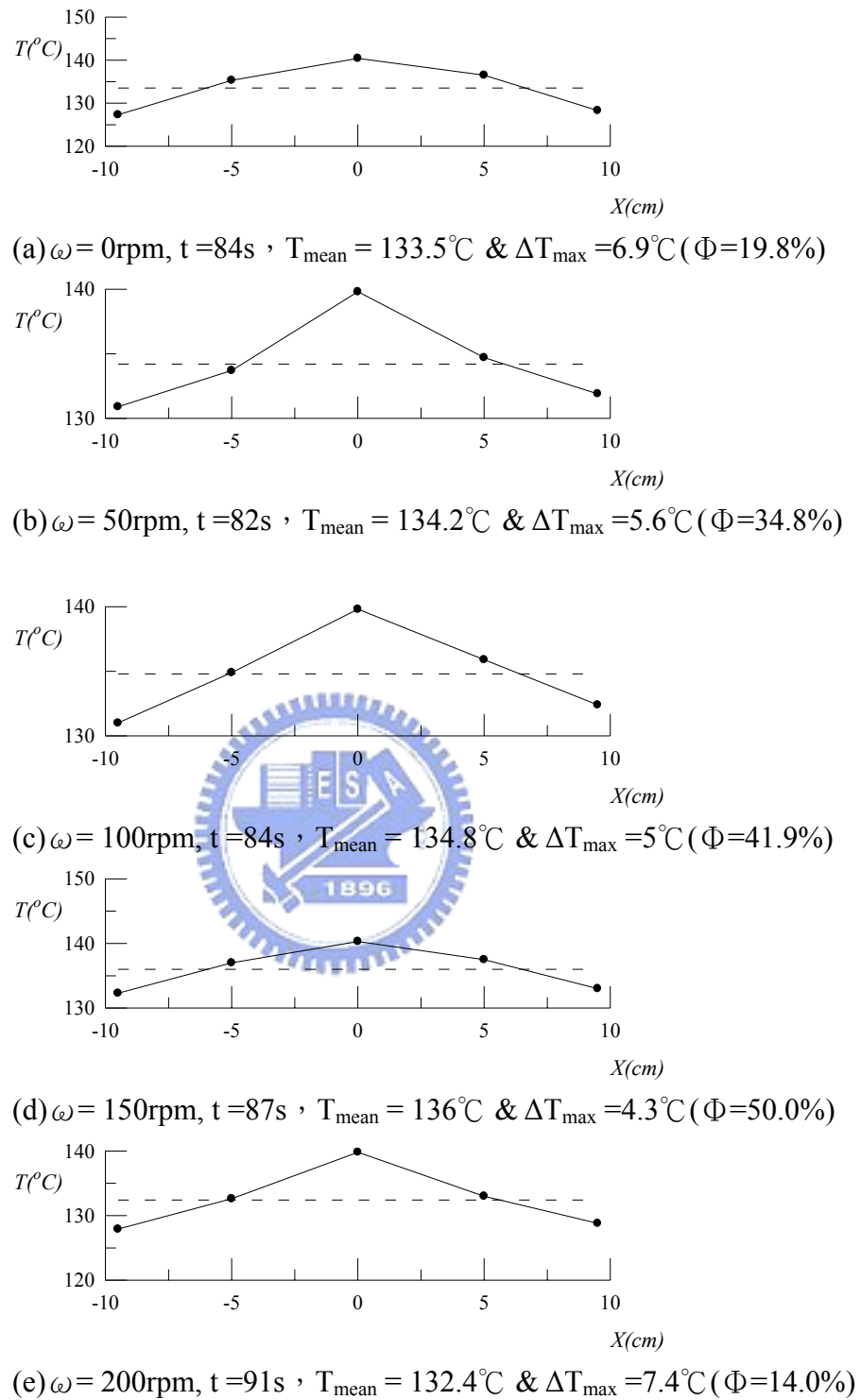


Fig. 4.11 The measured wafer temperature at selected locations for (a) $\omega = 0$ rpm, (b) $\omega = 50$ rpm, (c) $\omega = 100$ rpm, (d) $\omega = 150$ rpm and (e) $\omega = 200$ rpm at $H = 30$ mm and $V_d = 15$ mm/s for the wafer heated by one lamp.

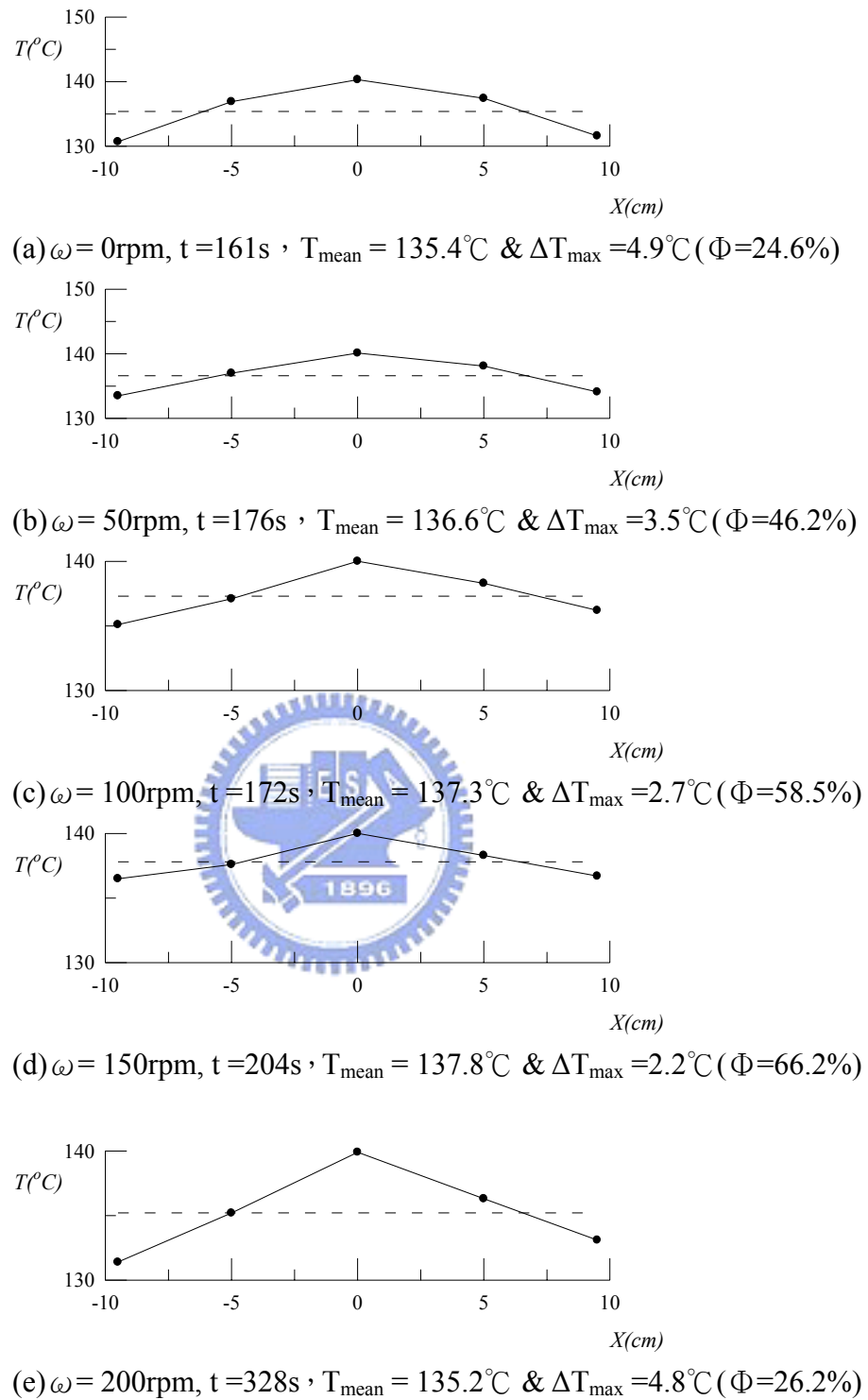
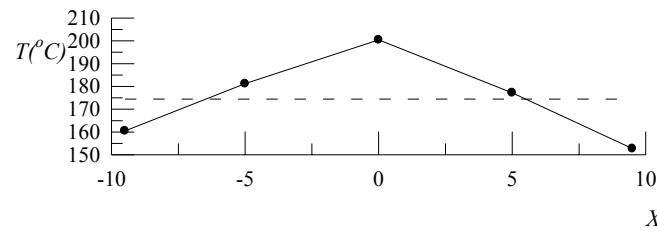
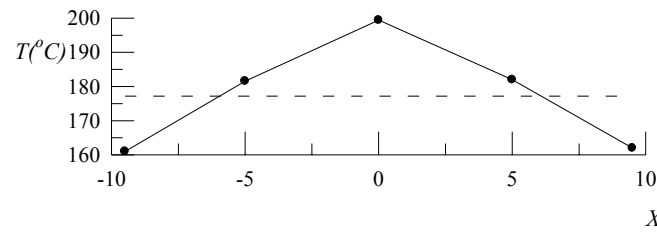


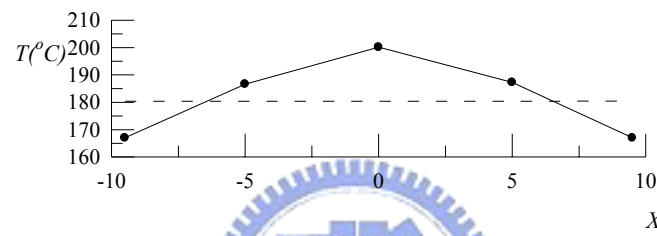
Fig. 4.12 The measured wafer temperature at selected locations for (a) $\omega = 0 \text{ rpm}$, (b) $\omega = 50 \text{ rpm}$, (c) $\omega = 100 \text{ rpm}$, (d) $\omega = 150 \text{ rpm}$ and (e) $\omega = 200 \text{ rpm}$ at $H = 60 \text{ mm}$ and $V_d = 15 \text{ mm/s}$ for the wafer heated by one lamp.



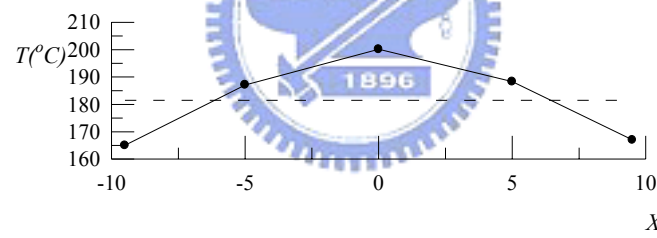
(a) $\omega=0\text{rpm}$, $t=40\text{s}$, $T_{\text{mean}}=174.4^{\circ}\text{C}$ & $\Delta T_{\text{max}}=26^{\circ}\text{C}$ ($\Phi=0\%$)



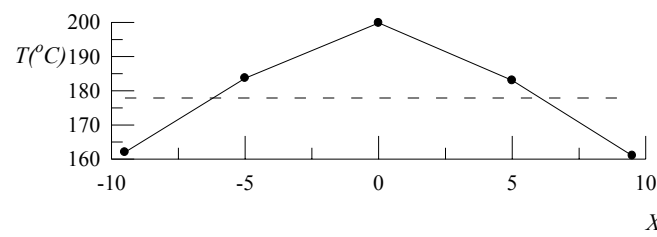
(b) $\omega=50\text{rpm}$, $t=40\text{s}$, $T_{\text{mean}}=177.2^{\circ}\text{C}$ & $\Delta T_{\text{max}}=22.2^{\circ}\text{C}$ ($\Phi=14.6\%$)



(c) $\omega=100\text{rpm}$, $t=40\text{s}$, $T_{\text{mean}}=180.4^{\circ}\text{C}$ & $\Delta T_{\text{max}}=19.7^{\circ}\text{C}$ ($\Phi=24.2\%$)



(d) $\omega=150\text{rpm}$, $t=38\text{s}$, $T_{\text{mean}}=181.5^{\circ}\text{C}$ & $\Delta T_{\text{max}}=18.6^{\circ}\text{C}$ ($\Phi=28.5\%$)



(e) $\omega=200\text{rpm}$, $t=62\text{s}$, $T_{\text{mean}}=177.9^{\circ}\text{C}$ & $\Delta T_{\text{max}}=21.9^{\circ}\text{C}$ ($\Phi=15.8\%$)

Fig. 4.13 The measured wafer temperature at selected locations for (a) $\omega=0\text{rpm}$, (b) $\omega=50\text{rpm}$, (c) $\omega=100\text{rpm}$, (d) $\omega=150\text{rpm}$ and (e) $\omega=200\text{rpm}$ at $H=30\text{mm}$ and $V_d=0\text{mm/s}$ for the wafer heated by three lamps.

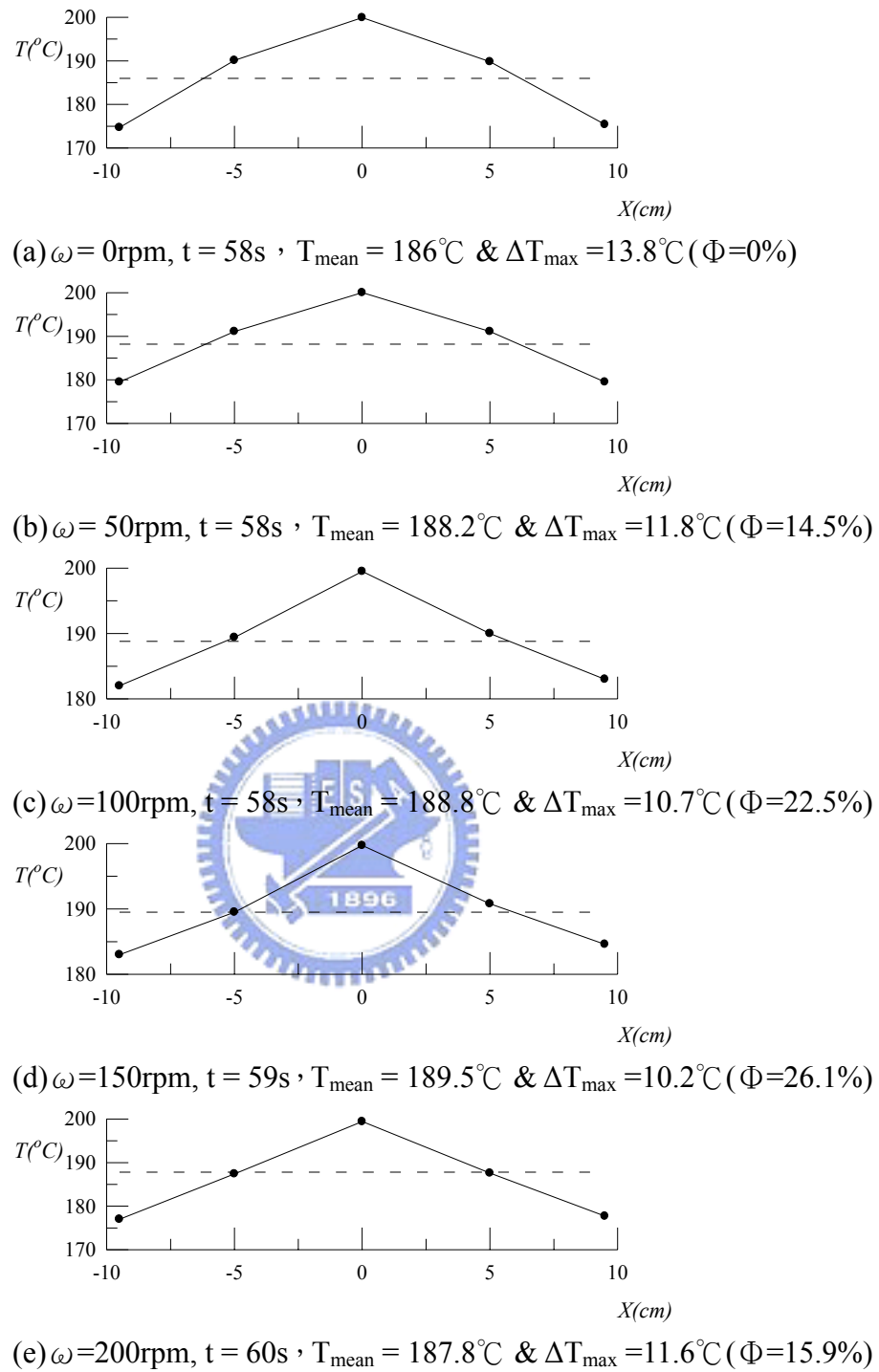


Fig. 4.14 The measured wafer temperature at selected locations for (a) $\omega = 0 \text{ rpm}$, (b) $\omega = 50 \text{ rpm}$, (c) $\omega = 100 \text{ rpm}$, (d) $\omega = 150 \text{ rpm}$ and (e) $\omega = 200 \text{ rpm}$ at $H = 60 \text{ mm}$ and $V_d = 0 \text{ mm/s}$ for the wafer heated by three lamps.

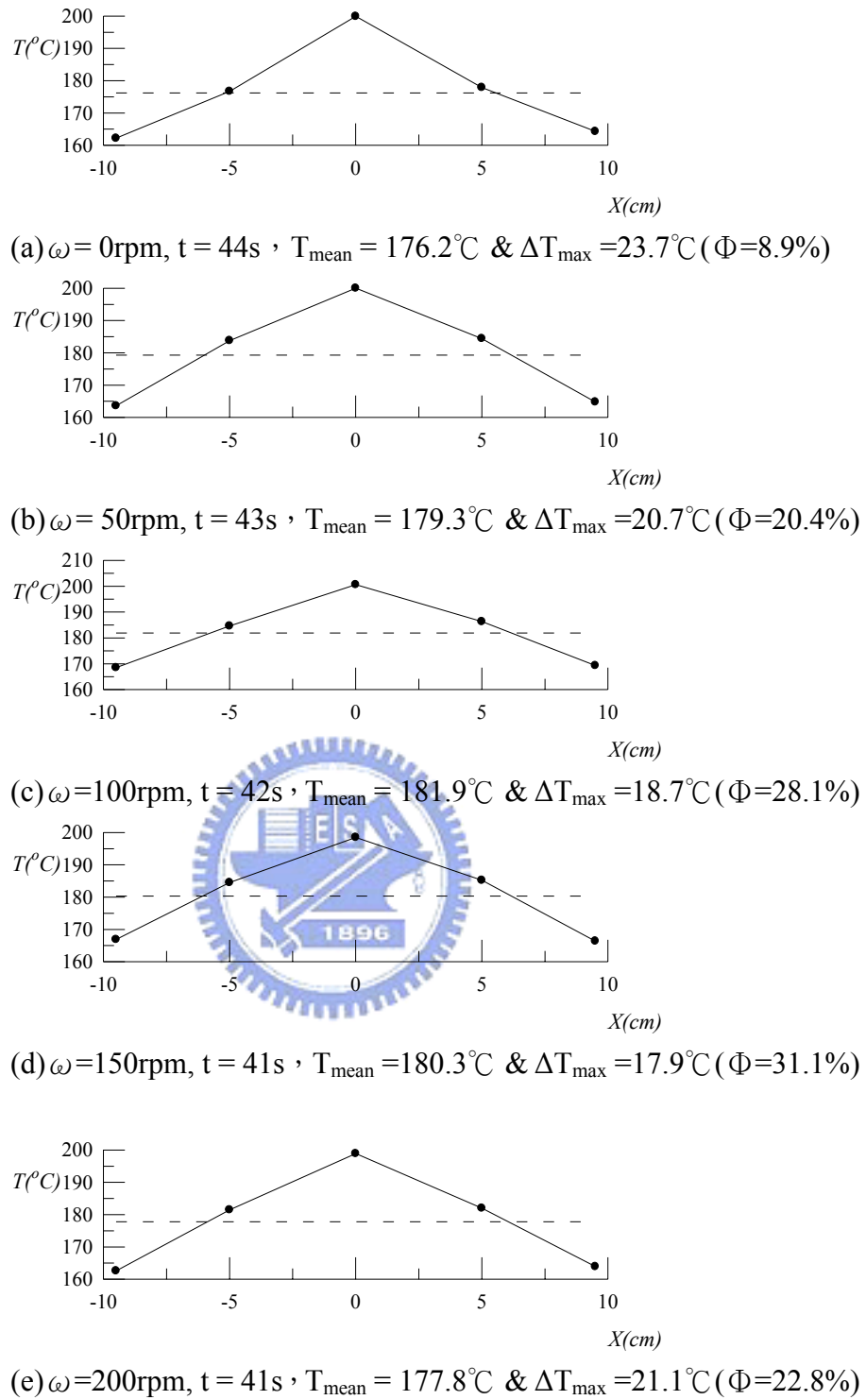


Fig. 4.15 The measured wafer temperature at selected locations for (a) $\omega = 0$ rpm, (b) $\omega = 50$ rpm, (c) $\omega = 100$ rpm, (d) $\omega = 150$ rpm and (e) $\omega = 200$ rpm at $H = 30$ mm and $V_d = 5$ mm/s for the wafer heated by three lamps.

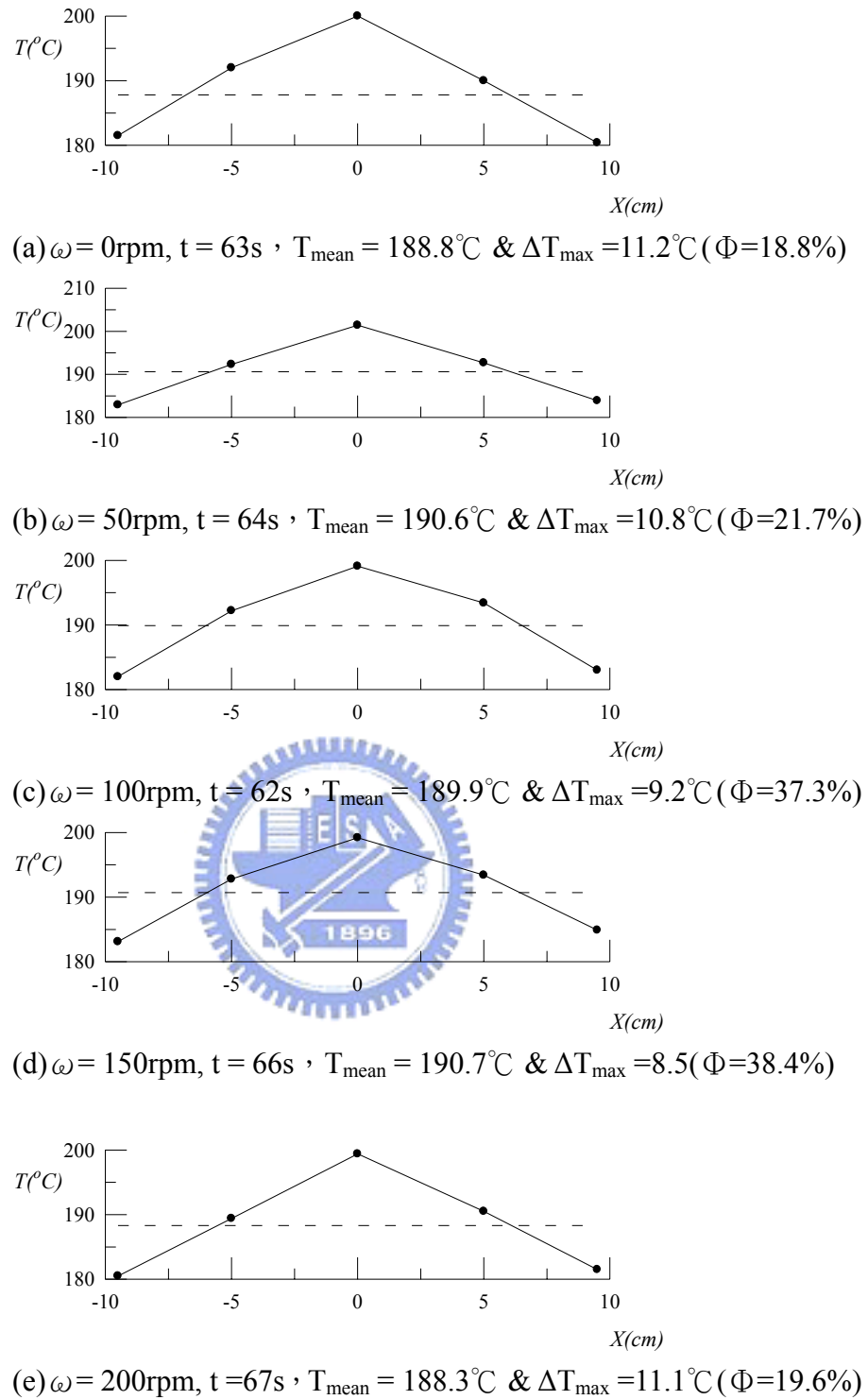


Fig. 4.16 The measured wafer temperature at selected locations for (a) $\omega = 0$ rpm, (b) $\omega = 50$ rpm, (c) $\omega = 100$ rpm, (d) $\omega = 150$ rpm and (e) $\omega = 200$ rpm at $H = 60$ mm and $V_d = 5$ mm/s for the wafer heated by three lamps.

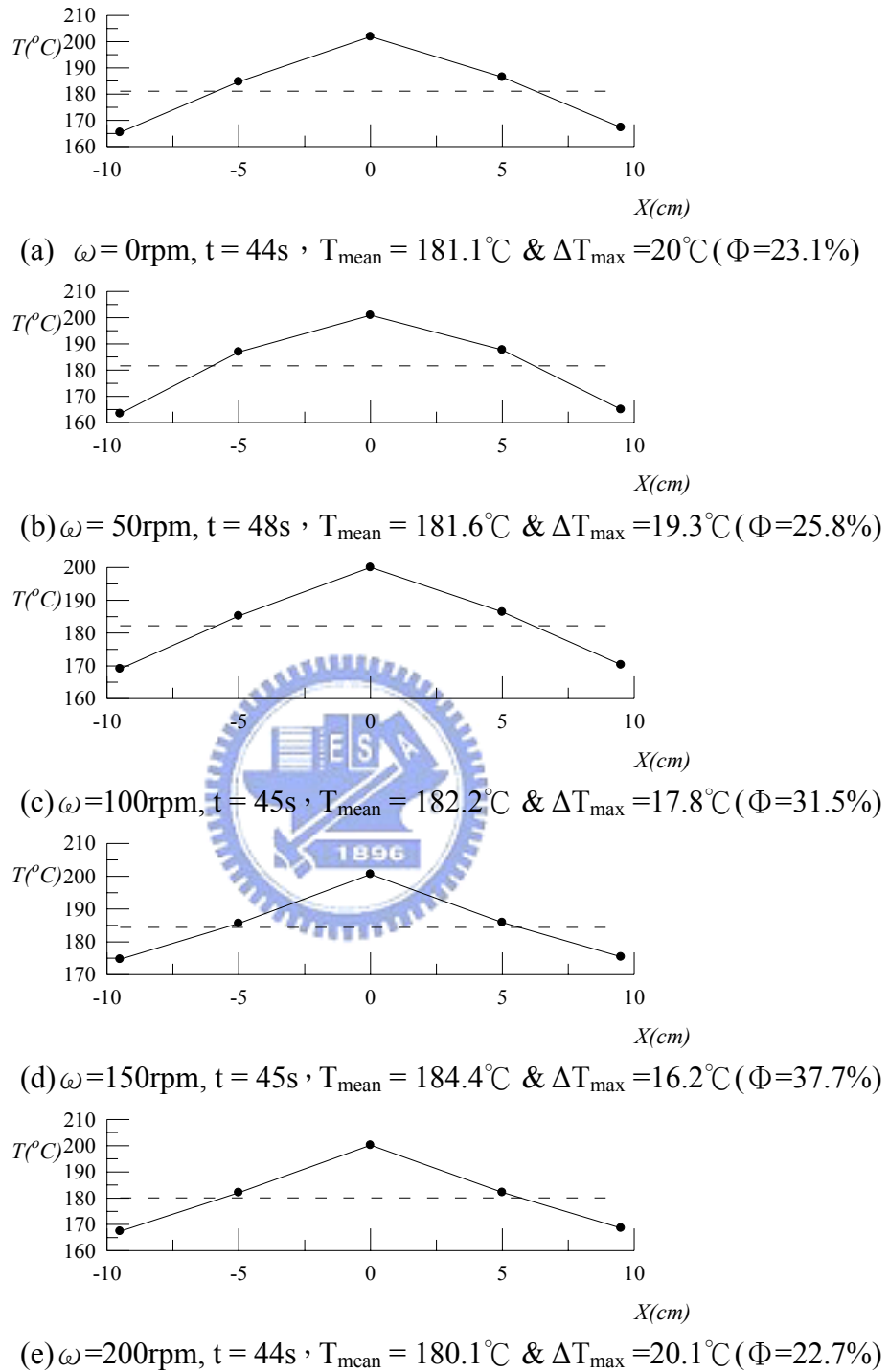


Fig. 4.17 The measured wafer temperature at selected locations for (a) $\omega = 0$ rpm, (b) $\omega = 50$ rpm, (c) $\omega = 100$ rpm, (d) $\omega = 150$ rpm and (e) $\omega = 200$ rpm at $H = 30$ mm and $V_d = 10$ mm/s for the wafer heated by three lamps.

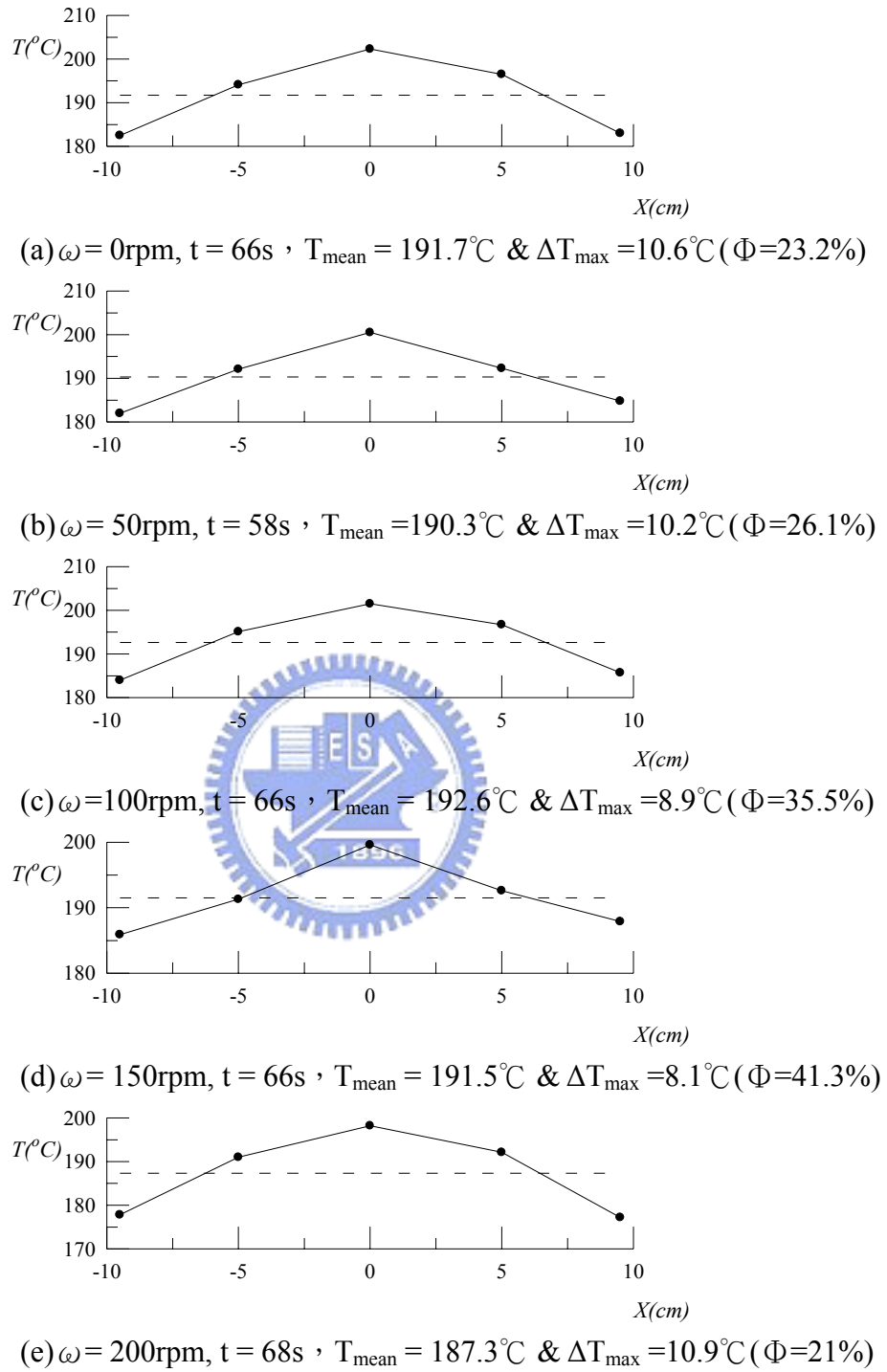
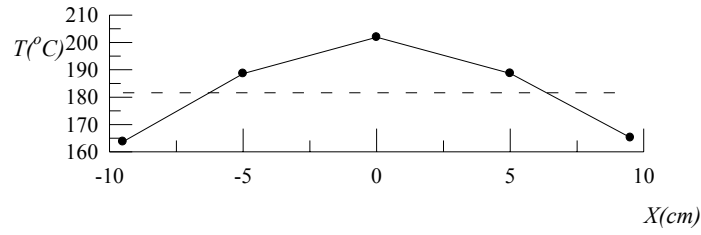
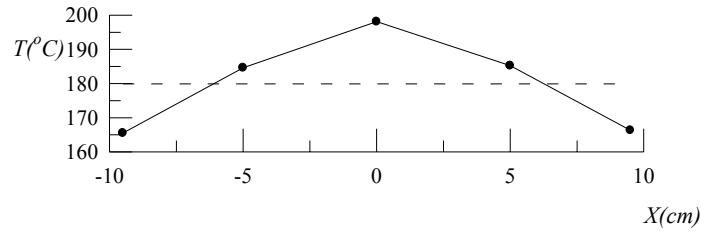


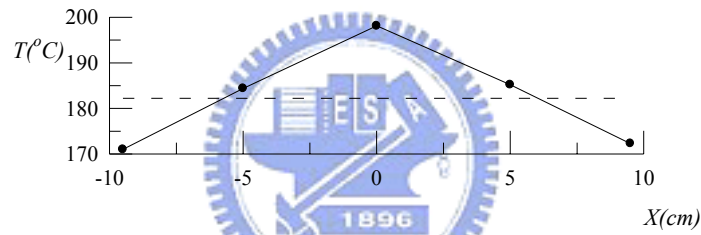
Fig. 4.18 The measured wafer temperature at selected locations for (a) $\omega = 0$ rpm, (b) $\omega = 50$ rpm, (c) $\omega = 100$ rpm, (d) $\omega = 150$ rpm and (e) $\omega = 200$ rpm at $H = 60$ mm and $V_d = 10$ mm/s for the wafer heated by three lamps.



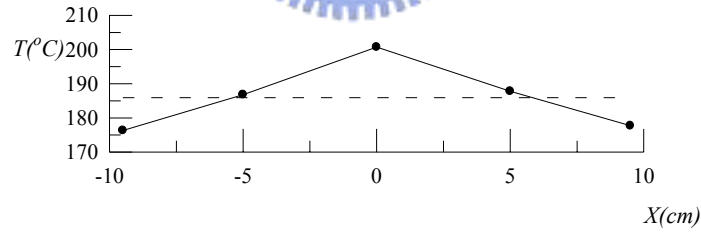
(a) $\omega = 0$ rpm, $t = 41$ s, $T_{\text{mean}} = 181.6^\circ\text{C}$ & $\Delta T_{\text{max}} = 17.9^\circ\text{C}$ ($\Phi = 31.2\%$)



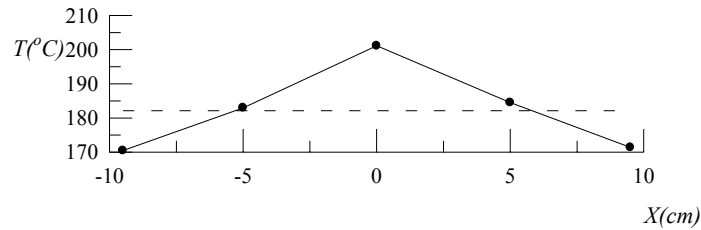
(b) $\omega = 50$ rpm, $t = 43$ s, $T_{\text{mean}} = 179.9^\circ\text{C}$ & $\Delta T_{\text{max}} = 18.2^\circ\text{C}$ ($\Phi = 30.0\%$)



(c) $\omega = 100$ rpm, $t = 43$ s, $T_{\text{mean}} = 182.2^\circ\text{C}$ & $\Delta T_{\text{max}} = 15.9^\circ\text{C}$ ($\Phi = 38.8\%$)



(d) $\omega = 150$ rpm, $t = 42$ s, $T_{\text{mean}} = 185.9^\circ\text{C}$ & $\Delta T_{\text{max}} = 14.8^\circ\text{C}$ ($\Phi = 43.1\%$)



(e) $\omega = 200$ rpm, $t = 44$ s, $T_{\text{mean}} = 182.1^\circ\text{C}$ & $\Delta T_{\text{max}} = 19^\circ\text{C}$ ($\Phi = 26.9\%$)

Fig. 4.19 The measured wafer temperature at selected locations for (a) $\omega = 0$ rpm, (b) $\omega = 50$ rpm, (c) $\omega = 100$ rpm, (d) $\omega = 150$ rpm and (e) $\omega = 200$ rpm at $H = 30$ mm and $V_d = 15$ mm/s for the wafer heated by three lamps.

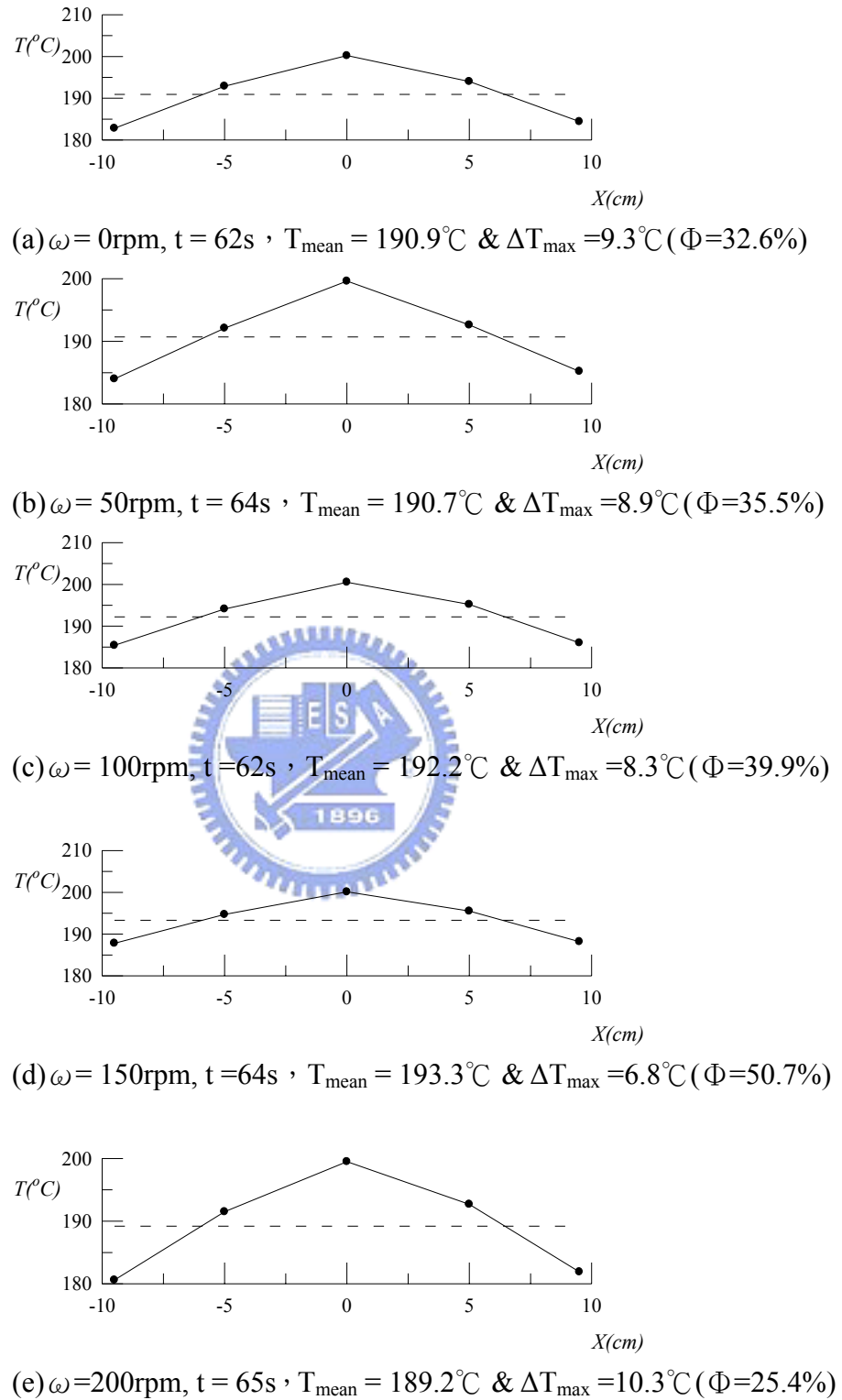
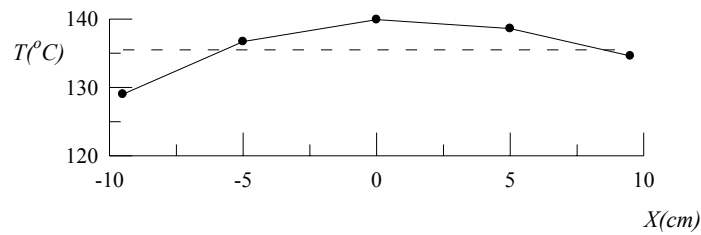
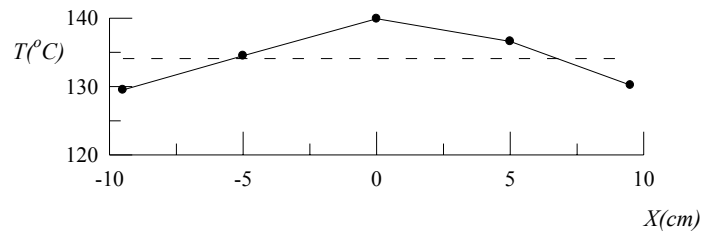


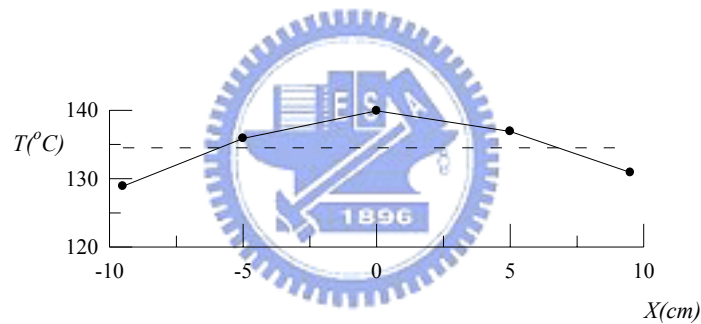
Fig. 4.20 The measured wafer temperature at selected locations for (a) $\omega = 0$ rpm, (b) $\omega = 50$ rpm, (c) $\omega = 100$ rpm, (d) $\omega = 150$ rpm and (e) $\omega = 200$ rpm at $H = 60$ mm and $V_d = 15$ mm/s for the wafer heated by three lamps.



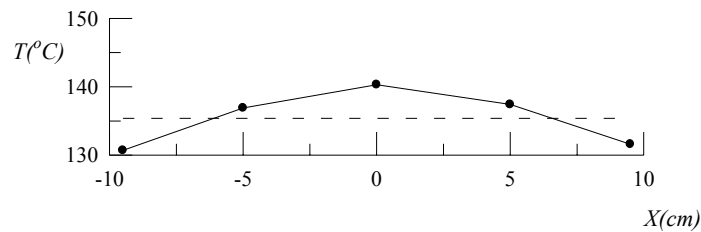
(a) $t=126s$, $T_{\text{mean}} = 135.5^{\circ}\text{C}$ & $\Delta T_{\text{max}} = 6.5^{\circ}\text{C}$ ($\Phi=0.0\%$)



(b) $t=163s$, $T_{\text{mean}} = 134.1^{\circ}\text{C}$ & $\Delta T_{\text{max}} = 5.8^{\circ}\text{C}$ ($\Phi=10.8\%$)

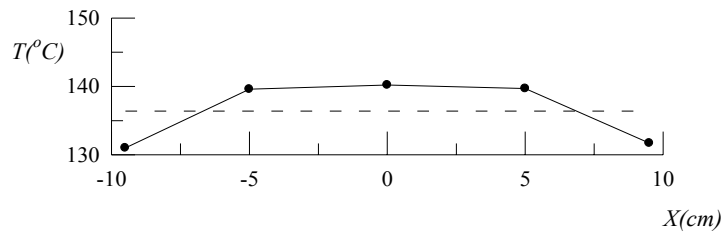


(c) $t=157s$, $T_{\text{mean}} = 134.5^{\circ}\text{C}$ & $\Delta T_{\text{max}} = 5.6^{\circ}\text{C}$ ($\Phi=13.8\%$)

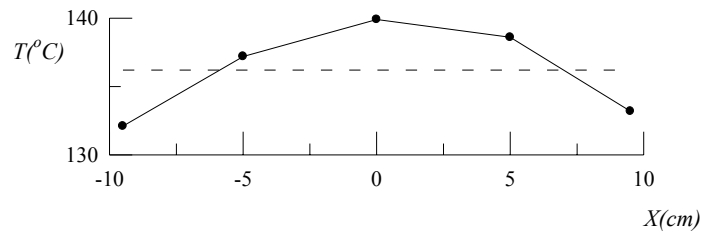


(d) $t=161s$, $T_{\text{mean}} = 135.4^{\circ}\text{C}$ & $\Delta T_{\text{max}} = 4.9^{\circ}\text{C}$ ($\Phi=24.6\%$)

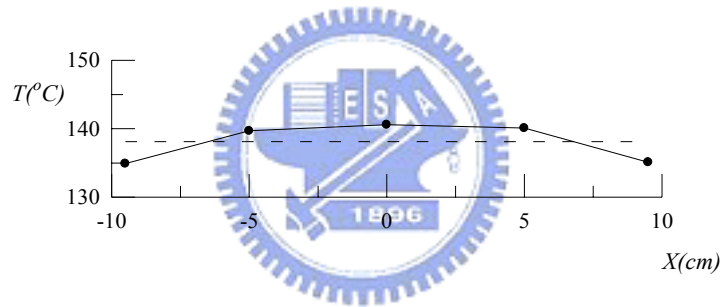
Fig. 4.21 The measured wafer temperature at selected locations during the ramp-up period for (a) $V_d=0$ mm/s, (b) $V_d=5$ mm/s, (c) $V_d=10$ mm/s and (d) $V_d=15$ mm/s with the wafer heated by a single lamp at $\omega=0$ rpm and $H=60$ mm for the final wafer temperature set at 140°C .



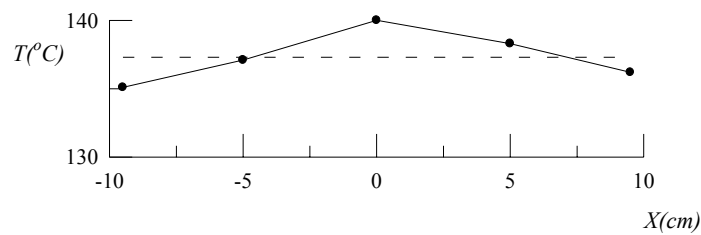
(a) $t=154s$, $T_{\text{mean}} = 136.4^{\circ}\text{C}$ & $\Delta T_{\text{max}} = 5.4^{\circ}\text{C}$ ($\Phi=16.9\%$)



(b) $t=184s$, $T_{\text{mean}} = 136.2^{\circ}\text{C}$ & $\Delta T_{\text{max}} = 4.1^{\circ}\text{C}$ ($\Phi=36.9\%$)

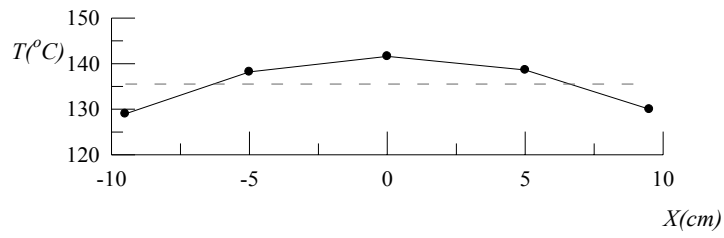


(c) $t=184s$, $T_{\text{mean}} = 138.1^{\circ}\text{C}$ & $\Delta T_{\text{max}} = 3.2^{\circ}\text{C}$ ($\Phi=50.8\%$)

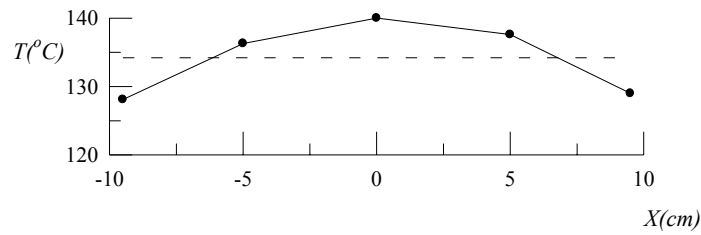


(d) $t=172s$, $T_{\text{mean}} = 137.3^{\circ}\text{C}$ & $\Delta T_{\text{max}} = 2.7^{\circ}\text{C}$ ($\Phi=58.5\%$)

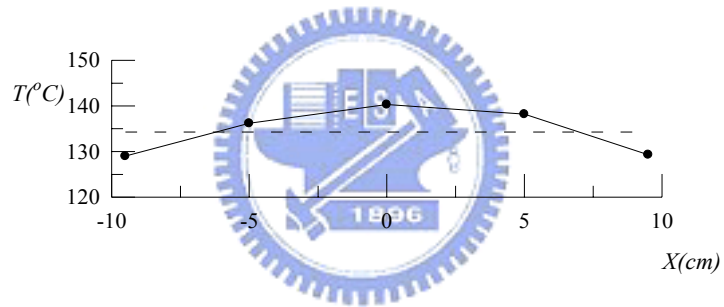
Fig. 4.22 The measured wafer temperature at selected locations during the ramp-up period for (a) $V_d=0$ mm/s, (b) $V_d=5$ mm/s, (c) $V_d=10$ mm/s and (d) $V_d=15$ mm/s with the wafer heated by a single lamp at $\omega=100$ rpm and $H=60$ mm for the final wafer temperature set at 140°C .



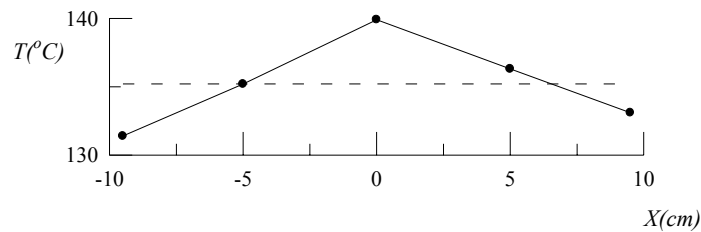
(a) $t=181\text{s}$, $T_{\text{mean}} = 135.5^{\circ}\text{C}$ & $\Delta T_{\text{max}} = 6.5^{\circ}\text{C}$ ($\Phi=0.0\%$)



(b) $t=238\text{s}$, $T_{\text{mean}} = 134.2^{\circ}\text{C}$ & $\Delta T_{\text{max}} = 6.1^{\circ}\text{C}$ ($\Phi=6.2\%$)

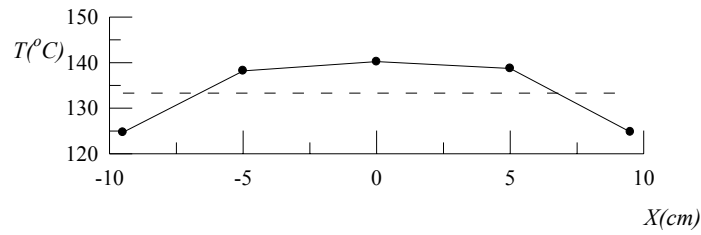


(c) $t=234\text{s}$, $T_{\text{mean}} = 134.6^{\circ}\text{C}$ & $\Delta T_{\text{max}} = 5.7^{\circ}\text{C}$ ($\Phi=12.3\%$)

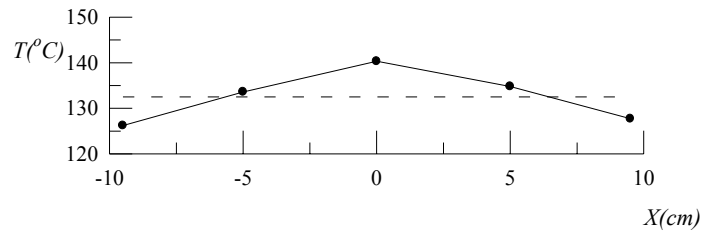


(d) $t=328\text{s}$, $T_{\text{mean}} = 135.2^{\circ}\text{C}$ & $\Delta T_{\text{max}} = 4.8^{\circ}\text{C}$ ($\Phi=26.2\%$)

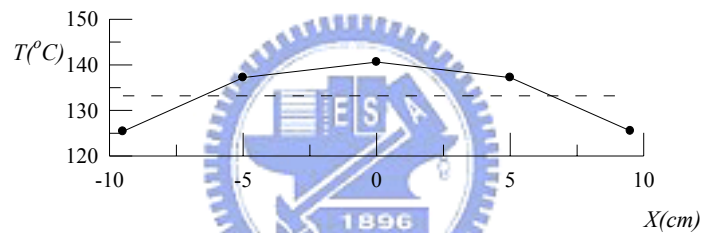
Fig. 4.23 The measured wafer temperature at selected locations during the ramp-up period for (a) $V_d=0$ mm/s, (b) $V_d=5$ mm/s, (c) $V_d=10$ mm/s and (d) $V_d=15$ mm/s with the wafer heated by a single lamp at $\omega=200$ rpm and $H=60$ mm for the final wafer temperature set at 140°C .



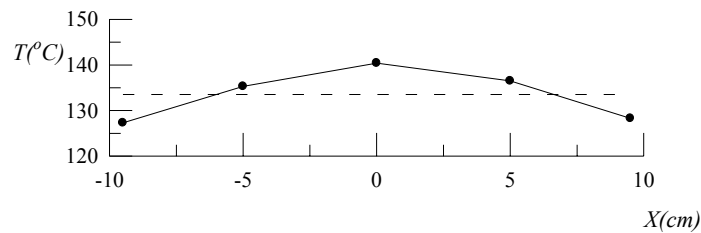
(a) $t=81\text{s}$, $T_{\text{mean}} = 133.3^{\circ}\text{C}$ & $\Delta T_{\text{max}} = 8.6^{\circ}\text{C}$ ($\Phi=0\%$)



(b) $t=81\text{s}$, $T_{\text{mean}} = 132.5^{\circ}\text{C}$ & $\Delta T_{\text{max}} = 7.8^{\circ}\text{C}$ ($\Phi=9.3\%$)

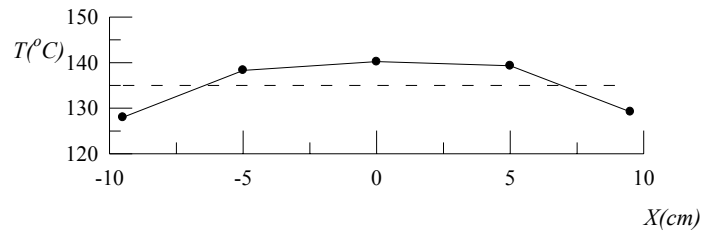


(c) $t=91\text{s}$, $T_{\text{mean}} = 133.2^{\circ}\text{C}$ & $\Delta T_{\text{max}} = 7.4^{\circ}\text{C}$ ($\Phi=14.0\%$)

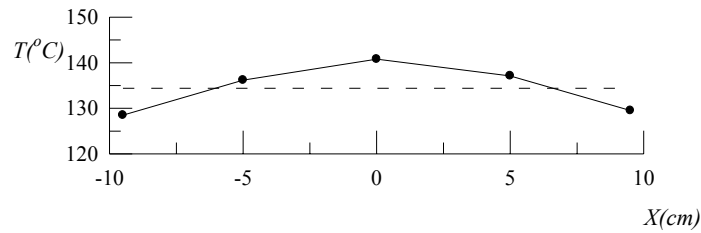


(d) $t=84\text{s}$, $T_{\text{mean}} = 133.5^{\circ}\text{C}$ & $\Delta T_{\text{max}} = 6.9^{\circ}\text{C}$ ($\Phi=19.8\%$)

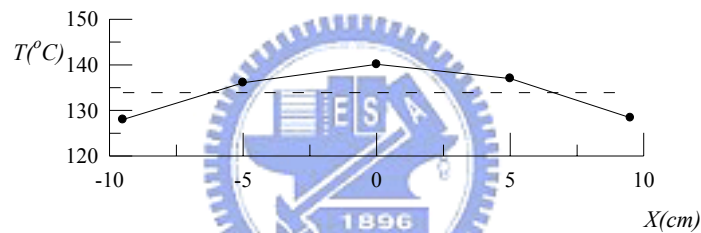
Fig. 4.24 The measured wafer temperature at selected locations during the ramp-up period for (a) $V_d=0$ mm/s, (b) $V_d=5$ mm/s, (c) $V_d=10$ mm/s and (d) $V_d=15$ mm/s with the wafer heated by a single lamp at $\omega=0$ rpm and $H=30$ mm for the final wafer temperature set at 140°C .



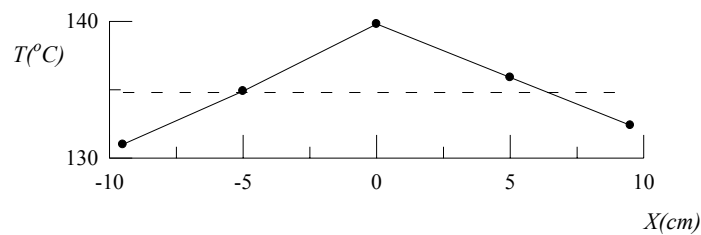
(a) $t=82\text{s}$, $T_{\text{mean}} = 135^{\circ}\text{C}$ & $\Delta T_{\text{max}} = 7^{\circ}\text{C}$ ($\Phi=18.6\%$)



(b) $t=83\text{s}$, $T_{\text{mean}} = 134.4^{\circ}\text{C}$ & $\Delta T_{\text{max}} = 6.4^{\circ}\text{C}$ ($\Phi=25.6\%$)

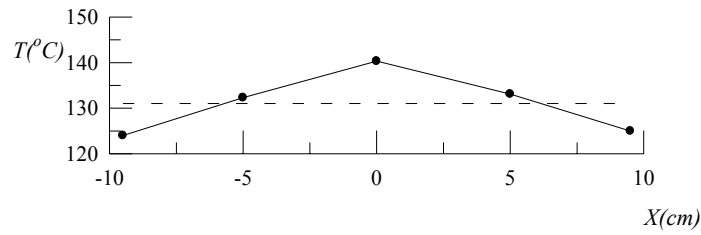


(c) $t=91\text{s}$, $T_{\text{mean}} = 133.9^{\circ}\text{C}$ & $\Delta T_{\text{max}} = 6.2^{\circ}\text{C}$ ($\Phi=27.9\%$)

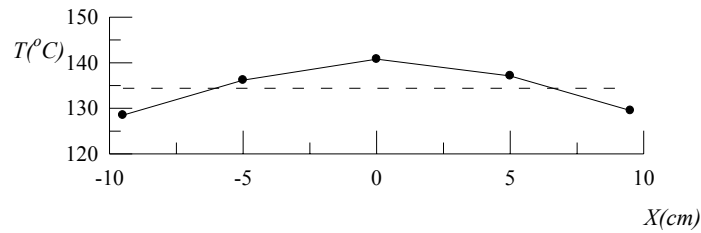


(d) $t=84\text{s}$, $T_{\text{mean}} = 134.8^{\circ}\text{C}$ & $\Delta T_{\text{max}} = 5^{\circ}\text{C}$ ($\Phi=41.9\%$)

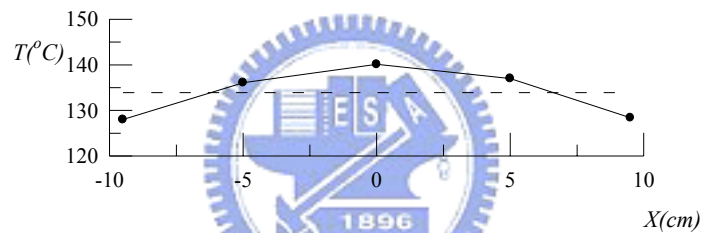
Fig. 4.25 The measured wafer temperature at selected locations during the ramp-up period for (a) $V_d=0$ mm/s, (b) $V_d=5$ mm/s, (c) $V_d=10$ mm/s and (d) $V_d=15$ mm/s with the wafer heated by a single lamp at $\omega=100$ rpm and $H=30$ mm for the final wafer temperature set at 140°C .



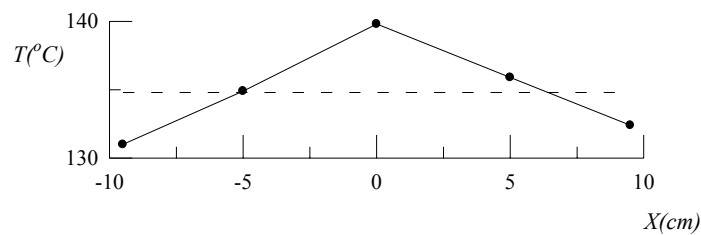
(a) $t=104\text{s}$, $T_{\text{mean}} = 131^{\circ}\text{C}$ & $\Delta T_{\text{max}} = 9.4^{\circ}\text{C}$ ($\Phi=-9.3\%$)



(b) $t=83\text{s}$, $T_{\text{mean}} = 134.4^{\circ}\text{C}$ & $\Delta T_{\text{max}} = 6.4^{\circ}\text{C}$ ($\Phi=21.0\%$)

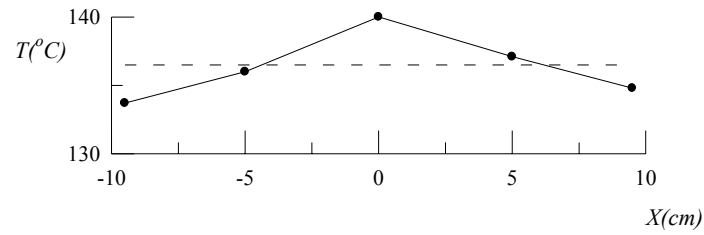


(c) $t=91\text{s}$, $T_{\text{mean}} = 133.9^{\circ}\text{C}$ & $\Delta T_{\text{max}} = 6.2^{\circ}\text{C}$ ($\Phi=27.9\%$)

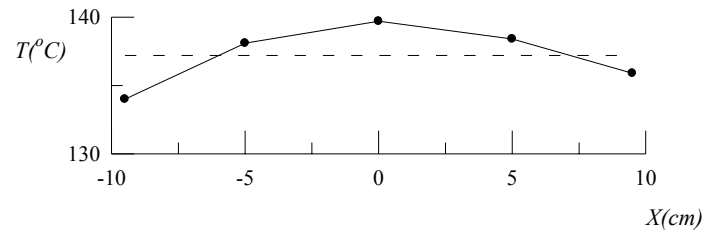


(d) $t=84\text{s}$, $T_{\text{mean}} = 134.8^{\circ}\text{C}$ & $\Delta T_{\text{max}} = 5^{\circ}\text{C}$ ($\Phi=41.9\%$)

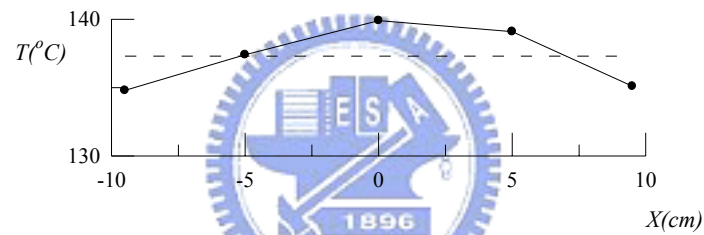
Fig. 4.26 The measured wafer temperature at selected locations during the ramp-up period for (a) $V_d=0$ mm/s, (b) $V_d=5$ mm/s, (c) $V_d=10$ mm/s and (d) $V_d=15$ mm/s with the wafer heated by a single lamp at $\omega=200$ rpm and $H=30$ mm for the final wafer temperature set at 140°C .



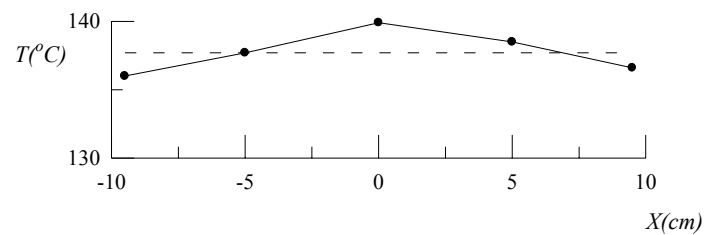
(a) $t=324\text{s}$, $T_{\text{mean}} = 136.5^{\circ}\text{C}$ & $\Delta T_{\text{max}} = 3.5^{\circ}\text{C}$ ($\Phi=0.0\%$)



(b) $t=376\text{s}$, $T_{\text{mean}} = 137.2^{\circ}\text{C}$ & $\Delta T_{\text{max}} = 3.2^{\circ}\text{C}$ ($\Phi=8.6\%$)

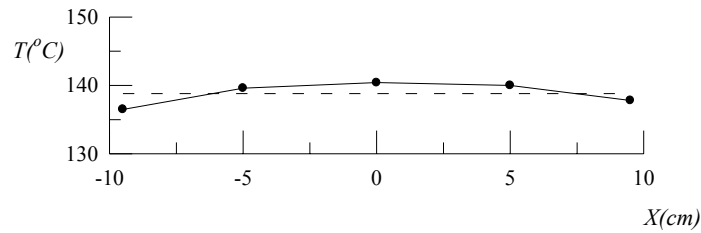


(c) $t=416\text{s}$, $T_{\text{mean}} = 137.3^{\circ}\text{C}$ & $\Delta T_{\text{max}} = 2.6^{\circ}\text{C}$ ($\Phi=25.7\%$)

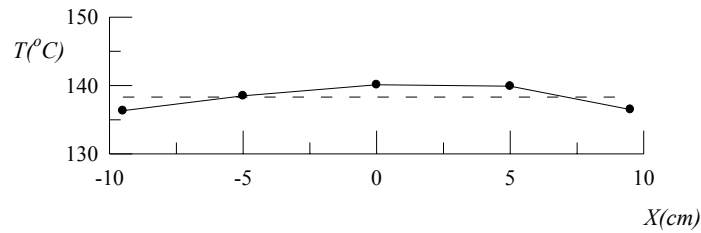


(d) $t=438\text{s}$, $T_{\text{mean}} = 137.7^{\circ}\text{C}$ & $\Delta T_{\text{max}} = 2.2^{\circ}\text{C}$ ($\Phi=37.1\%$)

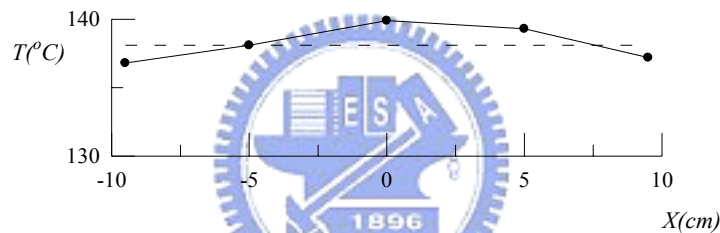
Fig. 4.27 The measured wafer temperature at selected locations during the ramp-up period for (a) $V_d=0$ mm/s, (b) $V_d=5$ mm/s, (c) $V_d=10$ mm/s and (d) $V_d=15$ mm/s with the wafer heated by a single lamp at $\omega=0$ rpm and $H=90$ mm for the final wafer temperature set at 140°C .



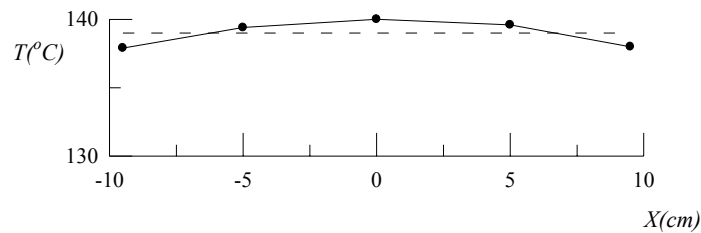
(a) $t=406\text{s}$, $T_{\text{mean}} = 138.8^{\circ}\text{C}$ & $\Delta T_{\text{max}} = 2.3^{\circ}\text{C}$ ($\Phi=24.3\%$)



(b) $t=455\text{s}$, $T_{\text{mean}} = 138.3^{\circ}\text{C}$ & $\Delta T_{\text{max}} = 2.0^{\circ}\text{C}$ ($\Phi=42.9\%$)

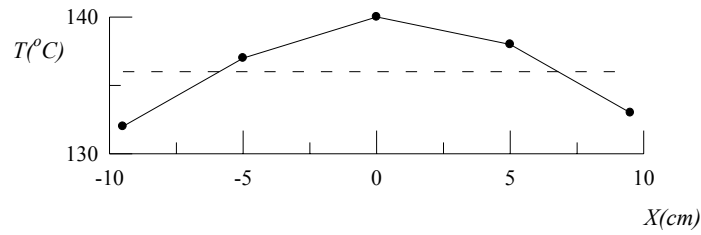


(c) $t=450\text{s}$, $T_{\text{mean}} = 138.1^{\circ}\text{C}$ & $\Delta T_{\text{max}} = 1.9^{\circ}\text{C}$ ($\Phi=45.7\%$)

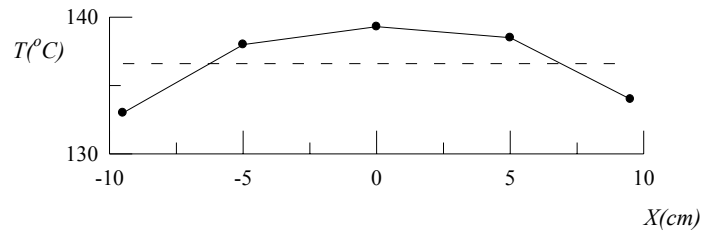


(d) $t=475\text{s}$, $T_{\text{mean}} = 139^{\circ}\text{C}$ & $\Delta T_{\text{max}} = 1.1^{\circ}\text{C}$ ($\Phi=68.6\%$)

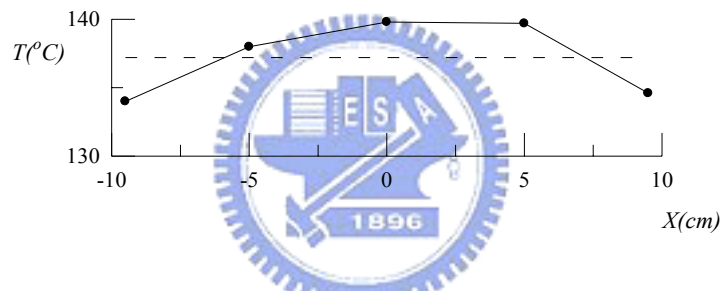
Fig. 4.28 The measured wafer temperature at selected locations during the ramp-up period for (a) $V_d=0$ mm/s, (b) $V_d=5$ mm/s, (c) $V_d=10$ mm/s and (d) $V_d=15$ mm/s with the wafer heated by a single lamp at $\omega=100$ rpm and $H=90$ mm for the final wafer temperature set at 140°C .



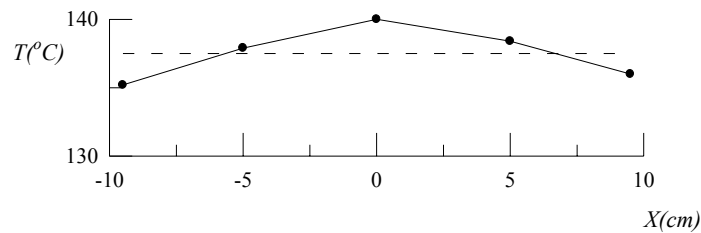
(a) $t=1421\text{s}$, $T_{\text{mean}} = 136^{\circ}\text{C}$ & $\Delta T_{\text{max}} = 4^{\circ}\text{C}$ ($\Phi = -14.3\%$)



(b) $t=2000\text{s}$, $T_{\text{mean}} = 136.6^{\circ}\text{C}$ & $\Delta T_{\text{max}} = 3.6^{\circ}\text{C}$ ($\Phi = -2.9\%$)

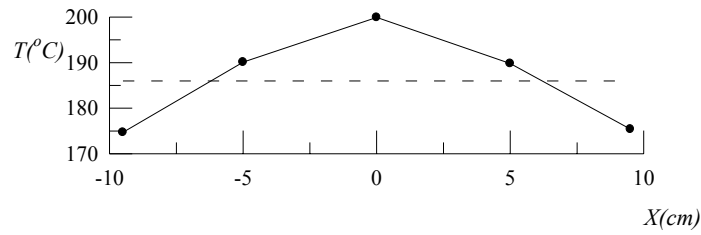


(c) $t=1900\text{s}$, $T_{\text{mean}} = 137.2^{\circ}\text{C}$ & $\Delta T_{\text{max}} = 3.2^{\circ}\text{C}$ ($\Phi = 8.6\%$)

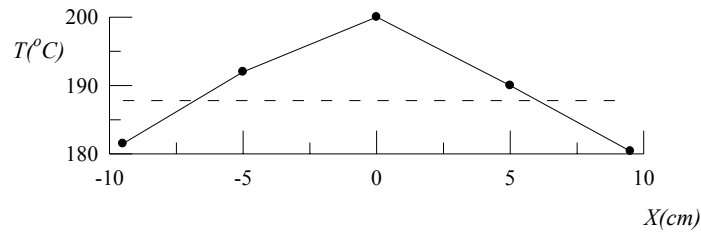


(d) $t=1962\text{s}$, $T_{\text{mean}} = 137.5^{\circ}\text{C}$ & $\Delta T_{\text{max}} = 2.3^{\circ}\text{C}$ ($\Phi = 34.3\%$)

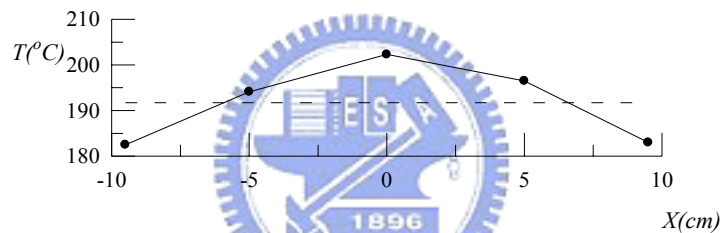
Fig. 4.29 The measured wafer temperature at selected locations during the ramp-up period for (a) $V_d=0$ mm/s, (b) $V_d=5$ mm/s, (c) $V_d=10$ mm/s and (d) $V_d=15$ mm/s with the wafer heated by a single lamp at $\omega=200$ rpm and $H=90$ mm for the final wafer temperature set at 140°C .



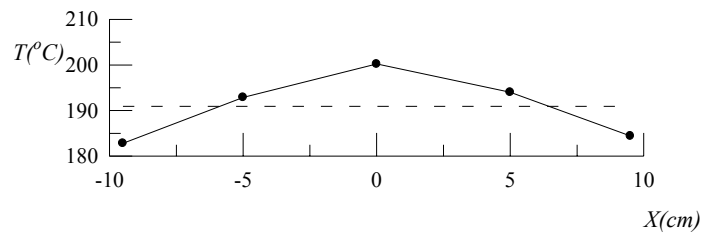
(a) $t = 58\text{s}$, $T_{\text{mean}} = 186^{\circ}\text{C}$ & $\Delta T_{\text{max}} = 13.8^{\circ}\text{C}$ ($\Phi = 0.0\%$)



(b) $t = 63\text{s}$, $T_{\text{mean}} = 188.8^{\circ}\text{C}$ & $\Delta T_{\text{max}} = 11.2^{\circ}\text{C}$ ($\Phi = 18.8\%$)

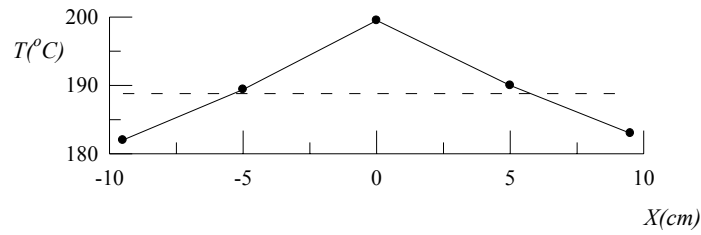


(c) $t = 66\text{s}$, $T_{\text{mean}} = 191.7^{\circ}\text{C}$ & $\Delta T_{\text{max}} = 10.6^{\circ}\text{C}$ ($\Phi = 23.2\%$)

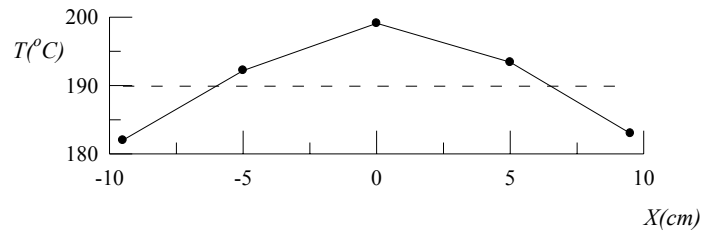


(d) $t = 62\text{s}$, $T_{\text{mean}} = 190.9^{\circ}\text{C}$ & $\Delta T_{\text{max}} = 9.3^{\circ}\text{C}$ ($\Phi = 32.6\%$)

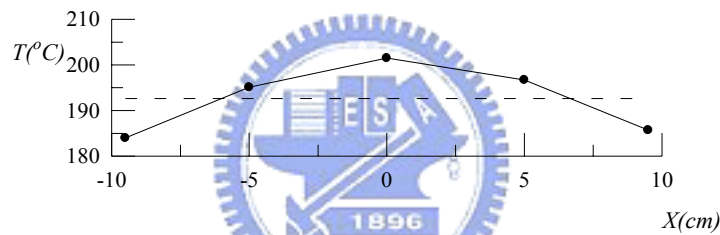
Fig. 4.30 The measured wafer temperature at selected locations during the ramp-up period for (a) $V_d = 0$ mm/s, (b) $V_d = 5$ mm/s, (c) $V_d = 10$ mm/s and (d) $V_d = 15$ mm/s with three heating lamps at $\omega = 0$ rpm and $H = 60$ mm for the final wafer temperature set at 200°C .



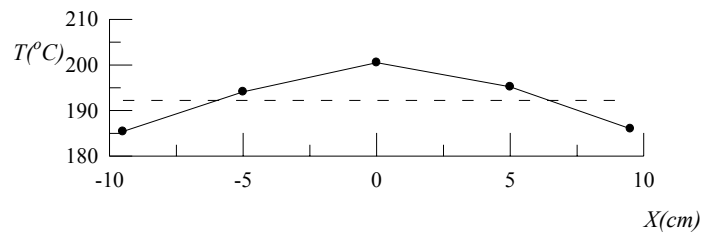
(a) $t = 58\text{s}$, $T_{\text{mean}} = 188.8^{\circ}\text{C}$ & $\Delta T_{\text{max}} = 10.7^{\circ}\text{C}$ ($\Phi = 22.5\%$)



(b) $t = 62\text{s}$, $T_{\text{mean}} = 189.9^{\circ}\text{C}$ & $\Delta T_{\text{max}} = 9.2^{\circ}\text{C}$ ($\Phi = 33.3\%$)

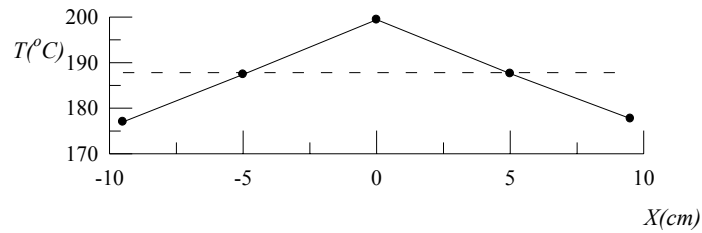


(c) $t = 66\text{s}$, $T_{\text{mean}} = 192.6^{\circ}\text{C}$ & $\Delta T_{\text{max}} = 8.9^{\circ}\text{C}$ ($\Phi = 35.5\%$)

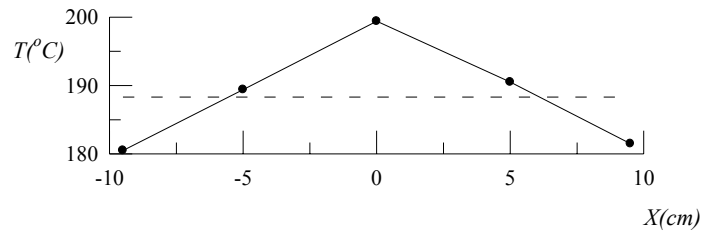


(d) $t = 62\text{s}$, $T_{\text{mean}} = 192.2^{\circ}\text{C}$ & $\Delta T_{\text{max}} = 8.3^{\circ}\text{C}$ ($\Phi = 39.9\%$)

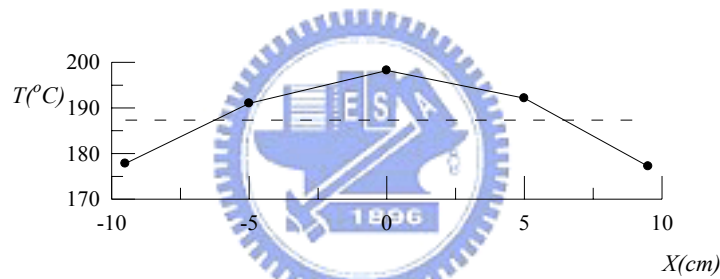
Fig. 4.31 The measured wafer temperature at selected locations during the ramp-up period for (a) $V_d = 0$ mm/s, (b) $V_d = 5$ mm/s, (c) $V_d = 10$ mm/s and (d) $V_d = 15$ mm/s with three heating lamps at $\omega = 100$ rpm and $H = 60$ mm for the final wafer temperature set at 200°C .



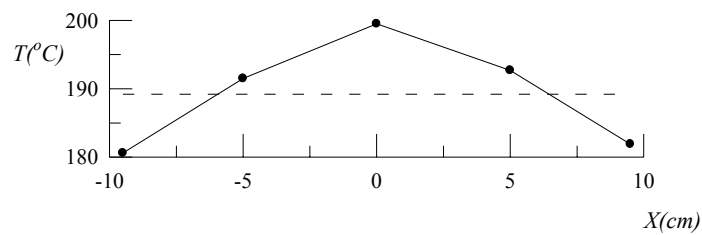
(a) $t = 60\text{s}$, $T_{\text{mean}} = 187.8^{\circ}\text{C}$ & $\Delta T_{\text{max}} = 11.6^{\circ}\text{C}$ ($\Phi=15.9\%$)



(b) $t = 67\text{s}$, $T_{\text{mean}} = 188.3^{\circ}\text{C}$ & $\Delta T_{\text{max}} = 11.1^{\circ}\text{C}$ ($\Phi=19.6\%$)

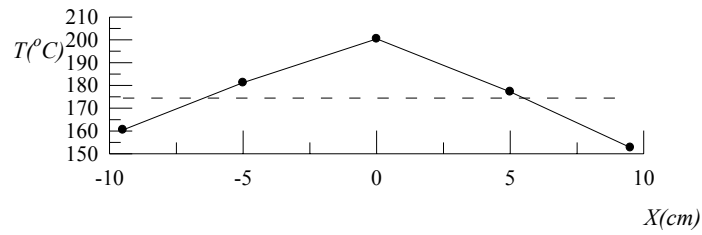


(c) $t = 68\text{s}$, $T_{\text{mean}} = 187.3^{\circ}\text{C}$ & $\Delta T_{\text{max}} = 10.9^{\circ}\text{C}$ ($\Phi=21.0\%$)

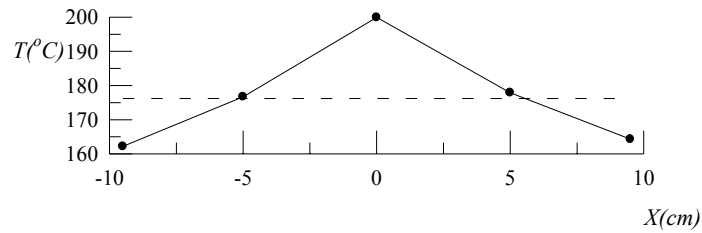


(d) $t = 65\text{s}$, $T_{\text{mean}} = 189.2^{\circ}\text{C}$ & $\Delta T_{\text{max}} = 10.3^{\circ}\text{C}$ ($\Phi=25.4\%$)

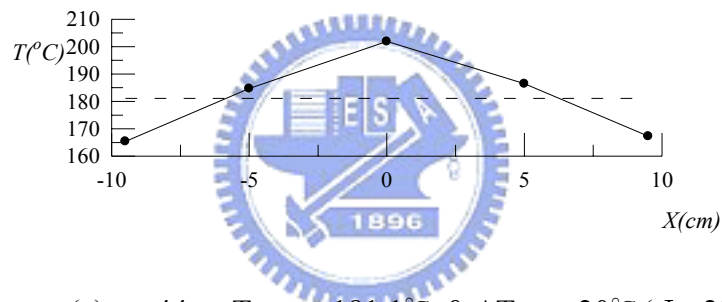
Fig. 4.32 The measured wafer temperature at selected locations during the ramp-up period for (a) $V_d=0$ mm/s, (b) $V_d=5$ mm/s, (c) $V_d=10$ mm/s and (d) $V_d=15$ mm/s with three heating lamps at $\omega=200$ rpm and $H= 60$ mm for the final wafer temperature set at 200°C .



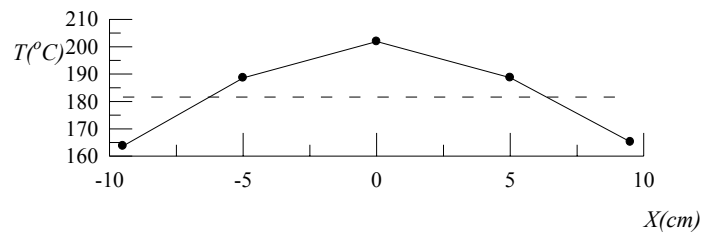
(a) $t = 40\text{s}$, $T_{\text{mean}} = 174.4^{\circ}\text{C}$ & $\Delta T_{\text{max}} = 26^{\circ}\text{C}$ ($\Phi = 0.0\%$)



(b) $t = 44\text{s}$, $T_{\text{mean}} = 176.2^{\circ}\text{C}$ & $\Delta T_{\text{max}} = 23.7^{\circ}\text{C}$ ($\Phi = 8.8\%$)

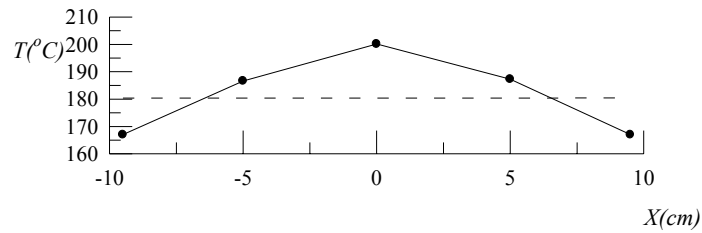


(c) $t = 44\text{s}$, $T_{\text{mean}} = 181.1^{\circ}\text{C}$ & $\Delta T_{\text{max}} = 20^{\circ}\text{C}$ ($\Phi = 23.1\%$)

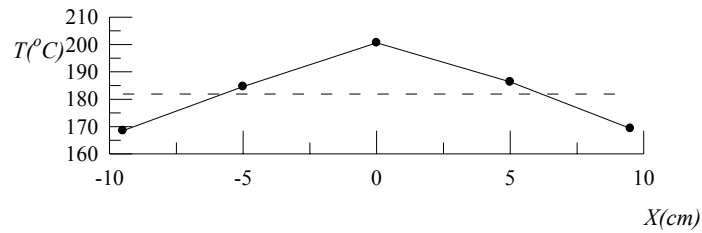


(d) $t = 41\text{s}$, $T_{\text{mean}} = 181.6^{\circ}\text{C}$ & $\Delta T_{\text{max}} = 17.9^{\circ}\text{C}$ ($\Phi = 31.2\%$)

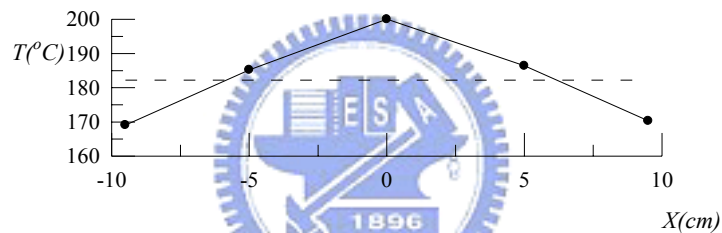
Fig. 4.33 The measured wafer temperature at selected locations during the ramp-up period for (a) $V_d = 0$ mm/s, (b) $V_d = 5$ mm/s, (c) $V_d = 10$ mm/s and (d) $V_d = 15$ mm/s with three heating lamps at $\omega = 0$ rpm and $H = 30$ mm for the final wafer temperature set at 200°C .



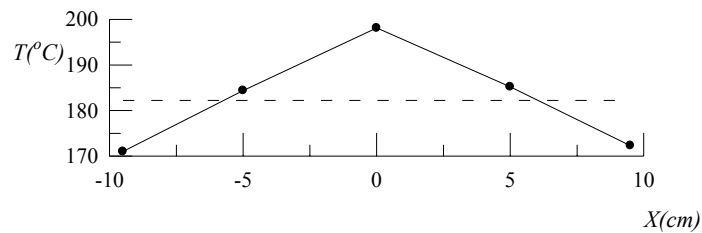
(a) $t = 40\text{s}$, $T_{\text{mean}} = 180.4^{\circ}\text{C}$ & $\Delta T_{\text{max}} = 19.7^{\circ}\text{C}$ ($\Phi = 24.2\%$)



(b) $t = 42\text{s}$, $T_{\text{mean}} = 181.9^{\circ}\text{C}$ & $\Delta T_{\text{max}} = 18.7^{\circ}\text{C}$ ($\Phi = 28.1\%$)

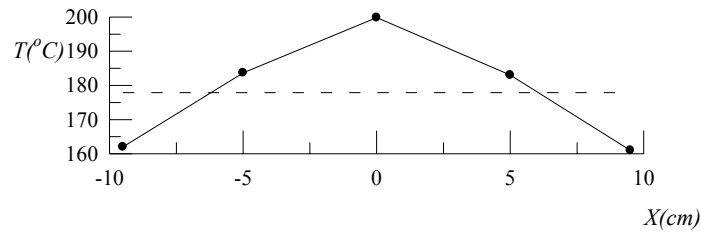


(c) $t = 45\text{s}$, $T_{\text{mean}} = 182.2^{\circ}\text{C}$ & $\Delta T_{\text{max}} = 17.8^{\circ}\text{C}$ ($\Phi = 31.5\%$)

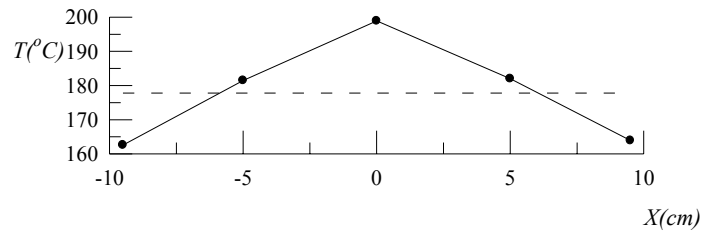


(d) $t = 43\text{s}$, $T_{\text{mean}} = 182.2^{\circ}\text{C}$ & $\Delta T_{\text{max}} = 15.9^{\circ}\text{C}$ ($\Phi = 38.8\%$)

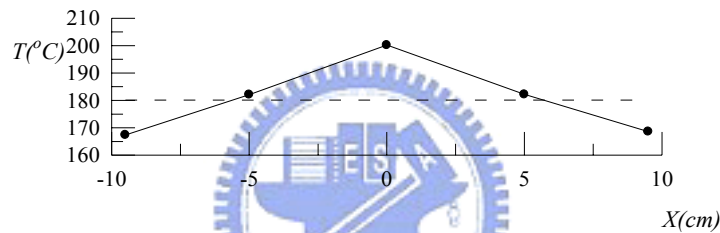
Fig. 4.34 The measured wafer temperature at selected locations during the ramp-up period for (a) $V_d = 0$ mm/s, (b) $V_d = 5$ mm/s, (c) $V_d = 10$ mm/s and (d) $V_d = 15$ mm/s with three heating lamps at $\omega = 100$ rpm and $H = 30$ mm for the final wafer temperature set at 200°C .



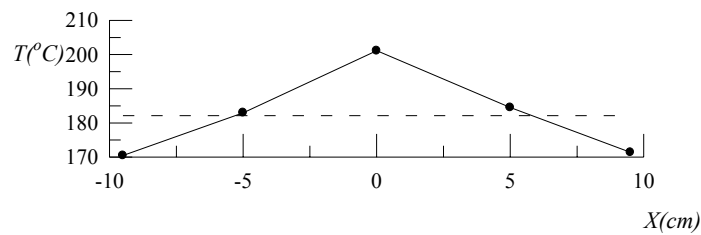
(a) $t = 62\text{s}$, $T_{\text{mean}} = 177.9^{\circ}\text{C}$ & $\Delta T_{\text{max}} = 21.9^{\circ}\text{C}$ ($\Phi = 15.8\%$)



(b) $t = 41\text{s}$, $T_{\text{mean}} = 177.8^{\circ}\text{C}$ & $\Delta T_{\text{max}} = 21.1^{\circ}\text{C}$ ($\Phi = 18.8\%$)

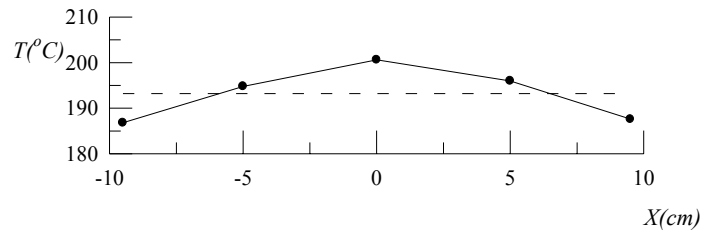


(c) $t = 44\text{s}$, $T_{\text{mean}} = 180.1^{\circ}\text{C}$ & $\Delta T_{\text{max}} = 20.1^{\circ}\text{C}$ ($\Phi = 22.7\%$)

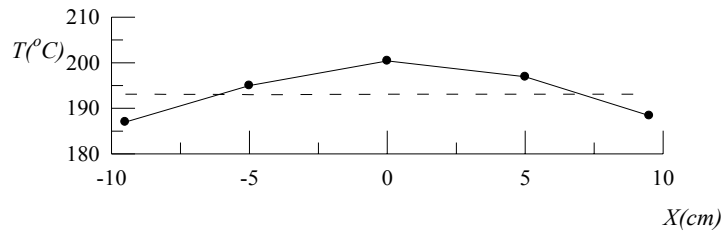


(d) $t = 44\text{s}$, $T_{\text{mean}} = 182.1^{\circ}\text{C}$ & $\Delta T_{\text{max}} = 19^{\circ}\text{C}$ ($\Phi = 26.9\%$)

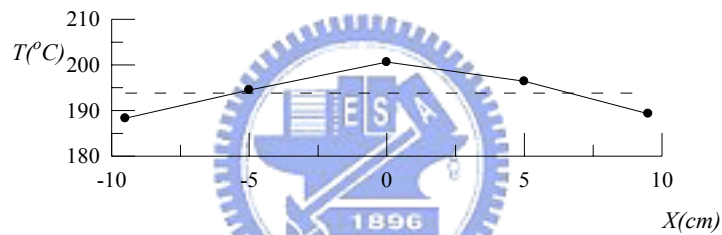
Fig. 4.35 The measured wafer temperature at selected locations during the ramp-up period for (a) $V_d = 0$ mm/s, (b) $V_d = 5$ mm/s, (c) $V_d = 10$ mm/s and (d) $V_d = 15$ mm/s with three heating lamps at $\omega = 200$ rpm and $H = 30$ mm for the final wafer temperature set at 200°C .



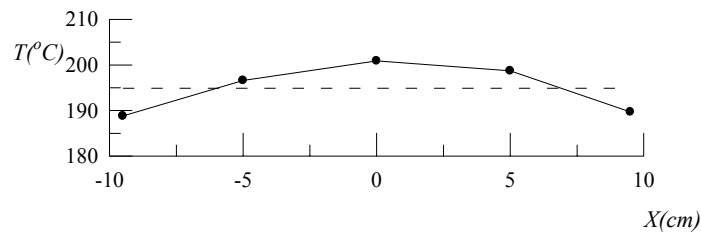
(a) $t=97\text{s}$, $T_{\text{mean}} = 193.2^{\circ}\text{C}$ & $\Delta T_{\text{max}} = 7.4^{\circ}\text{C}$ ($\Phi=0.0\%$)



(b) $t=88\text{s}$, $T_{\text{mean}} = 193.1^{\circ}\text{C}$ & $\Delta T_{\text{max}} = 7.2^{\circ}\text{C}$ ($\Phi=2.7\%$)

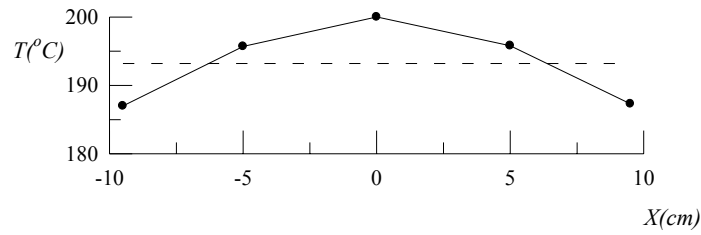


(c) $t=94\text{s}$, $T_{\text{mean}} = 193.8^{\circ}\text{C}$ & $\Delta T_{\text{max}} = 6.8^{\circ}\text{C}$ ($\Phi=8.0\%$)

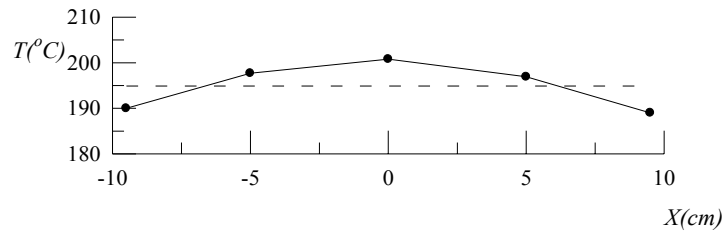


(d) $t=90\text{s}$, $T_{\text{mean}} = 194.9^{\circ}\text{C}$ & $\Delta T_{\text{max}} = 6.1^{\circ}\text{C}$ ($\Phi=17.6\%$)

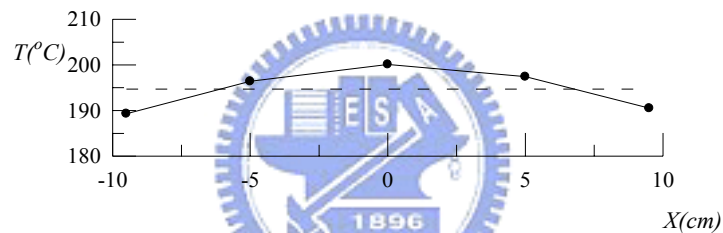
Fig. 4.36 The measured wafer temperature at selected locations during the ramp-up period for (a) $V_d=0$ mm/s, (b) $V_d=5$ mm/s, (c) $V_d=10$ mm/s and (d) $V_d=15$ mm/s with three heating lamps at $\omega=0$ rpm and $H=90$ mm for the final wafer temperature set at 200°C .



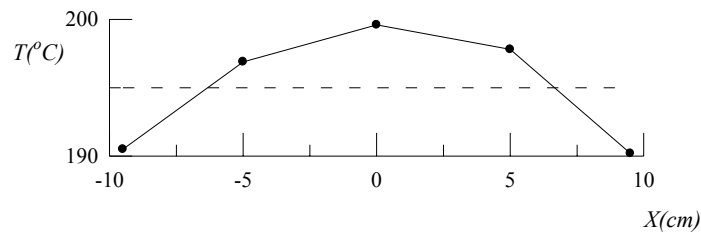
(a) $t=97\text{s}$, $T_{\text{mean}} = 193.2^{\circ}\text{C}$ & $\Delta T_{\text{max}} = 6.2^{\circ}\text{C}$ ($\Phi=16.2\%$)



(b) $t=89\text{s}$, $T_{\text{mean}} = 194.9^{\circ}\text{C}$ & $\Delta T_{\text{max}} = 5.9^{\circ}\text{C}$ ($\Phi=20.3\%$)

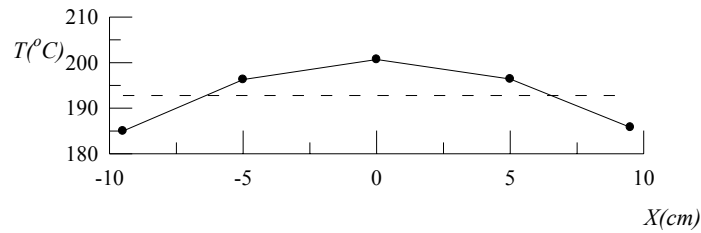


(c) $t=94\text{s}$, $T_{\text{mean}} = 194.7^{\circ}\text{C}$ & $\Delta T_{\text{max}} = 5.4^{\circ}\text{C}$ ($\Phi=27.0\%$)

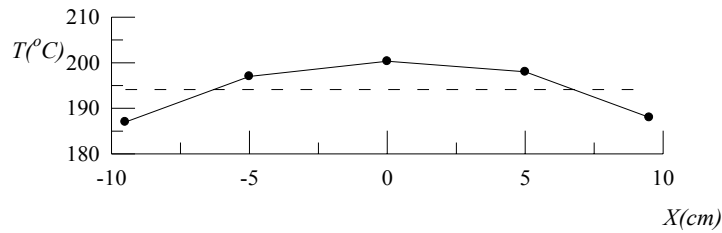


(d) $t=89\text{s}$, $T_{\text{mean}} = 195^{\circ}\text{C}$ & $\Delta T_{\text{max}} = 4.6^{\circ}\text{C}$ ($\Phi=37.8\%$)

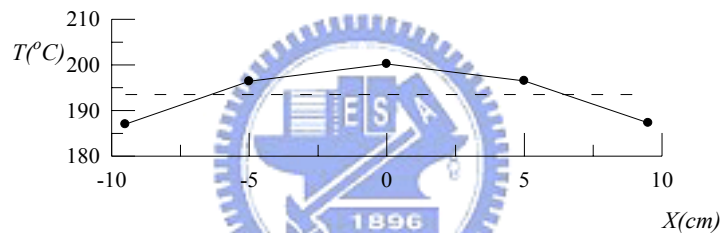
Fig. 4.37 The measured wafer temperature at selected locations during the ramp-up period for (a) $V_d=0$ mm/s, (b) $V_d=5$ mm/s, (c) $V_d=10$ mm/s and (d) $V_d=15$ mm/s with three heating lamps at $\omega=100$ rpm and $H=90$ mm for the final wafer temperature set at 200°C .



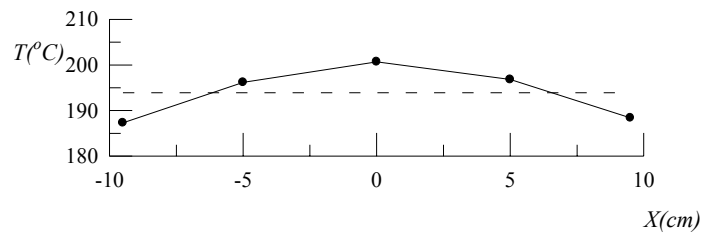
(a) $t=103\text{s}$, $T_{\text{mean}} = 192.8^{\circ}\text{C}$ & $\Delta T_{\text{max}} = 7.8^{\circ}\text{C}$ ($\Phi = -5.4\%$)



(b) $t=102\text{s}$, $T_{\text{mean}} = 194.1^{\circ}\text{C}$ & $\Delta T_{\text{max}} = 7.1^{\circ}\text{C}$ ($\Phi = 4.1\%$)

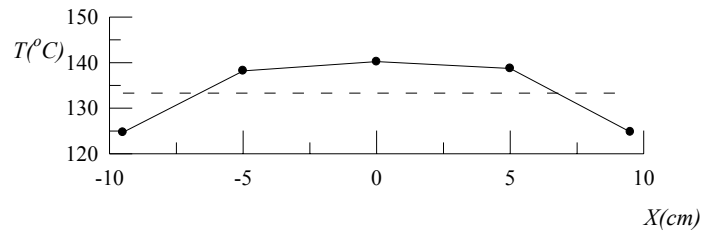


(c) $t=104\text{s}$, $T_{\text{mean}} = 193.5^{\circ}\text{C}$ & $\Delta T_{\text{max}} = 6.7^{\circ}\text{C}$ ($\Phi = 9.5\%$)

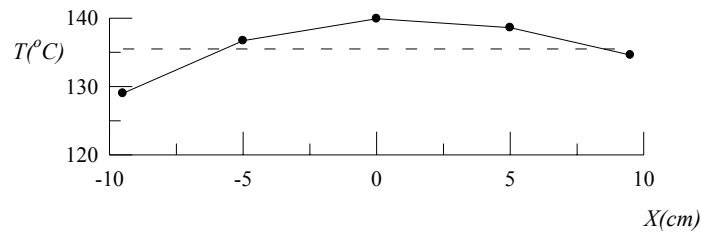


(d) $t=101\text{s}$, $T_{\text{mean}} = 193.9^{\circ}\text{C}$ & $\Delta T_{\text{max}} = 6.6^{\circ}\text{C}$ ($\Phi = 10.8\%$)

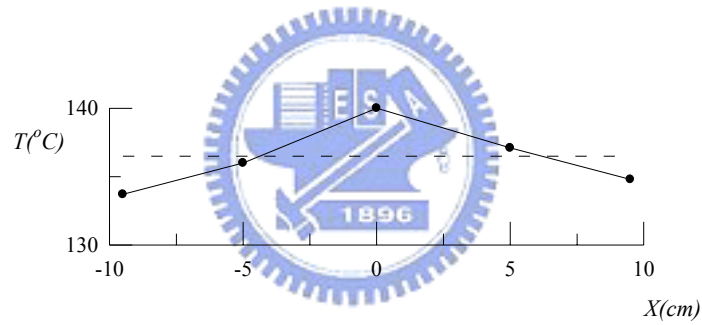
Fig. 4.38 The measured wafer temperature at selected locations during the ramp-up period for (a) $V_d=0$ mm/s, (b) $V_d=5$ mm/s, (c) $V_d=10$ mm/s and (d) $V_d=15$ mm/s with three heating lamps at $\omega=200$ rpm and $H=90$ mm for the final wafer temperature set at 200°C .



(a) $t=81\text{s}$, $T_{\text{mean}} = 133.3^{\circ}\text{C}$ & $\Delta T_{\text{max}} = 8.6^{\circ}\text{C}$ ($\Phi=0.0\%$)

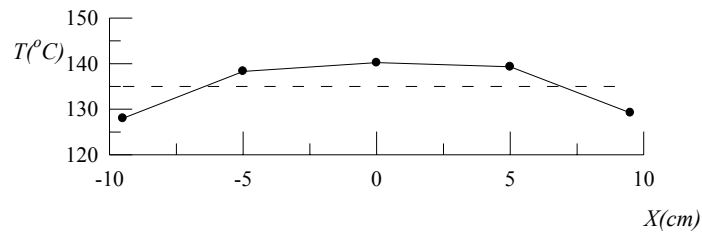


(b) $t=126\text{s}$, $T_{\text{mean}} = 135.5^{\circ}\text{C}$ & $\Delta T_{\text{max}} = 6.5^{\circ}\text{C}$ ($\Phi=24.4\%$)

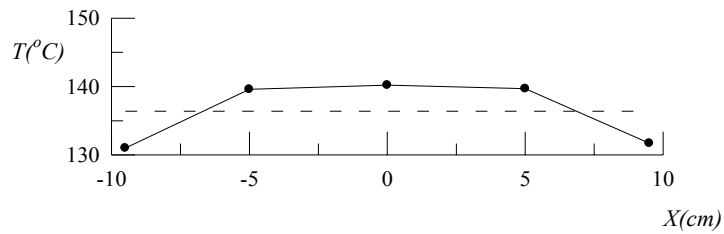


(c) $t=324\text{s}$, $T_{\text{mean}} = 136.5^{\circ}\text{C}$ & $\Delta T_{\text{max}} = 3.5^{\circ}\text{C}$ ($\Phi=59.3\%$)

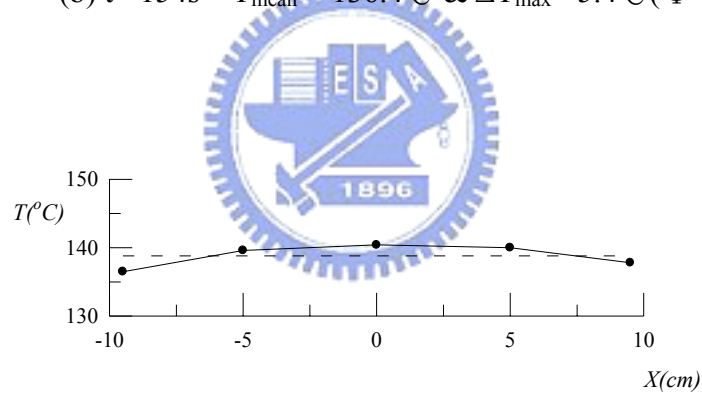
Fig. 4.39 The measured wafer temperature at selected locations during the ramp-up period for (a) $H=30\text{ mm}$, (b) $H=60\text{ mm}$, and (c) $H=90\text{ mm}$ with the wafer heated by a single lamp at $\omega=0\text{ rpm}$ and $V_d=0\text{ mm/s}$ for the final wafer temperature set at 140°C .



(a) $t=82\text{s}$, $T_{\text{mean}} = 135^{\circ}\text{C}$ & $\Delta T_{\text{max}} = 7^{\circ}\text{C}$ ($\Phi=18.6\%$)

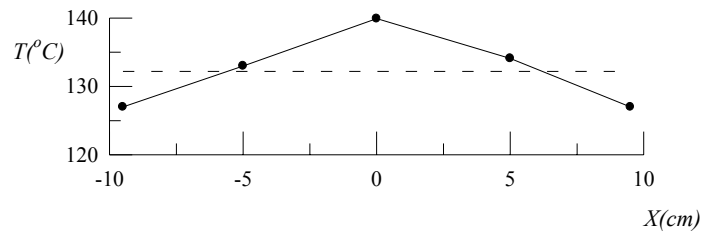


(b) $t=154\text{s}$, $T_{\text{mean}} = 136.4^{\circ}\text{C}$ & $\Delta T_{\text{max}} = 5.4^{\circ}\text{C}$ ($\Phi=33.2\%$)

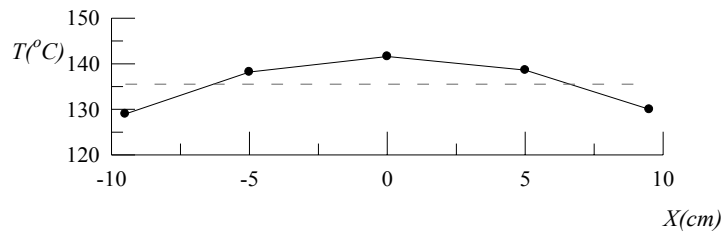


(c) $t=406\text{s}$, $T_{\text{mean}} = 138.8^{\circ}\text{C}$ & $\Delta T_{\text{max}} = 2.3^{\circ}\text{C}$ ($\Phi=73.3\%$)

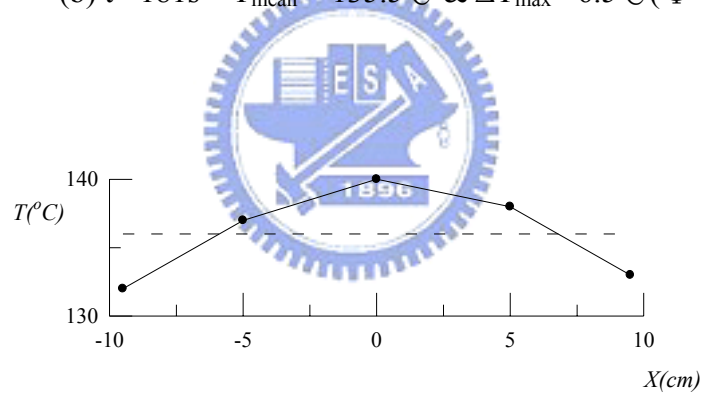
Fig. 4.40 The measured wafer temperature at selected locations during the ramp-up period for (a) $H=30\text{ mm}$, (b) $H=60\text{ mm}$, and (c) $H=90\text{ mm}$ with the wafer heated by a single lamp at $\omega=100\text{ rpm}$ and $V_d=0\text{ mm/s}$ for the final wafer temperature set at 140°C .



(a) $t=94\text{s}$, $T_{\text{mean}} = 132.2^{\circ}\text{C}$ & $\Delta T_{\text{max}} = 7.7^{\circ}\text{C}$ ($\Phi=10.5\%$)

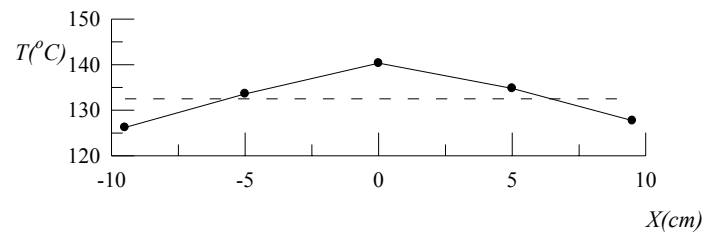


(b) $t=181\text{s}$, $T_{\text{mean}} = 135.5^{\circ}\text{C}$ & $\Delta T_{\text{max}} = 6.5^{\circ}\text{C}$ ($\Phi=24.4\%$)

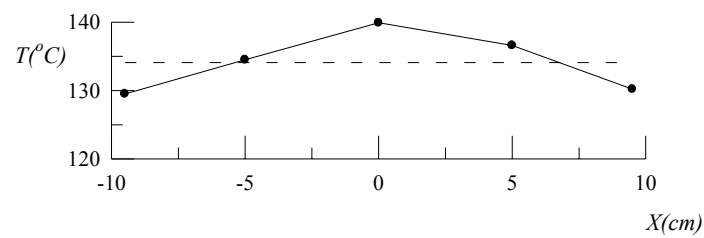


(c) $t=1421\text{s}$, $T_{\text{mean}} = 136^{\circ}\text{C}$ & $\Delta T_{\text{max}} = 4^{\circ}\text{C}$ ($\Phi=53.5\%$)

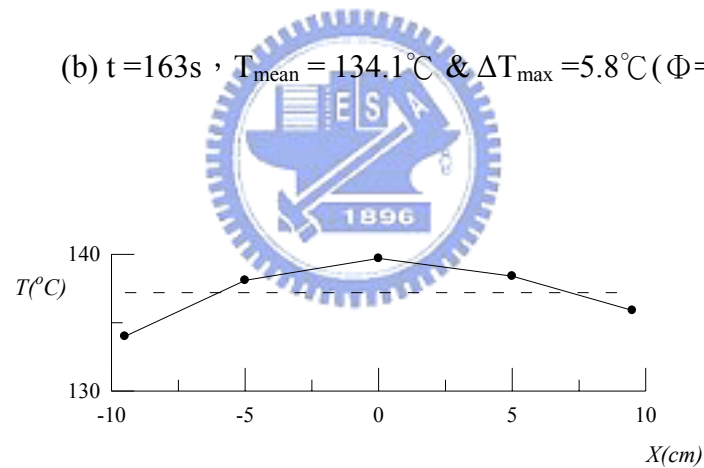
Fig. 4.41 The measured wafer temperature at selected locations during the ramp-up period for (a) $H=30\text{ mm}$, (b) $H=60\text{ mm}$, and (c) $H=90\text{ mm}$ with the wafer heated by a single lamp at $\omega=200\text{ rpm}$ and $V_d=0\text{ mm/s}$ for the final wafer temperature set at 140°C .



(a) $t=81\text{s}$, $T_{\text{mean}} = 132.5^{\circ}\text{C}$ & $\Delta T_{\text{max}} = 7.8^{\circ}\text{C}$ ($\Phi=9.3\%$)

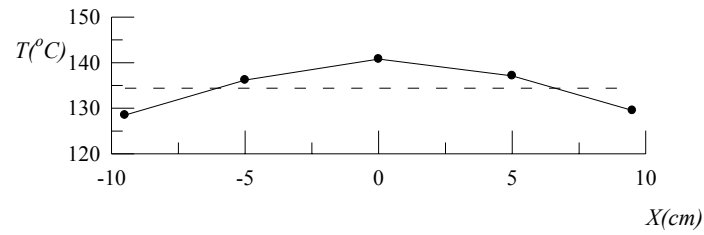


(b) $t=163\text{s}$, $T_{\text{mean}} = 134.1^{\circ}\text{C}$ & $\Delta T_{\text{max}} = 5.8^{\circ}\text{C}$ ($\Phi=32.6\%$)

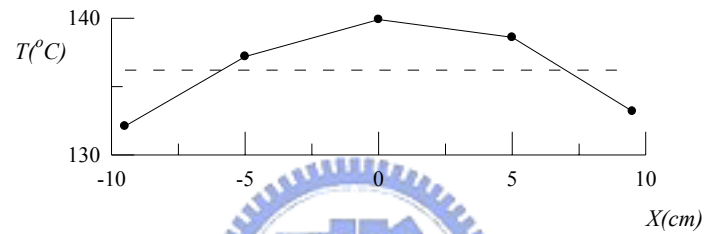


(c) $t=376\text{s}$, $T_{\text{mean}} = 137.2^{\circ}\text{C}$ & $\Delta T_{\text{max}} = 3.2^{\circ}\text{C}$ ($\Phi=62.8\%$)

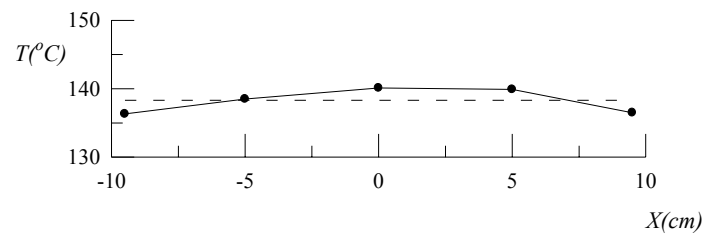
Fig. 4.42 The measured wafer temperature at selected locations during the ramp-up period for (a) $H=30\text{ mm}$, (b) $H=60\text{ mm}$, and (c) $H=90\text{ mm}$ with the wafer heated by a single lamp at $\omega=0\text{ rpm}$ and $V_d=5\text{ mm/s}$ for the final wafer temperature set at 140°C .



(a) $t = 83\text{s}$, $T_{\text{mean}} = 134.4^\circ\text{C}$ & $\Delta T_{\text{max}} = 6.4^\circ\text{C}$ ($\Phi = 25.6\%$)

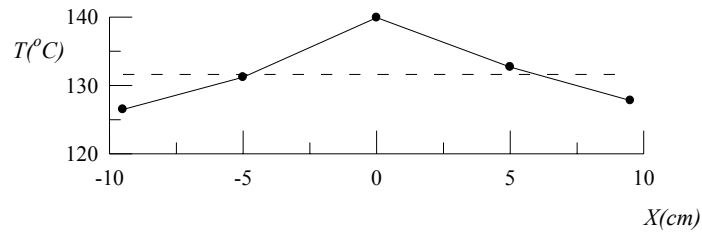


(b) $t = 184\text{s}$, $T_{\text{mean}} = 136.2^\circ\text{C}$ & $\Delta T_{\text{max}} = 4.1^\circ\text{C}$ ($\Phi = 52.3\%$)

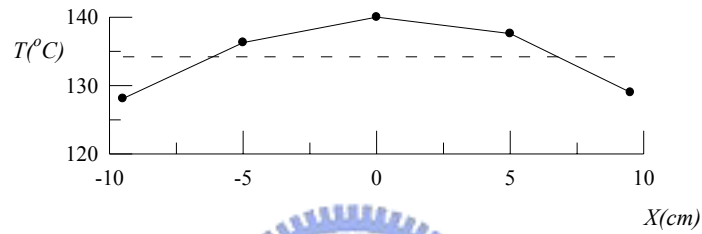


(c) $t = 455\text{s}$, $T_{\text{mean}} = 138.3^\circ\text{C}$ & $\Delta T_{\text{max}} = 2.0^\circ\text{C}$ ($\Phi = 76.7\%$)

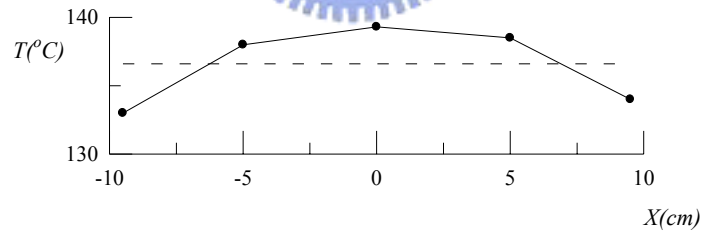
Fig. 4.43 The measured wafer temperature at selected locations during the ramp-up period for (a) $H=30\text{ mm}$, (b) $H=60\text{ mm}$, and (c) $H=90\text{ mm}$ with the wafer heated by a single lamp at $\omega=100\text{ rpm}$ and $V_d=5\text{ mm/s}$ for the final wafer temperature set at 140°C .



(a) $t=99\text{s}$, $T_{\text{mean}} = 131.6^\circ\text{C}$ & $\Delta T_{\text{max}} = 8.3^\circ\text{C}$ ($\Phi=3.5\%$)

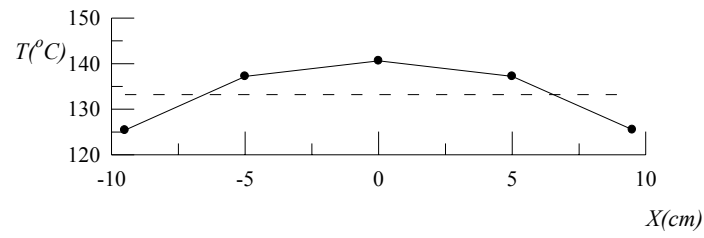


(b) $t=238\text{s}$, $T_{\text{mean}} = 134.2^\circ\text{C}$ & $\Delta T_{\text{max}} = 6.1^\circ\text{C}$ ($\Phi=29.1\%$)

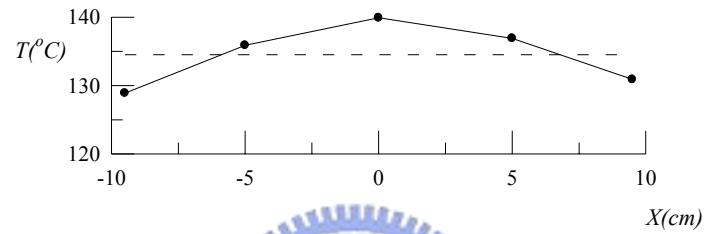


(c) $t=2000\text{s}$, $T_{\text{mean}} = 136.6^\circ\text{C}$ & $\Delta T_{\text{max}} = 3.6^\circ\text{C}$ ($\Phi=58.1\%$)

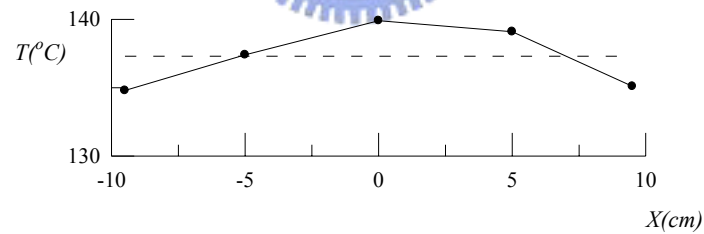
Fig. 4.44 The measured wafer temperature at selected locations during the ramp-up period for (a) $H=30\text{ mm}$, (b) $H=60\text{ mm}$, and (c) $H=90\text{ mm}$ with the wafer heated by a single lamp at $\omega=200\text{ rpm}$ and $V_d=5\text{ mm/s}$ for the final wafer temperature set at 140°C .



(a) $t=91\text{s}$, $T_{\text{mean}} = 133.2^\circ\text{C}$ & $\Delta T_{\text{max}} = 7.4^\circ\text{C}$ ($\Phi=14.0\%$)

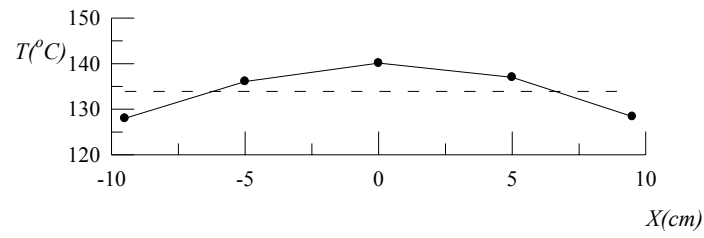


(b) $t=157\text{s}$, $T_{\text{mean}} = 134.5^\circ\text{C}$ & $\Delta T_{\text{max}} = 5.6^\circ\text{C}$ ($\Phi=34.9\%$)

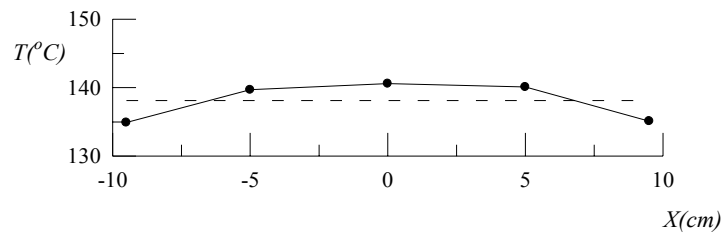


(c) $t=416\text{s}$, $T_{\text{mean}} = 137.3^\circ\text{C}$ & $\Delta T_{\text{max}} = 2.6^\circ\text{C}$ ($\Phi=69.8\%$)

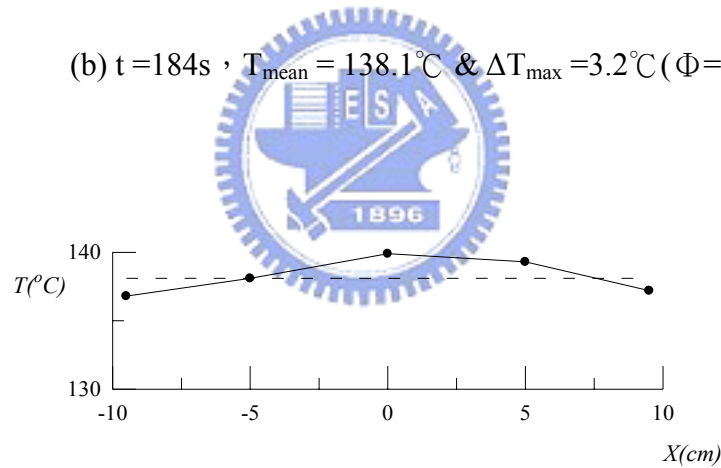
Fig. 4.45 The measured wafer temperature at selected locations during the ramp-up period for (a) $H=30\text{ mm}$, (b) $H=60\text{ mm}$, and (c) $H=90\text{ mm}$ with the wafer heated by a single lamp at $\omega=0\text{ rpm}$ and $V_d=10\text{ mm/s}$ for the final wafer temperature set at 140°C .



(a) $t=91\text{s}$, $T_{\text{mean}} = 133.9^{\circ}\text{C}$ & $\Delta T_{\text{max}} = 6.2^{\circ}\text{C}$ ($\Phi=27.9\%$)

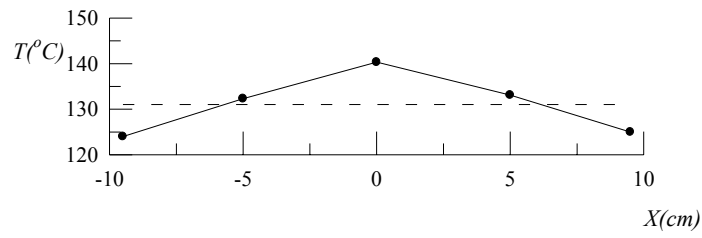


(b) $t=184\text{s}$, $T_{\text{mean}} = 138.1^{\circ}\text{C}$ & $\Delta T_{\text{max}} = 3.2^{\circ}\text{C}$ ($\Phi=62.8\%$)

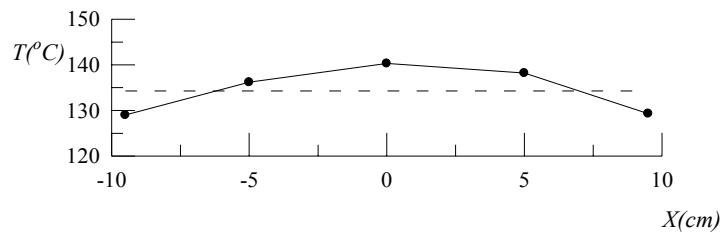


(c) $t=450\text{s}$, $T_{\text{mean}} = 138.1^{\circ}\text{C}$ & $\Delta T_{\text{max}} = 1.9^{\circ}\text{C}$ ($\Phi=77.9\%$)

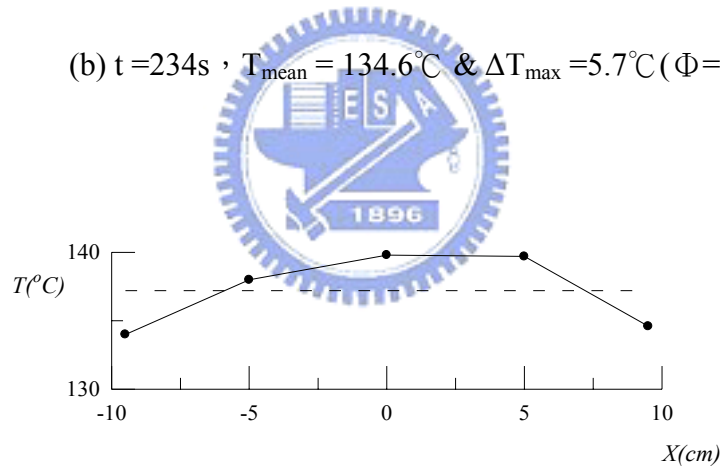
Fig. 4.46 The measured wafer temperature at selected locations during the ramp-up period for (a) $H=30\text{ mm}$, (b) $H=60\text{ mm}$, and (c) $H=90\text{ mm}$ with the wafer heated by a single lamp at $\omega=100\text{ rpm}$ and $V_d=10\text{ mm/s}$ for the final wafer temperature set at 140°C .



(a) $t=104\text{s}$, $T_{\text{mean}} = 131^{\circ}\text{C}$ & $\Delta T_{\text{max}} = 9.4^{\circ}\text{C}$ ($\Phi = -9.3\%$)

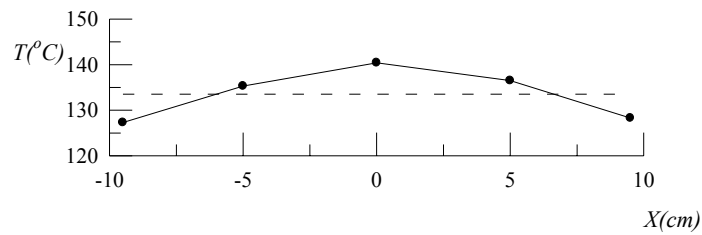


(b) $t=234\text{s}$, $T_{\text{mean}} = 134.6^{\circ}\text{C}$ & $\Delta T_{\text{max}} = 5.7^{\circ}\text{C}$ ($\Phi = 33.7\%$)

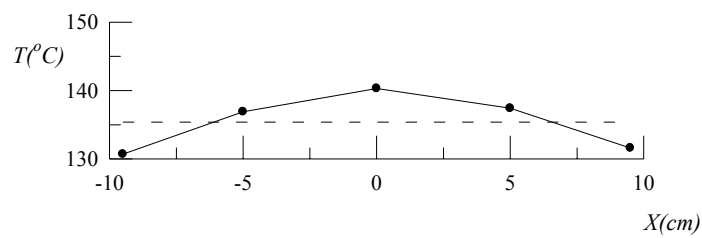


(c) $t=1900\text{s}$, $T_{\text{mean}} = 137.2^{\circ}\text{C}$ & $\Delta T_{\text{max}} = 3.2^{\circ}\text{C}$ ($\Phi = 62.8\%$)

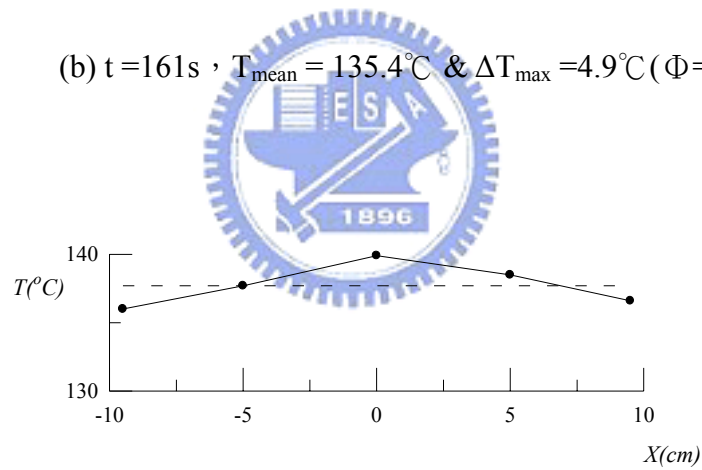
Fig. 4.47 The measured wafer temperature at selected locations during the ramp-up period for (a) $H=30\text{ mm}$, (b) $H=60\text{ mm}$, and (c) $H=90\text{ mm}$ with the wafer heated by a single lamp at $\omega=200\text{ rpm}$ and $V_d=10\text{ mm/s}$ for the final wafer temperature set at 140°C .



(a) $t=84\text{s}$, $T_{\text{mean}} = 133.5^{\circ}\text{C}$ & $\Delta T_{\text{max}} = 6.9^{\circ}\text{C}$ ($\Phi=19.8\%$)

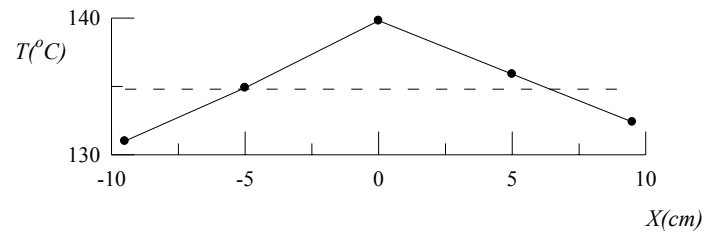


(b) $t=161\text{s}$, $T_{\text{mean}} = 135.4^{\circ}\text{C}$ & $\Delta T_{\text{max}} = 4.9^{\circ}\text{C}$ ($\Phi=43.0\%$)

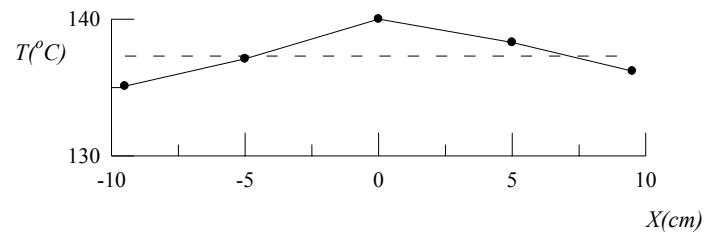


(c) $t=438\text{s}$, $T_{\text{mean}} = 137.7^{\circ}\text{C}$ & $\Delta T_{\text{max}} = 2.2^{\circ}\text{C}$ ($\Phi=74.4\%$)

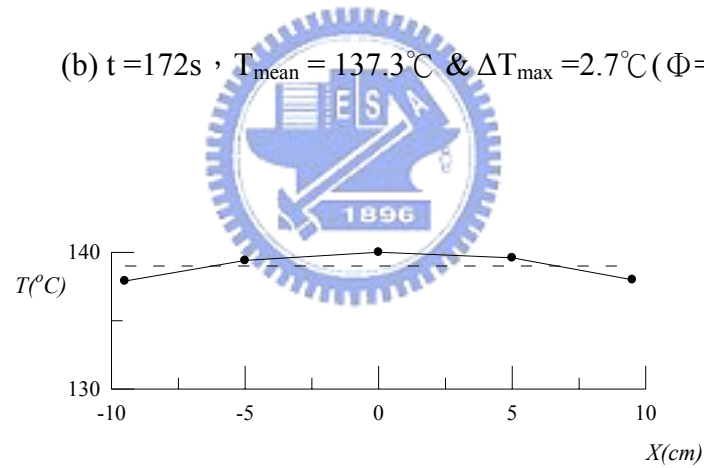
Fig. 4.48 The measured wafer temperature at selected locations during the ramp-up period for (a) $H=30\text{ mm}$, (b) $H=60\text{ mm}$, and (c) $H=90\text{ mm}$ with the wafer heated by a single lamp at $\omega=0\text{ rpm}$ and $V_d=15\text{ mm/s}$ for the final wafer temperature set at 140°C .



(a) $t=84\text{s}$, $T_{\text{mean}} = 134.8^{\circ}\text{C}$ & $\Delta T_{\text{max}} = 5^{\circ}\text{C}$ ($\Phi=41.9\%$)

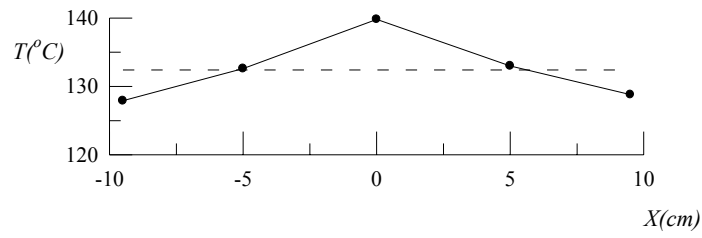


(b) $t=172\text{s}$, $T_{\text{mean}} = 137.3^{\circ}\text{C}$ & $\Delta T_{\text{max}} = 2.7^{\circ}\text{C}$ ($\Phi=68.6\%$)

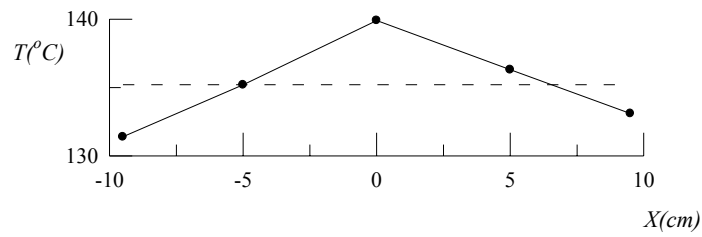


(c) $t=475\text{s}$, $T_{\text{mean}} = 139^{\circ}\text{C}$ & $\Delta T_{\text{max}} = 1.1^{\circ}\text{C}$ ($\Phi=87.2\%$)

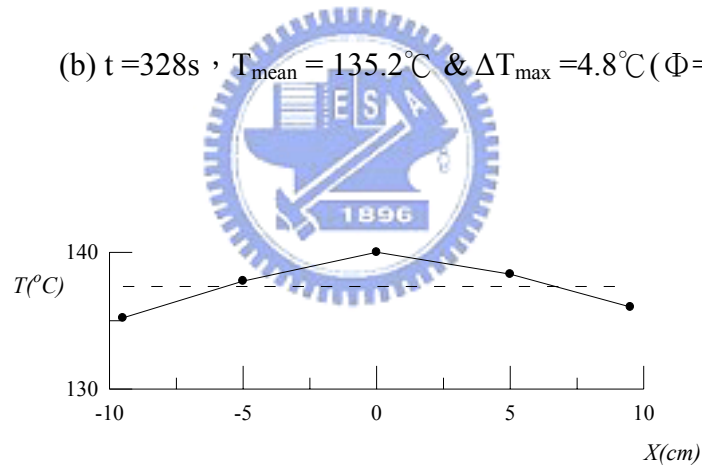
Fig. 4.49 The measured wafer temperature at selected locations during the ramp-up period for (a) $H=30\text{ mm}$, (b) $H=60\text{ mm}$, and (c) $H=90\text{ mm}$ with the wafer heated by a single lamp at $\omega=100\text{ rpm}$ and $V_d=15\text{ mm/s}$ for the final wafer temperature set at 140°C .



(a) $t = 91\text{s}$, $T_{\text{mean}} = 132.4^\circ\text{C}$ & $\Delta T_{\text{max}} = 7.4^\circ\text{C}$ ($\Phi = 14.0\%$)

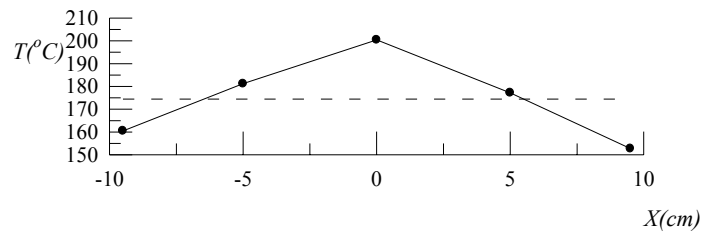


(b) $t = 328\text{s}$, $T_{\text{mean}} = 135.2^\circ\text{C}$ & $\Delta T_{\text{max}} = 4.8^\circ\text{C}$ ($\Phi = 44.2\%$)

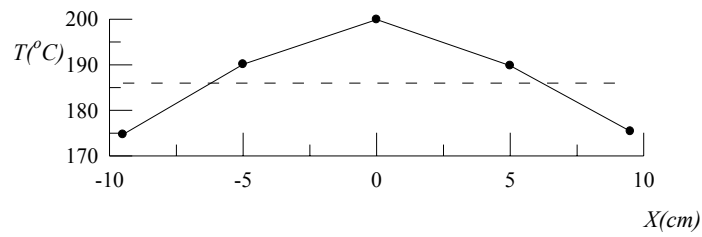


(c) $t = 1352\text{s}$, $T_{\text{mean}} = 137.5^\circ\text{C}$ & $\Delta T_{\text{max}} = 2.3^\circ\text{C}$ ($\Phi = 73.3\%$)

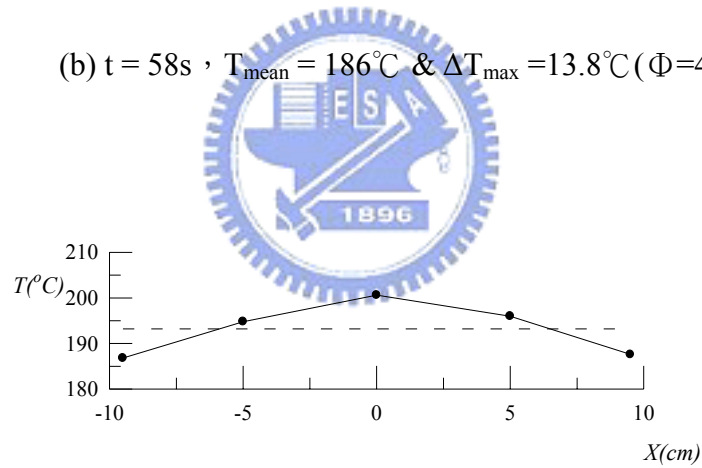
Fig. 4.50 The measured wafer temperature at selected locations during the ramp-up period for (a) $H=30\text{ mm}$, (b) $H=60\text{ mm}$, and (c) $H=90\text{ mm}$ with the wafer heated by a single lamp at $\omega=200\text{ rpm}$ and $V_d=15\text{ mm/s}$ for the final wafer temperature set at 140°C .



(a) $t = 40\text{s}$, $T_{\text{mean}} = 174.4^{\circ}\text{C}$ & $\Delta T_{\text{max}} = 26^{\circ}\text{C}$ ($\Phi = 0.0\%$)

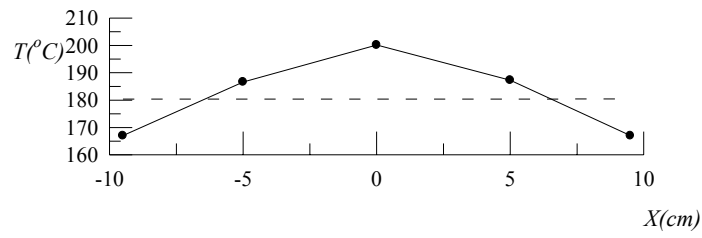


(b) $t = 58\text{s}$, $T_{\text{mean}} = 186^{\circ}\text{C}$ & $\Delta T_{\text{max}} = 13.8^{\circ}\text{C}$ ($\Phi = 46.9\%$)

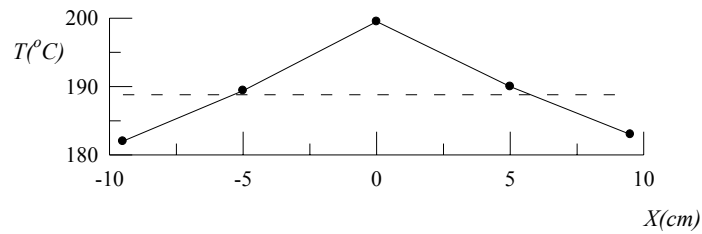


(c) $t = 97\text{s}$, $T_{\text{mean}} = 193.2^{\circ}\text{C}$ & $\Delta T_{\text{max}} = 7.4^{\circ}\text{C}$ ($\Phi = 71.5\%$)

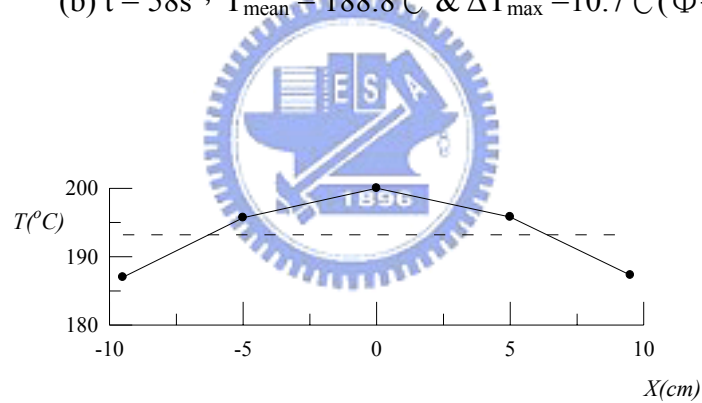
Fig. 4.51 The measured wafer temperature at selected locations during the ramp-up period for (a) $H=30\text{ mm}$, (b) $H=60\text{ mm}$, and (c) $H=90\text{ mm}$ with the wafer heated by a three lamps at $\omega=0\text{ rpm}$ and $V_d=0\text{ mm/s}$ for the final wafer temperature set at 200°C .



(a) $t = 40\text{s}$, $T_{\text{mean}} = 180.4^{\circ}\text{C}$ & $\Delta T_{\text{max}} = 19.7^{\circ}\text{C}$ ($\Phi = 24.2\%$)

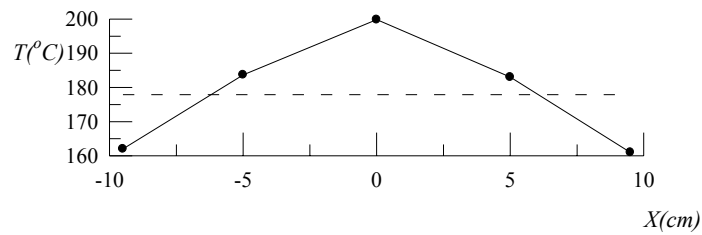


(b) $t = 58\text{s}$, $T_{\text{mean}} = 188.8^{\circ}\text{C}$ & $\Delta T_{\text{max}} = 10.7^{\circ}\text{C}$ ($\Phi = 58.8\%$)

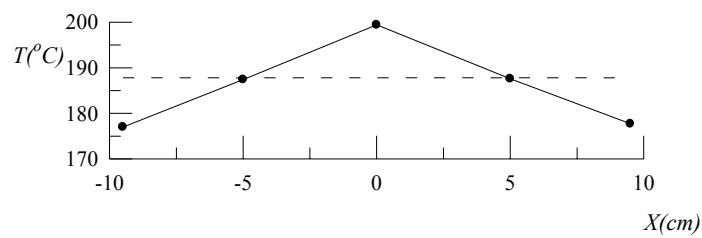


(c) $t = 97\text{s}$, $T_{\text{mean}} = 193.2^{\circ}\text{C}$ & $\Delta T_{\text{max}} = 6.2^{\circ}\text{C}$ ($\Phi = 76.2\%$)

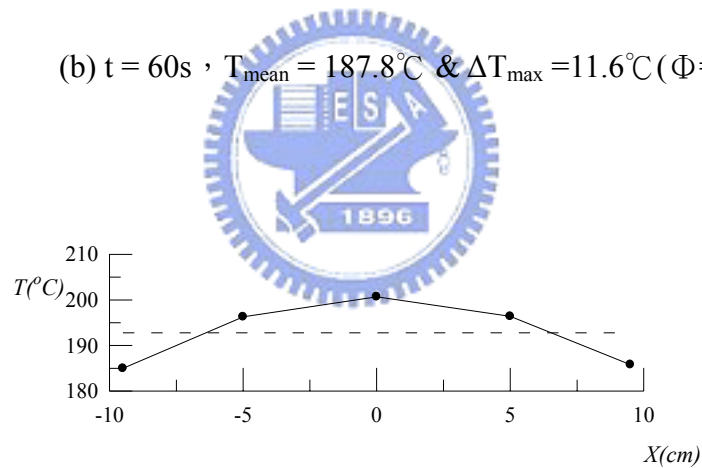
Fig. 4.52 The measured wafer temperature at selected locations during the ramp-up period for (a) $H=30\text{ mm}$, (b) $H=60\text{ mm}$, and (c) $H=90\text{ mm}$ with three heating lamps at $\omega=100\text{ rpm}$ and $V_d=0\text{ mm/s}$ for the final wafer temperature set at 200°C .



(a) $t = 62\text{s}$, $T_{\text{mean}} = 177.9^{\circ}\text{C}$ & $\Delta T_{\text{max}} = 21.9^{\circ}\text{C}$ ($\Phi = 15.8\%$)

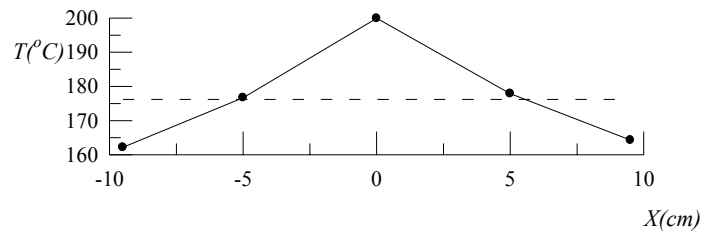


(b) $t = 60\text{s}$, $T_{\text{mean}} = 187.8^{\circ}\text{C}$ & $\Delta T_{\text{max}} = 11.6^{\circ}\text{C}$ ($\Phi = 55.4\%$)

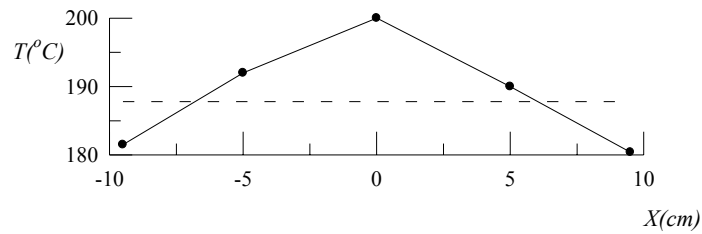


(c) $t = 103\text{s}$, $T_{\text{mean}} = 192.8^{\circ}\text{C}$ & $\Delta T_{\text{max}} = 7.8^{\circ}\text{C}$ ($\Phi = 70\%$)

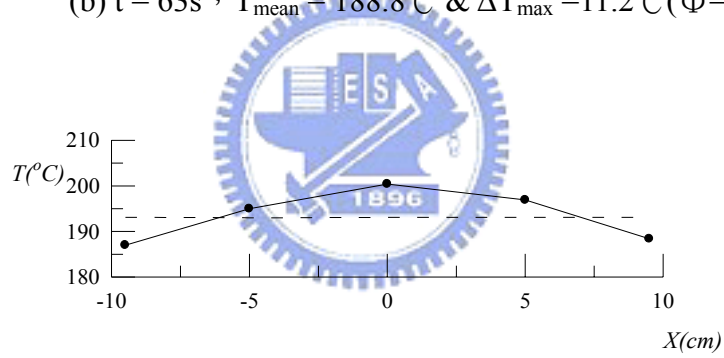
Fig. 4.53 The measured wafer temperature at selected locations during the ramp-up period for (a) $H=30\text{ mm}$, (b) $H=60\text{ mm}$, and (c) $H=90\text{ mm}$ with three heating lamps at $\omega=200\text{ rpm}$ and $V_d=0\text{ mm/s}$ for the final wafer temperature set at 200°C .



(a) $t = 44\text{s}$, $T_{\text{mean}} = 176.2^{\circ}\text{C}$ & $\Delta T_{\text{max}} = 23.7^{\circ}\text{C}$ ($\Phi = 8.8\%$)

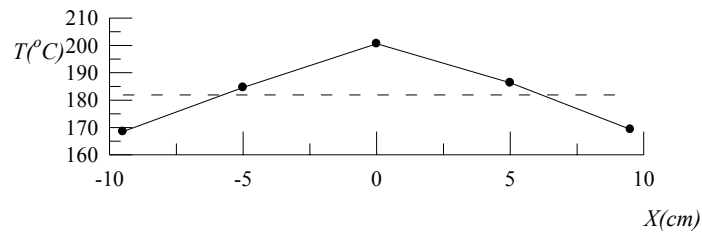


(b) $t = 63\text{s}$, $T_{\text{mean}} = 188.8^{\circ}\text{C}$ & $\Delta T_{\text{max}} = 11.2^{\circ}\text{C}$ ($\Phi = 56.9\%$)

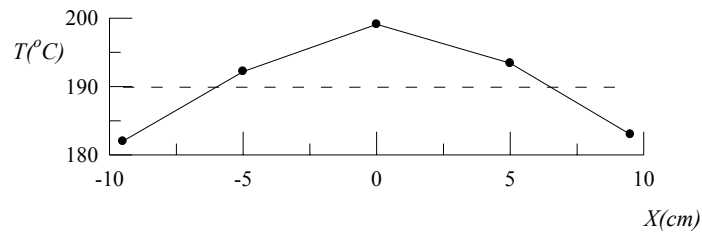


(c) $t = 88\text{s}$, $T_{\text{mean}} = 193.1^{\circ}\text{C}$ & $\Delta T_{\text{max}} = 7.2^{\circ}\text{C}$ ($\Phi = 72.3\%$)

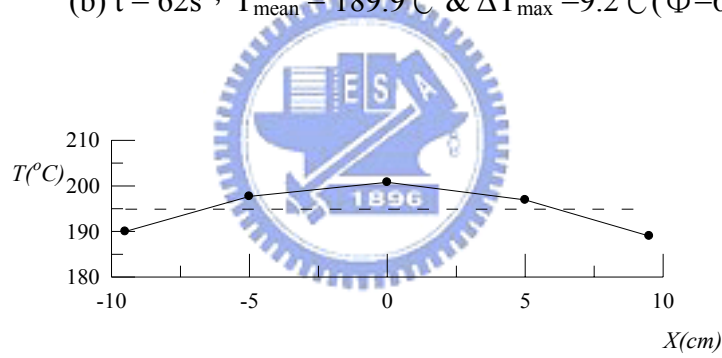
Fig. 4.54 The measured wafer temperature at selected locations during the ramp-up period for (a) $H=30\text{ mm}$, (b) $H=60\text{ mm}$, and (c) $H=90\text{ mm}$ with three heating lamps at $\omega=0\text{ rpm}$ and $V_d=5\text{ mm/s}$ for the final wafer temperature set at 200°C .



(a) $t = 42\text{s}$, $T_{\text{mean}} = 181.9^{\circ}\text{C}$ & $\Delta T_{\text{max}} = 18.7^{\circ}\text{C}$ ($\Phi = 28.1\%$)

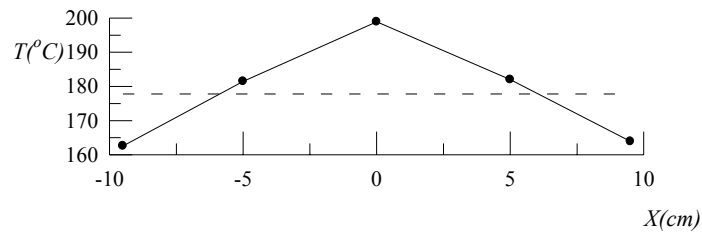


(b) $t = 62\text{s}$, $T_{\text{mean}} = 189.9^{\circ}\text{C}$ & $\Delta T_{\text{max}} = 9.2^{\circ}\text{C}$ ($\Phi = 64.6\%$)

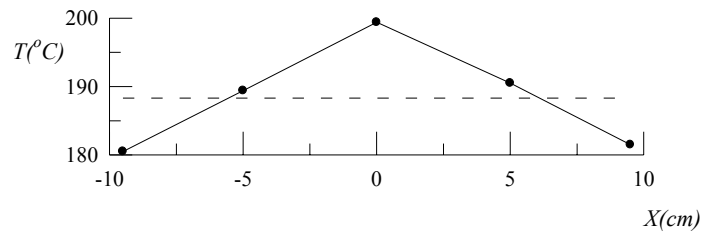


(c) $t = 89\text{s}$, $T_{\text{mean}} = 194.9^{\circ}\text{C}$ & $\Delta T_{\text{max}} = 5.9^{\circ}\text{C}$ ($\Phi = 77.3\%$)

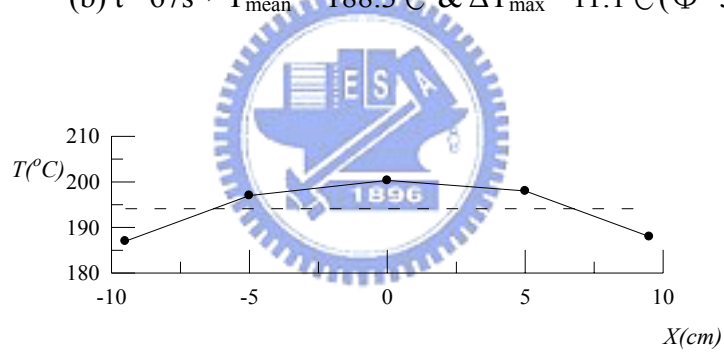
Fig. 4.55 The measured wafer temperature at selected locations during the ramp-up period for (a) $H=30\text{ mm}$, (b) $H=60\text{ mm}$, and (c) $H=90\text{ mm}$ with three heating lamps at $\omega=100\text{ rpm}$ and $V_d=5\text{ mm/s}$ for the final wafer temperature set at 200°C .



(a) $t = 41\text{s}$, $T_{\text{mean}} = 177.8^{\circ}\text{C}$ & $\Delta T_{\text{max}} = 21.1^{\circ}\text{C}$ ($\Phi = 18.8\%$)

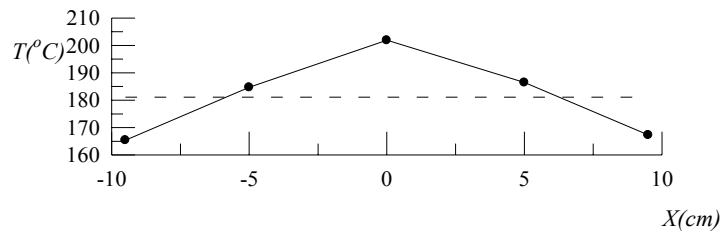


(b) $t = 67\text{s}$, $T_{\text{mean}} = 188.3^{\circ}\text{C}$ & $\Delta T_{\text{max}} = 11.1^{\circ}\text{C}$ ($\Phi = 57.3\%$)

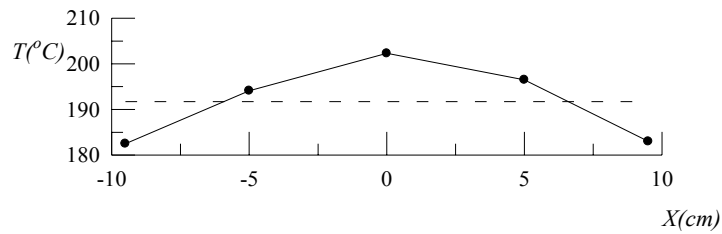


(c) $t = 102\text{s}$, $T_{\text{mean}} = 194.1^{\circ}\text{C}$ & $\Delta T_{\text{max}} = 7.1^{\circ}\text{C}$ ($\Phi = 72.7\%$)

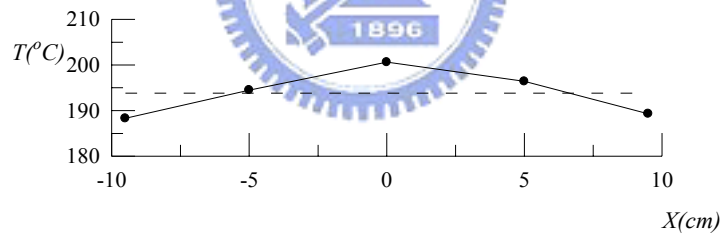
Fig. 4.56 The measured wafer temperature at selected locations during the ramp-up period for (a) $H=30\text{ mm}$, (b) $H=60\text{ mm}$, and (c) $H=90\text{ mm}$ with three heating lamps at $\omega=200\text{ rpm}$ and $V_d=5\text{ mm/s}$ for the final wafer temperature set at 200°C .



(a) $t = 44\text{s}$, $T_{\text{mean}} = 181.1^{\circ}\text{C}$ & $\Delta T_{\text{max}} = 20^{\circ}\text{C}$ ($\Phi = 23.1\%$)

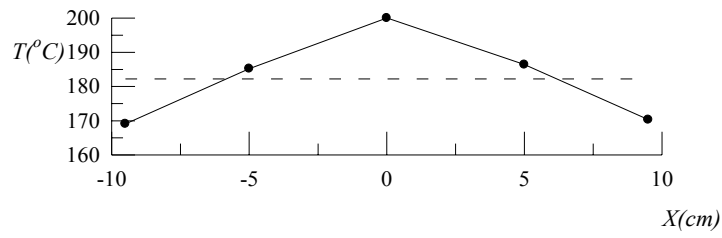


(b) $t = 66\text{s}$, $T_{\text{mean}} = 191.7^{\circ}\text{C}$ & $\Delta T_{\text{max}} = 10.6^{\circ}\text{C}$ ($\Phi = 59.2\%$)

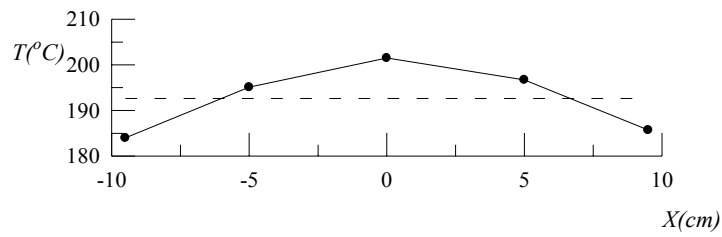


(c) $t = 94\text{s}$, $T_{\text{mean}} = 193.8^{\circ}\text{C}$ & $\Delta T_{\text{max}} = 6.8^{\circ}\text{C}$ ($\Phi = 73.8\%$)

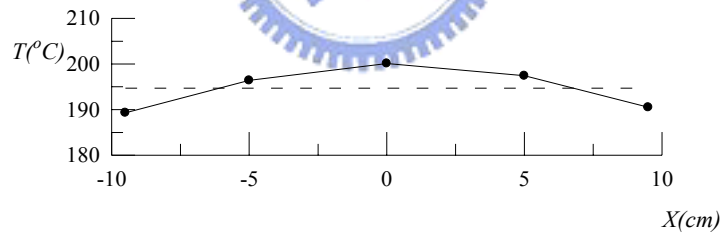
Fig. 4.57 The measured wafer temperature at selected locations during the ramp-up period for (a) $H=30\text{ mm}$, (b) $H=60\text{ mm}$, and (c) $H=90\text{ mm}$ with three heating lamps at $\omega=0\text{ rpm}$ and $V_d=10\text{ mm/s}$ for the final wafer temperature set at 200°C .



(a) $t = 45\text{s}$, $T_{\text{mean}} = 182.2^{\circ}\text{C}$ & $\Delta T_{\text{max}} = 17.8^{\circ}\text{C}$ ($\Phi = 31.5\%$)

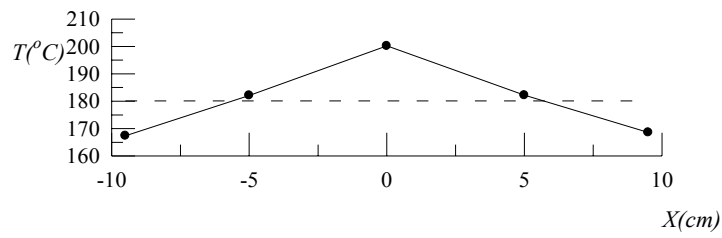


(b) $t = 66\text{s}$, $T_{\text{mean}} = 192.6^{\circ}\text{C}$ & $\Delta T_{\text{max}} = 8.9^{\circ}\text{C}$ ($\Phi = 65.8\%$)

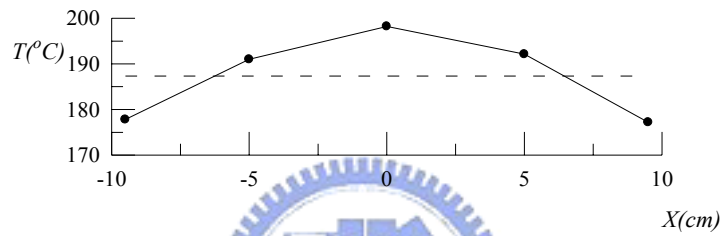


(c) $t = 94\text{s}$, $T_{\text{mean}} = 194.7^{\circ}\text{C}$ & $\Delta T_{\text{max}} = 5.4^{\circ}\text{C}$ ($\Phi = 79.2\%$)

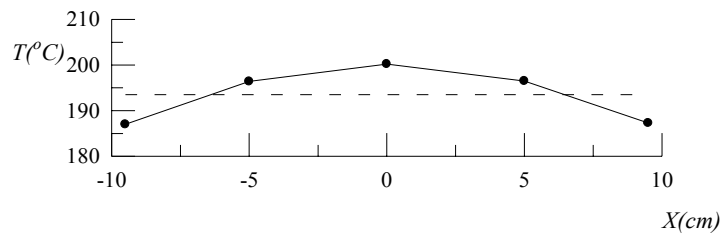
Fig. 4.58 The measured wafer temperature at selected locations during the ramp-up period for (a) $H=30\text{ mm}$, (b) $H=60\text{ mm}$, and (c) $H=90\text{ mm}$ with three heating lamps at $\omega=100\text{ rpm}$ and $V_d=10\text{ mm/s}$ for the final wafer temperature set at 200°C .



(a) $t = 44\text{s}$, $T_{\text{mean}} = 180.1^{\circ}\text{C}$ & $\Delta T_{\text{max}} = 20.1^{\circ}\text{C}$ ($\Phi = 22.7\%$)

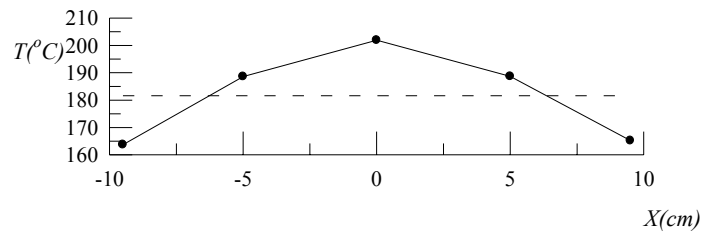


(b) $t = 68\text{s}$, $T_{\text{mean}} = 187.3^{\circ}\text{C}$ & $\Delta T_{\text{max}} = 10.9^{\circ}\text{C}$ ($\Phi = 58.1\%$)

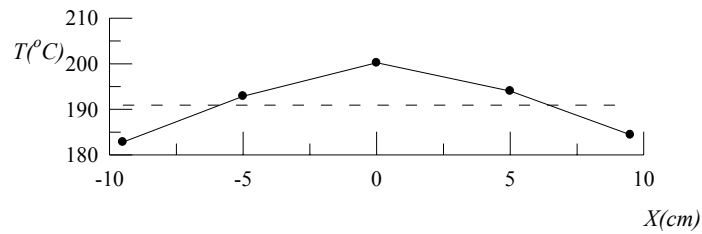


(c) $t = 104\text{s}$, $T_{\text{mean}} = 193.5^{\circ}\text{C}$ & $\Delta T_{\text{max}} = 6.7^{\circ}\text{C}$ ($\Phi = 74.2\%$)

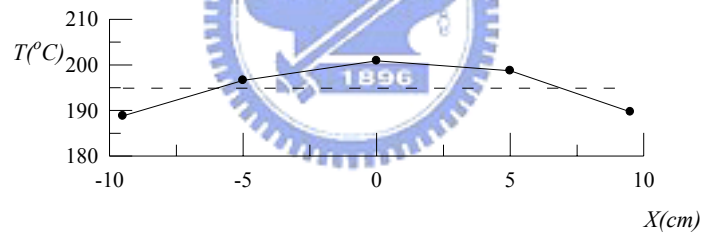
Fig. 4.59 The measured wafer temperature at selected locations during the ramp-up period for (a) $H=30\text{ mm}$, (b) $H=6\text{ mm}$, and (c) $H=9\text{ mm}$ with three heating lamps at $\omega=200\text{ rpm}$ and $V_d=10\text{ mm/s}$ for the final wafer temperature set at 200°C .



(a) $t = 41\text{s}$, $T_{\text{mean}} = 181.6^{\circ}\text{C}$ & $\Delta T_{\text{max}} = 17.9^{\circ}\text{C}$ ($\Phi = 31.2\%$)

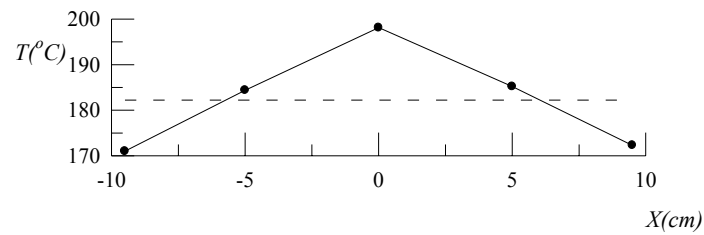


(b) $t = 62\text{s}$, $T_{\text{mean}} = 190.9^{\circ}\text{C}$ & $\Delta T_{\text{max}} = 9.3^{\circ}\text{C}$ ($\Phi = 64.2\%$)

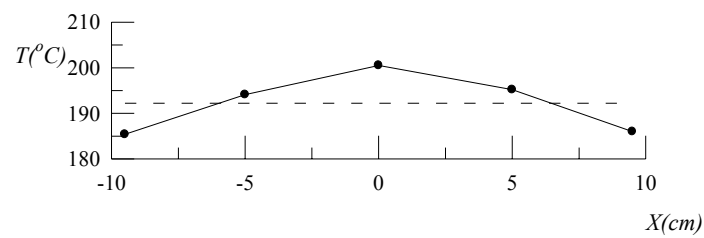


(c) $t = 90\text{s}$, $T_{\text{mean}} = 194.9^{\circ}\text{C}$ & $\Delta T_{\text{max}} = 6.1^{\circ}\text{C}$ ($\Phi = 76.5\%$)

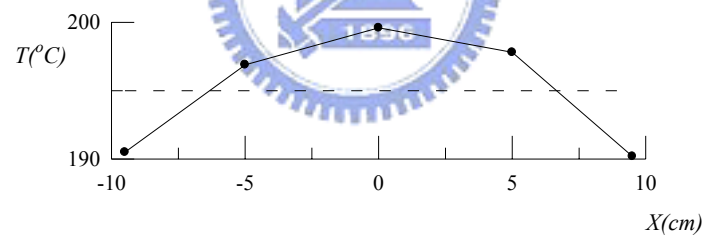
Fig. 4.60 The measured wafer temperature at selected locations during the ramp-up period for (a) $H=30\text{ mm}$, (b) $H=60\text{ mm}$, and (c) $H=90\text{ mm}$ with three heating lamps at $\omega=0\text{ rpm}$ and $V_d=15\text{ mm/s}$ for the final wafer temperature set at 200°C .



(a) $t = 43\text{s}$, $T_{\text{mean}} = 182.2^{\circ}\text{C}$ & $\Delta T_{\text{max}} = 15.9^{\circ}\text{C}$ ($\Phi = 38.8\%$)

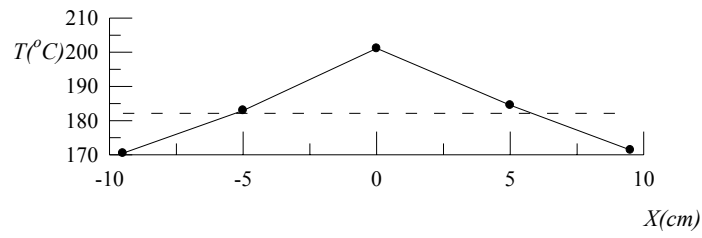


(b) $t = 62\text{s}$, $T_{\text{mean}} = 192.2^{\circ}\text{C}$ & $\Delta T_{\text{max}} = 8.3^{\circ}\text{C}$ ($\Phi = 68.1\%$)

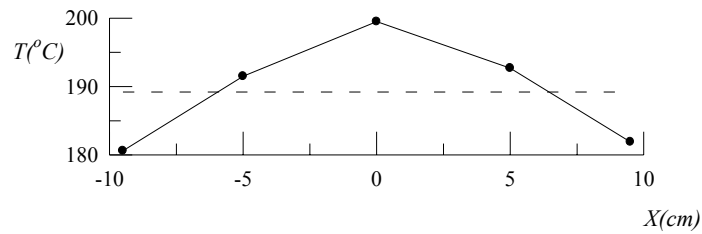


(c) $t = 89\text{s}$, $T_{\text{mean}} = 195^{\circ}\text{C}$ & $\Delta T_{\text{max}} = 4.6^{\circ}\text{C}$ ($\Phi = 82.3\%$)

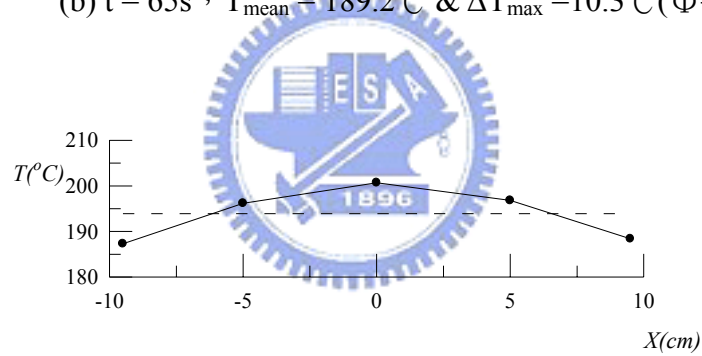
Fig. 4.61 The measured wafer temperature at selected locations during the ramp-up period for (a) $H=30\text{ mm}$, (b) $H=60\text{ mm}$, and (c) $H=90\text{ mm}$ with three heating lamps at $\omega=100\text{ rpm}$ and $V_d=15\text{ mm/s}$ for the final wafer temperature set at 200°C .



(a) $t = 44\text{s}$, $T_{\text{mean}} = 182.1^{\circ}\text{C}$ & $\Delta T_{\text{max}} = 19^{\circ}\text{C}$ ($\Phi = 26.9\%$)

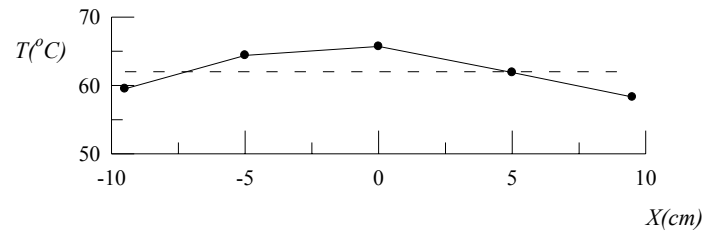


(b) $t = 65\text{s}$, $T_{\text{mean}} = 189.2^{\circ}\text{C}$ & $\Delta T_{\text{max}} = 10.3^{\circ}\text{C}$ ($\Phi = 60.4\%$)

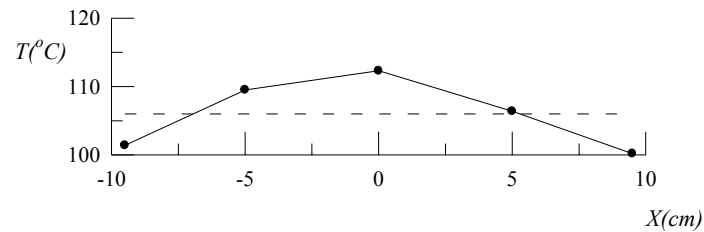


(c) $t = 101\text{s}$, $T_{\text{mean}} = 193.9^{\circ}\text{C}$ & $\Delta T_{\text{max}} = 6.6^{\circ}\text{C}$ ($\Phi = 74.6\%$)

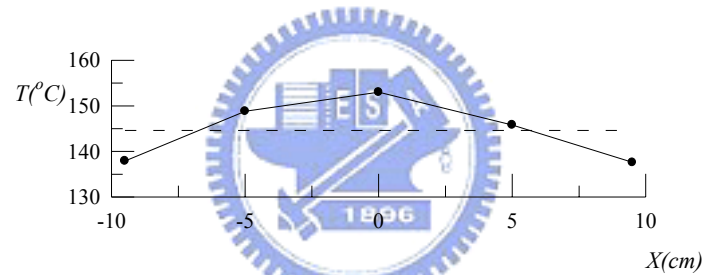
Fig. 4.62 The measured wafer temperature at selected locations during the ramp-up period for (a) $H=30\text{ mm}$, (b) $H=60\text{ mm}$, and (c) $H=90\text{ mm}$ with three heating lamps at $\omega=200\text{ rpm}$ and $V_d=15\text{ mm/s}$ for the final wafer temperature set at 200°C .



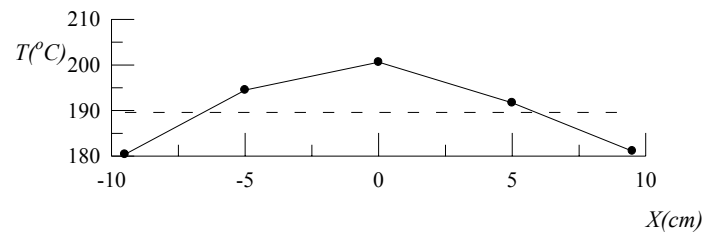
(a) $t = 15\text{ s}$, $T_{\text{mean}} = 62^{\circ}\text{C}$ & $\Delta T_{\text{max}} = 3.7^{\circ}\text{C}$



(b) $t = 30\text{ s}$, $T_{\text{mean}} = 106^{\circ}\text{C}$ & $\Delta T_{\text{max}} = 6.3^{\circ}\text{C}$

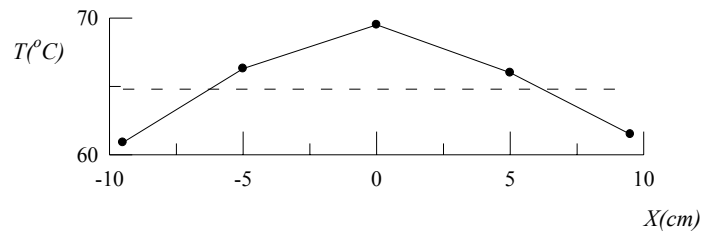


(c) $t = 45\text{ s}$, $T_{\text{mean}} = 144.6^{\circ}\text{C}$ & $\Delta T_{\text{max}} = 8.4^{\circ}\text{C}$

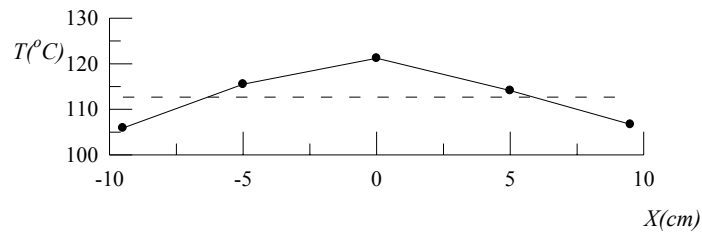


(d) $t = 66\text{ s}$, $T_{\text{mean}} = 189.6^{\circ}\text{C}$ & $\Delta T_{\text{max}} = 11^{\circ}\text{C}$

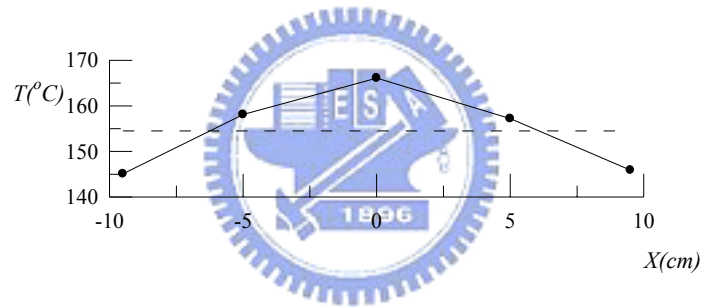
Fig. 4.63 The measured wafer temperature at selected locations for the wafer heated by three lamps arranged as Fig. 2.2(c) at $\omega = 0\text{ rpm}$, $V_d = 0\text{ mm/s}$ and $H = 60\text{ mm}$ for the final wafer temperature set at 200°C .



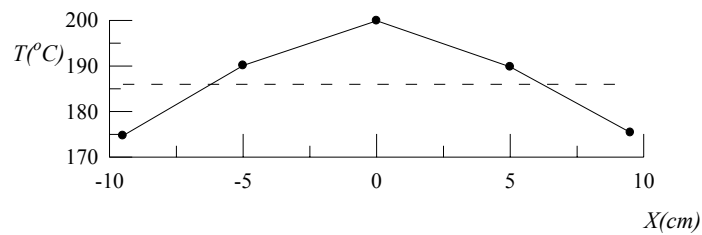
(a) $t = 15\text{s}$, $T_{\text{mean}} = 64.8^{\circ}\text{C}$ & $\Delta T_{\text{max}} = 4.7^{\circ}\text{C}$



(b) $t = 30\text{s}$, $T_{\text{mean}} = 112.7^{\circ}\text{C}$ & $\Delta T_{\text{max}} = 8.52^{\circ}\text{C}$



(c) $t = 45\text{s}$, $T_{\text{mean}} = 154.5^{\circ}\text{C}$ & $\Delta T_{\text{max}} = 11.6^{\circ}\text{C}$



(d) $t = 58\text{s}$, $T_{\text{mean}} = 186^{\circ}\text{C}$ & $\Delta T_{\text{max}} = 13.8^{\circ}\text{C}$

Fig. 4.64 The measured wafer temperature at selected locations for the wafer heated by three lamps arranged as Fig. 2.2(b) at $\omega = 0$ rpm, $V_d = 0$ mm/s and $H = 60$ mm for the final wafer temperature set at 200°C .

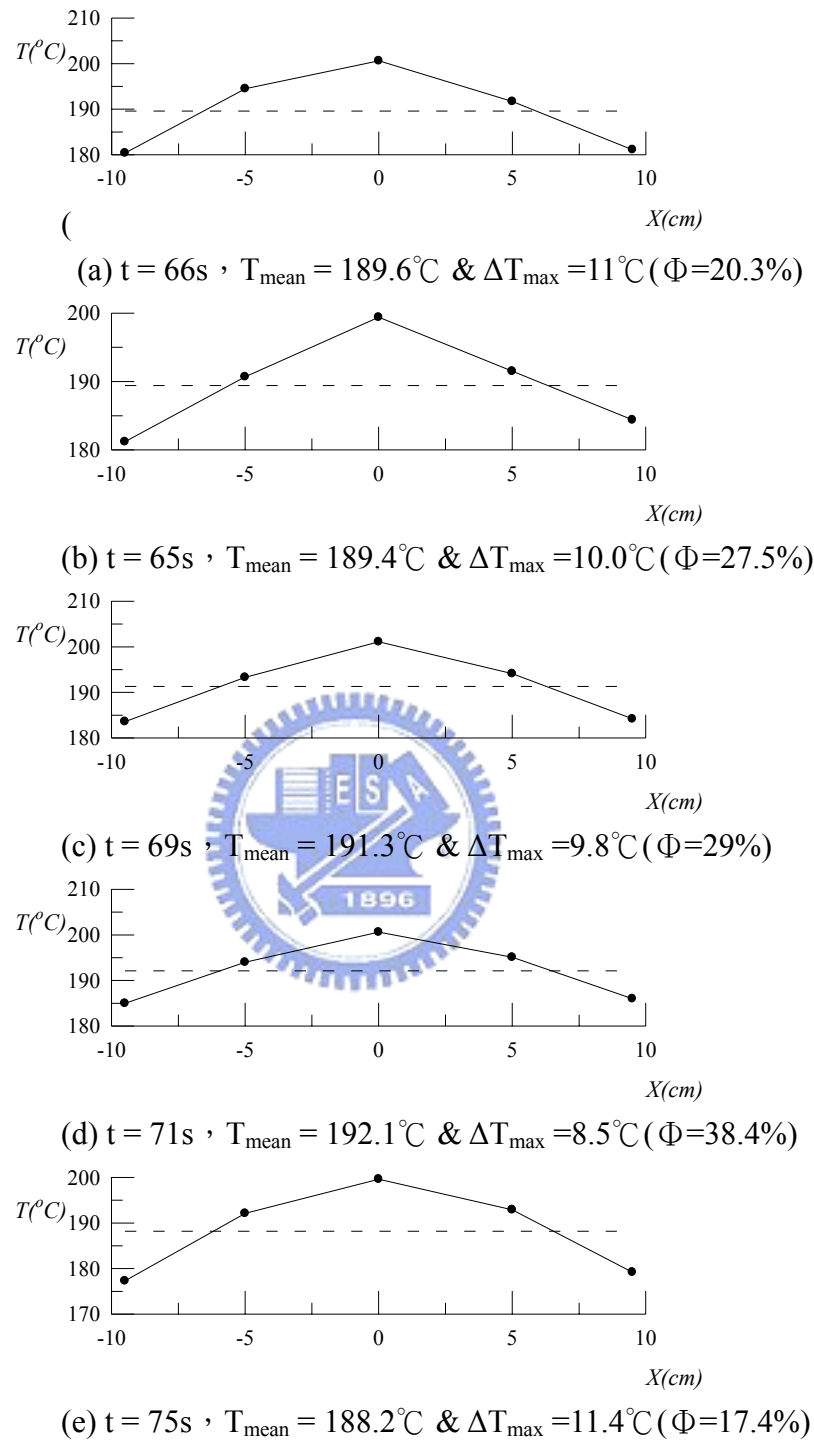


Fig. 4.65 The measured wafer temperature at selected locations during the ramp-up period for (a) $\omega = 0$ rpm, (b) $\omega = 50$ rpm, (c) $\omega = 100$ rpm, (d) $\omega = 150$ rpm and (e) $\omega = 200$ rpm with the wafer heated by three lamps arranged as Fig. 2.2(c) at $H = 60$ mm and $V_d = 0$ mm/s for the final wafer temperature set at 200°C .

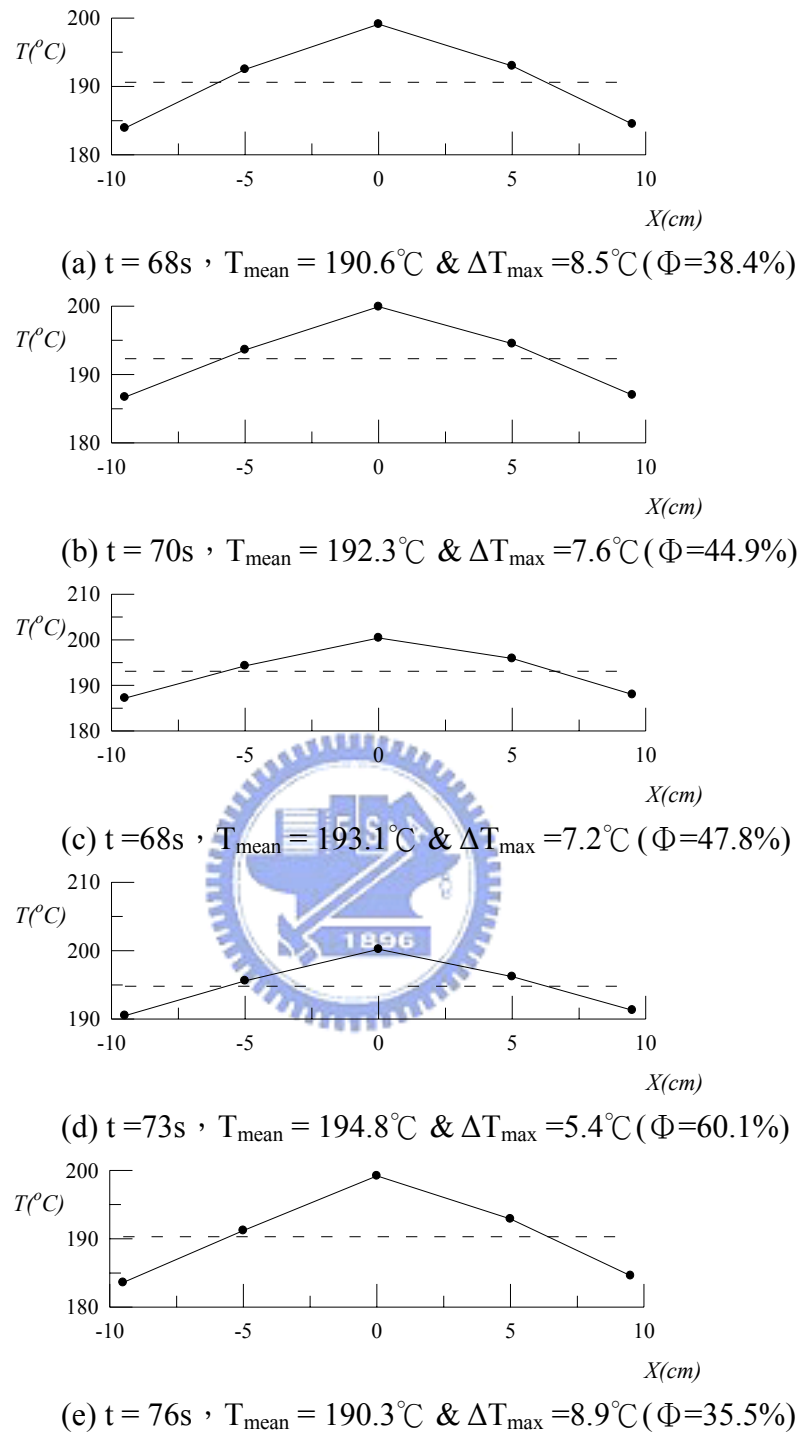
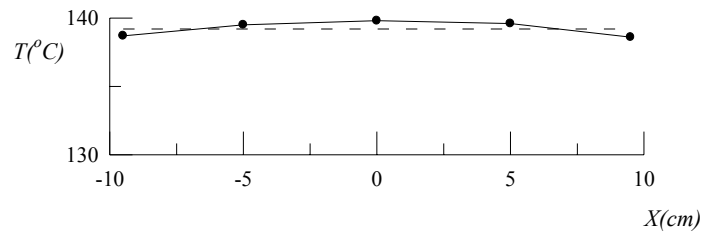
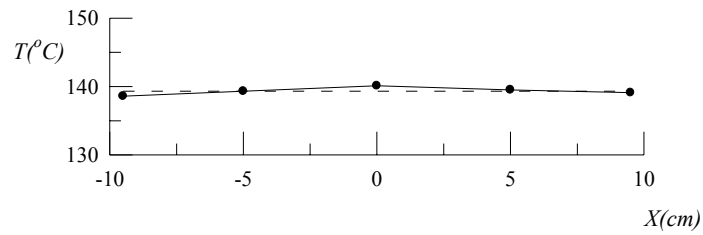


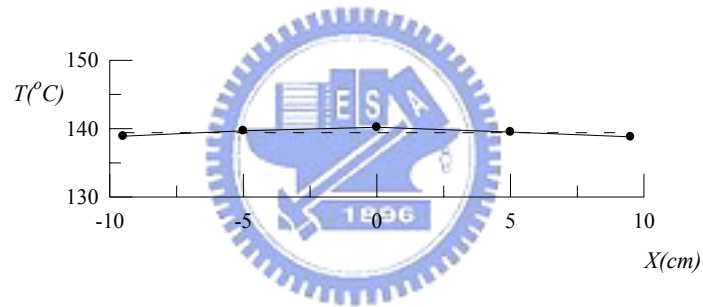
Fig. 4.66 The measured wafer temperature at selected locations during the ramp-up period for (a) $\omega = 0$ rpm, (b) $\omega = 50$ rpm, (c) $\omega = 100$ rpm, (d) $\omega = 150$ rpm and (e) $\omega = 200$ rpm with the wafer heated by three lamps arranged as Fig. 2.2(b) at $H = 60$ mm and $V_d = 15$ mm/s for the final wafer temperature set at 200°C .



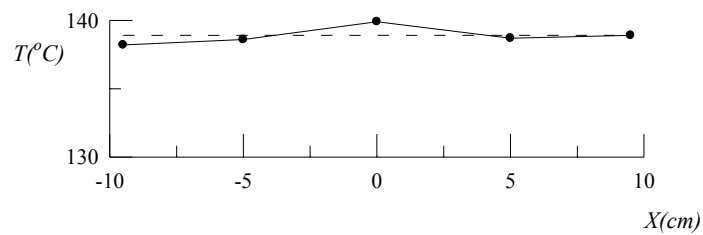
(a) $t=1348s$, $T_{\text{mean}} = 139.2^{\circ}\text{C}$ & $\Delta T_{\text{max}} = 0.6^{\circ}\text{C}$ ($\Phi=82.9\%$)



(b) $t=1362s$, $T_{\text{mean}} = 139.3^{\circ}\text{C}$ & $\Delta T_{\text{max}} = 0.7^{\circ}\text{C}$ ($\Phi=80.0\%$)



(c) $t=1350s$, $T_{\text{mean}} = 139.4^{\circ}\text{C}$ & $\Delta T_{\text{max}} = 0.5^{\circ}\text{C}$ ($\Phi=85.7\%$)



(d) $t=1320s$, $T_{\text{mean}} = 138.9^{\circ}\text{C}$ & $\Delta T_{\text{max}} = 0.7^{\circ}\text{C}$ ($\Phi=80.0\%$)

Fig.4.67 The measured wafer temperature at selected locations during the ramp-up period for (a) $V_d=15$ mm/s, (b) $V_d=16$ mm/s, (c) $V_d=17$ mm/s and (d) $V_d=18$ mm/s with a heating lamp at $\omega=170$ rpm and $H=90$ mm for the final wafer temperature set at 140°C .

CHAPTER 5

CONCLUDING REMARKS

An experimental study is carried out here to investigate the improvement of the temperature uniformity of a lamp heated eight-inch silicon wafer through the wafer rotation and translation during the ramp-up period. The effects of the rotation rate and translation speed of the wafer have been examined in detail. Moreover, the effects of the lamp-to-wafer distance and the power level of the heated lamps have been inspected. The results clearly indicate that increasing the wafer rotation rate up to certain value can improve the wafer temperature uniformity. Beyond that rotation rate an opposite effect is obtained. A similar trend is also noted for the increases of the wafer translation speed on the wafer temperature uniformity. Furthermore, the wafer temperature is more uniform for a longer lamp-to-wafer distance and lower power level of the lamps.

Our experimental data also suggest that a better arrangement of the three heated lamps can result in a better wafer temperature uniformity. For a suitable choice of the wafer rotation rate and translation speed the temperature nonuniformity on the wafer can be relatively small. At the wafer rotation speed $\omega = 170$ rpm, wafer translation velocity $V_d = 17$ mm/s and lamp-to-wafer separation distance $H = 90$ mm for the wafer heated by a single lamp, the maximum temperature difference across the wafer can be as low as 0.5°C for the mean wafer temperature $T_{\text{mean}} \approx 140^\circ\text{C}$.

References

1. R. S. Gyurcsik, R. K. Cavin and F. Y. Sorrell, Model-based control of semiconductor processing equipment : rapid thermal processing example, “systems engineering in the services of humans” conference proceedings, international conference Vol. 2 (1993) 13 -18.
2. Moslehi, M. M., Velo, L., Ajit Paranjpt, Kuehne, J., Huang S., Chapman R., Schaper S., Breedijk B., Najm H., Yin D., Lee Y. J., Anderson D. and Daves C., Fast-cycle-time single-wafer IC manufacturing, Microelectronic Engineering 25, (1994) 93-130.
3. K. G. Reid and A. R. Sitaram, High temperature thermal processing for ULSI application, Mat. Res. Soc. Symp. Proc. 387 (1995) 201-211.
4. C. P. Yin, C. C. Hsiao and T. F. Lin, Improvement in wafer temperature uniformity and flow pattern in a lamp heated rapid thermal processor, Journal of Crystal Growth 217 (2000) 201-210.
5. J. M. Dilhac, N. Nolhier, C. Ganibal, and C. Zanchi, Thermal modeling of a wafer in a rapid thermal processor, IEEE Transactions on Semiconductor Manufacturing, Vol. 8, No. 4 (1995) 432-439.
6. M. C. Öztürk, F. Y. Sorrell, J. J. Wortman and F. S. Johnson, Manufacturability issues in rapid thermal chemical vapor deposition, IEEE Transactions on Semiconductor Manufacturing, Vol.4, No.2 (1991) 155-165.
7. J. M. Ranish, Design of halogen lamps for rapid thermal processing, 11th IEEE International Conference on Advanced Thermal Processing of Semiconductors-RTP 2003, 195-202.
8. P. J. Timans, Rapid thermal processing technology for the 21st century, Materials Science in Semiconductor Processing 1 (1998) 169-179.

9. W. S. Yoo, T. Fukada, T. Setokubo, K. Aizawa, T. Ohsawa, N. Takahashi and R. Komatubara, Comparative study on implant anneal using single wafer furnace and lamp-based rapid thermal processor, 9th Int. Conference on Advanced Thermal Processing of Semiconductors-RTP 2001, 240-245.
10. F. Y. Sorrell, M. J. Fordham, M. C. Öztürk and J. J. Wortman, Temperature uniformity in RTP Furnaces , IEEE Transactions on Electron Devices Vol 39, No 1 (1992) 75-80.
11. H. A. Lord, Thermal and stress analysis of semiconductor wafers in a rapid thermal processing oven, IEEE Transactions on Semiconductor Manufacturing, Vol. 1, No. 3 (1988) 105-114.
12. R. S. Gyurcsik, R. K. Cavin and F. Y. Sorrell, Model-based control of semiconductor processing equipment: rapid thermal processing example, National science foundation and SEMATECH (1993) 13-18.
13. T. S. Wong, C. T. Wang, K. H. Chen, L. C. Chen and K. J. Ma, Carbon nanotube growth by rapid thermal processing, Diamond and Related Materials 10 (2001) 1810-1813.
14. S. Hirasawa, T. Suzuki and S. Maruyama, Optimal heating control conditions to unify temperature distribution in a wafer during rapid thermal processing with lamp heaters, 9th Int. Conference on Advanced Thermal Processing of Semiconductors-RTP' (2001) 210-216.
15. K. S. Balakrishnan and T. F. Edgar, Model-based control in thermal processing, Thin Solid Films 365 (2000) 322-333.
16. C. W. Liu, M. H. Lee, C. Y. Chao, C. Y. Chen, C. C. Yang and Y. Chang, The design of rapid thermal process for large diameter applications, 61-70.
17. B. J. Cho, P. Vandenabeele, and Karen Maex, Development of a hexagonal-shaper rapid thermal processor using a vertical tube, IEEE Transactions on

- Semiconductor Manufacturing, Vol. 7, No. 3, (1994) 345-353.
18. J. D. Stuber, I. T. Trachtenberg and T. F. Edgar, Design and modeling of rapid thermal processing systems, IEEE Transactions on Semiconductor Manufacturing, Vol. 11, No. 3, (1998) 442-457.
 19. S. Poscher and T. Theiler, Coupled simulation of gas flow and heat transfer in an RTP-system with rotating wafer, Materials Science in Semiconductor Processing 1 (1998) 201-205.
 20. C. J. Huang, C. C. Yu and S. H. Shen, Selection of measurement locations for the control of the rapid thermal processor, Automatica 36 (2000) 705-715.
 21. J. P. Zöllner, V. C. Cimalla and J. Pezoldt, RTP-temperature monitoring by means of oxidation, Journal of Non-Crystalline Solids 187 (1995) 23-28.
 22. Y. Chen, L. Booth, C. Schaper, B. T. Khuri-Yakub and K. C. Saraswat, 3D Modeling of rapid thermal processors for design optimization of a new flexible RTP system, IEEE (1994) 1-4.
 23. T. Fukada, W. S. Yoo, Y. Hiraga and N. Takahashi, Rapid thermal processing using single wafer rapid thermal furnaces, Extended Abstracts of International Workshop on Junction Technology 2001 (4.3.1- 4.3.4).
 24. J. Urban, W. Blersch and S. Paul, Thermal Model of Rapid Thermal Processing System.
 25. P. P. Apte and K. C. Saraswat, Rapid thermal processing uniformity using multivariable control of a circularly symmetric 3 Zone Lamp, IEEE Transaction on Semiconductor Manufacturing, Vol. 5, No. 3 (1992) 180-188.
 26. S. A. Norman, Optimization of transient temperature uniformity in RTP System, IEEE Transaction on Electron Devices, Vol. 39, No. 1 (1992) 205-207.
 27. J. Y. Choi, H. M. Do and H. S. Choi, Adaptive control of wafer temperature in RTP, ISIE 2001, 1219-1224.

28. Y. M. Cho, A. Paulraj and T. Kailath, A contribution to optimal lamp design in rapid thermal processing, IEEE Transaction on Semiconductor Manufacturing, Vol. 7, No. 1 (1994) 34-41.
29. Y. Liu, J. Hebb and J. Willis, Fast ambient switching for the multiple-step rapid thermal processing of wafers using a furnace-based RTP system, 9th Int. Conference on Advanced Thermal Processing of Semiconductors-RTP 2001, 306-314.
30. P. Park, C. D. Schaper and T. Kailath, control strategy for temperature tracking in rapid thermal processing of semiconductor wafers, Proceeding of the 31st Conference on Decision and control , (1992) 2568-2573.
31. S. A. Norman, Optimization of wafer temperature uniformity in rapid thermal processing systems, IEEE Transactions on Electron Devices (1991) 1-46.
32. P. J. Gyugyi and R. H. Roy, Model-based control of rapid thermal processing system, (1992) 374-381.
33. Y. K. Jan and C. A. Lin, Lamp configuration design for rapid thermal processing systems, IEEE Transactions on Semiconductor Manufacturing, Vol. 11, No. 1, (1998) 75-84.
34. A. Theodoropoulou, R. A. Adomaitis and E. Zafirou, Model reduction for optimization of rapid thermal chemical vapor deposition systems, IEEE Transactions on Semiconductor Manufacturing, Vol. 11, No. 1, (1998) 85-98.
35. Lee k. C., Chang H. Y. and Hu J. G., A new temperature compensation method for SI wafer in rapid thermal processor using separated SI rings as susceptor, Res. Soc. Symp. Proc. 470, (1997) 187-192.
36. C. Schaper, M. Moslehi, K. Saraswat and T. Kailath, Control of MMST RTP: repeatability, uniformity, and integration for flexible manufacturing, IEEE Transactions on Semiconductor Manufacturing, Vol. 7, No. 2, (1994) 202-219.

37. K. L. Knutson and S. A. Campbell, Modeling of three-dimensional effects on temperature uniformity in rapid thermal processing of eight inch wafers, IEEE Transactions on Semiconductor Manufacturing Vol. 7 No 1 (1994) 68-72.
38. S. Yu, F. Y. Sorrell and W. J. Keither, Temperature control strategies for RTP systems, (1993) 229-234.
39. F. Y. Sorrell, J. A. Harris and R. S. Gyurcsik, A global model for rapid thermal processors, IEEE Transactions on Semiconductor Manufacturing, Vol. 3, No. 4, (1990) 183-188.
40. S. Hirasawa, T. Watanabe, T. Takagaki and T. Uchino, Temperature distribution in semiconductor wafers heated in a hot-wall-type rapid diffusion furnace, IEEE Transactions on Semiconductor Manufacturing, Vol. 7, No. 4, (1994) 423-429.
41. A. Kersch and T. Schafbauer, Thermal modeling of RTP and RTCVD processes, Thin Solid Films 365 (2000) 307-321.
42. C. A. Lin and Y. K. Jan, Control system design for a rapid thermal processing system, IEEE Transaction on Control Systems Technology, Vol. 9, No.1 (2001) 122-129.
43. A. E. Naeini, Jon L. Ebert, D. D. Roover , R. L. Kosut , M. Dettori, L. M. L. Porter and S. Ghosal, Modeling and control of distributed thermal systems, IEEE transactions on control systems technology, Vol. 11, No.5 (2003) 668-683.
44. Y. M. Cho and T. K. Kailath, improvement of pyrometric sensing in rapid thermal processing via adaptive cancellation of lamplight interference, Control Engineering Practice, Vol. 3, (1995) 643-649.
45. S. J. Kline, and F. A. Mcclinkock, Describing uncertainties in single-sample experiment, MeChanical Engineering 75 (1953) 3-8.
46. R. J. Moffat, Contributions to the theory of single-sample uncertainty analysis, J. Fluid Eng., 104 (1982) 250-260.

47. Thermophysical properties of fluid, JSME Data Book (1983).

